FEDERAL UNIVERSITY OF SÃO CARLOS

EXACT SCIENCE AND TECHNOLOGY CENTER

GRADUATE PROGRAM IN PRODUCTION ENGINEERING

GISELLE ELIAS COUTO

EFFECT OF MEASUREMENT ERRORS ON DOUBLE SAMPLING S^2 CONTROL CHART

SÃO CARLOS-SP

2023

FEDERAL UNIVERSITY OF SÃO CARLOS

EXACT SCIENCE AND TECHNOLOGY CENTER

GRADUATE PROGRAM IN PRODUCTION ENGINEERING

GISELLE ELIAS COUTO

EFFECT OF MEASUREMENT ERRORS ON DOUBLE SAMPLING S^2 CONTROL CHART

Thesis presented to the Graduate Program in Production Engineering of the Federal University of São Carlos (UFSCar) to obtain the title of Doctor in Production Engineering.

Advisor: Prof. Dr. Pedro Carlos Oprime

SÃO CARLOS-SP

2023

UNIVERSIDADE FEDERAL DE SÃO CARLOS

Centro de Ciências Exatas e de Tecnologia
Programa de Pós-Graduação em Engenharia de Produção

Folha de Aprovação

Defesa de Tese de Doutorado da candidata Giselle Elias Couto, realizada em 02/06/2023.

Comissão Julgadora:

Prof. Dr. Pedro Carlos Oprime (UFSCar)

Prof. Dr. Ricardo Coser Mergulhão (UFSCar)

Prof. Dr. Antônio Fernando Branco Costa (UNIFEI)

Profa. Dra. Marcela Aparecida Guerreiro Machado de Freitas (UNESP)

Prof. Dr. Felipe Schoemer Jardim (UFF)

O Relatório de Defesa assinado pelos membros da Comissão Julgadora encontra-se arquivado junto ao Programa de Pós-Graduação em Engenharia de Produção.

Dedicated to Wallace

ACKNOWLEDGMENTS

"When you can measure what you are speaking about, and express it in numbers, you know something about it."

William Thomson, 1st Baron Kelvin (1983)

RESUMO

A qualidade de um produto pode ser entendida como inversamente proporcional à variabilidade presente em seu processo produtivo. Nesse sentido, o gráfico de controle é uma ferramenta estatística bem estabelecida para quantificar e analisar a variabilidade de um processo com base em informações observadas sobre algumas de suas características mensuráveis. Para simplificar a aplicação dos gráficos de controle, alguns pesquisadores e usuários assumem que os dados usados para avaliar o processo são exatos. No entanto, visto que a construção e a utilização dos gráficos de controle baseiam-se em resultados de medições e que nenhum sistema de medição é perfeito, a presença de erros de medição nos dados monitorados é inevitável. Estudos recentes indicam que o gráfico de controle do tipo Double Sampling pode ser uma alternativa favorável para o monitoramento de processos. No entanto, ainda há uma lacuna sobre estudos que investiguem o impacto dos erros de medição sobre gráficos Double Sampling voltados para o monitoramento da variância. Com base no exposto, o presente trabalho visa estudar como o desempenho do gráfico de controle Double Sampling S^2 é afetado pela presença dos erros de medição. Inicialmente, propõem-se uma revisão sistemática da literatura visando explorar estudos sobre o tema. Como metodologia principal de pesquisa tem-se a modelagem matemática e a simulação. Estuda-se a modelagem necessária para consideração dos erros de medição no design do gráfico de controle Double Sampling S^2. Por meio de simulação, verifica-se o impacto sobre o número médio de amostras até se obter um sinal (ARL) para diferentes valores de erro de medição. Utilizando algoritmo genético, propõe-se um estudo de otimização do gráfico de controle Double Sampling S^2 para operação com erros de medição. Por fim, um exemplo de simulação é apresentado para verificar a utilização do gráfico Double Sampling S^2 com os parâmetros otimizados. Os resultados obtidos indicam que a presença do erro de medição deteriora o desempenho do gráfico Double Sampling S^2 e que o impacto é maior quanto maior o erro de medição. Por meio do estudo de simulação, verificou-se a vantagem de se utilizar o gráfico Double Sampling S^2 otimizado, principalmente para erros de medição de maior magnitude. O presente estudo contribui com o conhecimento necessário para aplicação prática do gráfico de controle Double Sampling S^2 à medida que fornece parâmetros para sua utilização quando na presença de erros de medição.

Keywords: monitoramento de processos; gráfico de controle Double Sampling; erros de medição.

ABSTRACT

Product quality can be understood as inversely proportional to the variability in its production process. The control chart is a well-established statistical tool for quantifying and analyzing this process' variability based on observed information about some of its measurable characteristics. To simplify the control chart application, some researchers and users assume that the data used to evaluate the process is accurate. However, since the construction and use of control charts are based on measurement and no measurement system is perfect, errors in the measured data are inevitable. Recent studies indicate that the Double Sampling control chart can be an alternative for process monitoring. However, there is still a lack of studies that investigate the impact of measurement errors on Double Sampling control chart to monitor process variability. Based on the preceding, the present work aims to study how the performance of the Double Sampling S^2 control chart is affected by the presence of measurement errors. Initially, a systematic review of the literature is proposed in order to explore studies on the subject. The main methodology of the research is mathematical modeling and simulation. A design modeling for considering measurement errors in the Double Sampling S^2 control chart is proposed. The impact on the average run length (ARL) for different measurement error values is verified through simulation. Using a genetic algorithm, we propose an optimization study of the Double Sampling S^2 control chart for operation with measurement errors. Finally, a simulation example is presented to verify using the Double Sampling S^2 chart with the optimized parameters. The results indicate that measurement error deteriorates the performance of the Double Sampling S^2 chart, and the impact rises as measurement error increases. The simulation analysis showed the advantage of using the optimized Double Sampling S^2 chart, particularly for larger measurement errors. The present study contributes to the practical application knowledge of the Double Sampling S^2 control chart, providing parameters for its use in the presence of measurement errors.

Keywords: process monitoring; Double Sampling control chart; measurement errors.

GLOSSARY

$\hat{\sigma}_0^{2\prime}$	Estimator for the in-control process variance in ME case
$S_{Y_1}{}^2$	Sample variance computed for n_1
$S_{Y_2}{}^2$	Sample variance computed for n_2
$S_{Yp}{}^2$	Pooled sample variance
$\hat{\sigma}_0^2$	Estimator for the in-control process variance
$\hat{}$	Used to indicate estimation from the sample
$F_v(.)$	Chi-square cumulative distribution function
L_1	First control limit in the stage 1 of DS chart
L_2	Second control limit in the stage 1 of DS chart
L_3	Control limit of stage 2 of DS chart
P_{a1}	Probability that the process is in-control at stage 1
P_{a2}	Probability that the process is in-control at stage 2
S^2	Sample variance
$\bar{X}$	Sample mean
k_1	L_1 control limit constant
k_2	L_2 control limit constant
k_3	L_3 control limit constant
n_1	Stage 1 sample
n_2	Stage 2 sample
μ_0	In-control process mean
σ_0^2	In-control process variance
σ_1^2	Out-of-control process variance
σ_ε^2	Variance of the measurement error term ε
$*$	Used to indicate Phase I
A	Constant that represents the intercept in the measurement error model
AIB	Auxiliary information based
ARL	Average Run Length
ARL_0	In-control Average Run Length
ASS	Average sample size
ASS_0	In-control average sample size
B	Constant that represents the slope in the measurement error model
BDS	Bivariate double sampling
CL	Center line
CRL	Conforming Run Length
CV	Coefficient of variation

DS	Double sampling
DSATL	Double Sampling Adaptive Thresholding LASSO
EWMA	Exponentially weighted moving average
FAR	False alarm rate
FIR	Fast Initial Response
GA	Genetic Algorithm
HWMA	Homogenously weighted moving average
IC	In-control
LCL	Lower Control limit
MAX-EWMAMS	Maximum Exponentially Weighted Moving Average and Mean Squared Deviation
ME	Measurement error
MMS	Multivariate multiple sampling
MRL	Median run length
OOC	Out-of-control
R	Range
RL	Run length distribution
SDANOS	Standard deviation of the average number of observations to signal
SDRL	Standard deviation of the run length
SPC	Statistical Process Control
SSMGRDS	Side-sensitive modified group runs double sampling
TS	Triple Sampling
UCL	Upper control limit
VSI	Variable sampling interval
VSSI	Variable sample size and sampling interval
X	True value of the quality characteristic
Y	Observed value of the quality characteristic
Γ	Gamma function
$f(.)$	Chi-square probability density function
m	Number of Phase I samples
n	Number of items in a sample
α	Type I error
β	Type II error
δ	Standard deviation shift
ε	Random error term for measurement imprecision
ν	Degrees of freedom

LIST OF FIGURES

LIST OF TABLES

TABLE OF CONTENTS

1. INTRODUCTION

This chapter contextualizes the research presenting its motivation, research questions, objectives, and the proposed document structure.

1.1. CONTEXTUALIZATION

The quality concept has been studied, defined, and refined over the years. Quality specialists such as Shewhart and Taguchi devoted their work to researching ways to improve production systems by raising the processes' quality (WOODALL; MONTGOMERY, 1999). To make this enhancement attainable, it is crucial to translate the customer's expect quality into practical and measurable terms. In this regard, a useful interpretation of quality to make it more quantifiable is to consider it as inversely proportional to variability (MONTGOMERY, 2013). This definition underscores the importance of studying and reducing process variation to improve product quality.

Walter Shewhart was a pioneer in the field of variability monitoring, studying how to lower variation in order to increase industrial process quality, a thought that was not common at the time (BEST; NEUHAUSER, 2006). Following Shewhart's ideas about reducing variation were some of the greatest names in the Quality Management field, such as W. Edwards Deming, Philip B. Crosby, and Joseph M. Juran (ZAIRI, 2013). Deming reportedly stated that: "If I had to replace my message to managers to just a few words, I'd say it all had to do with reducing variation" (BANK, 1992 cited in ZAIRI, 2013, pg. 659).

Statistical process control (SPC) is a useful set of tools that seeks to reduce the process variation to an acceptable level by identifying the sources of undesired disturbances so that they can be removed by appropriate online or offline action (WETHERILL; ROWLANDS, 1991). SPC refers to statistics used to monitor and enhance the quality of the respective operations and enable appropriate decision-making by collecting data at various stages of the process and analyzing it statistically. It ensures that the overall process remains controlled, and that the final product satisfies the specified parameters. For this reason, it is used extensively by practitioners in academic research and engineering applications (GODINA *et al.*, 2018; STATSOFT, 2011).

SPC application involves following the processes, identifying problem areas, recommending methods to reduce variation and verify that they work, optimizing the process, testing the reliability of parts, and performing other analytical operations. Basic and more advanced statistical quality control methods can be used in SPC, including control charts, Pareto charts, capability analysis, gauge repeatability/reproducibility analysis, design of experiments, and reliability analysis (GODINA *et al.*, 2018; STATSOFT, 2011).

Due to their proven effectiveness, control charts are one of the most used tools in Statistical Quality Control. It is a well-established statistical tool for quantifying and analyzing process variability. It can be used to monitor a manufacturing process based on some measurable quality characteristics from individual items or subgroups (ASLAM *et al.*, 2021).

The first control chart was developed by Walter A. Shewhart in the 1920s at the Bell Telephone Laboratories, using normal curve's widely known properties to monitor the manufacturing process's quality characteristics. Because of their simplicity, versatility, and ease of use, Shewhart-type control charts are still among the most essential and widely used tools in industrial statistics applications (ALEVIZAKOS; CHATTERJEE; KOUKOUVINOS, 2021; BRADFORD; MIRANTI, 2019; STOUMBOS *et al.*, 2001).

The general principle of quality control charting is simple: samples of a specified size should be extracted from the ongoing manufacturing process. Then, using line charts to represent the variability of those samples, one should examine how close they are to the target parameters. If a pattern arises along those lines or samples exceed pre-determined limits, the process is considered out-of-control, and actions should be taken to identify the problem's source (LEWICKI; HILL, 2006).

No process or control system is perfect. Regardless of the type of process studied and the control system used, a portion of variability will always be present. An important part of using control charts is identifying whether or not this variability is acceptable. This variability may be due to common causes of variation arising from factors inherent in the process, or special causes, representing sporadic deviations in their behavior. A process is considered in-control (IC) if it operates only in the presence of common causes. If special causes of variation are present, it is said that the process is out-of-control (OOC). In this case, the data will exhibit non-random behavior, and the chart may also indicate points outside the control limits. This occurrence is called an alarm or signaling event (CHAKRABORTI; GRAHAM, 2018).

The control charts' conventional structure generally includes the following three elements: Center Line (CL), Upper Control Limit (UCL), and Lower Control Limit (LCL). The center line represents the target value, and the control limits represent the boundaries that, if trespassed, will result in an out-of-control event. Both are frequently set using the mean and standard deviation of a random variable representing the quality characteristic (HRYNIEWICZ; KACZMAREK-MAJER, 2018; VACHÁLEK *et al.*, 2021).

A control chart's performance is evaluated by how well it can discriminate between process shifts due to random causes and those due to special causes. It involves its ability to detect rapidly process deviations and the ability to not signal when they are not present. Aiming to improve the performance of the traditional control chart structure, Daudin (1992) proposed a monitoring scheme based on two evaluation stages. He named this scheme a Double Sampling (DS) control chart. In this scheme, a small sample of size n_1 is evaluated in the chart's first stage. Depending on its location in the chart, the process can be considered in-control, out-of-control, or a new small sample of size n_2 can be collected. Before determining if the process is out-of-control, the second sample is evaluated in the chart's second stage. Recent research, such as those proposed by Huang, Yang, and Xie (2020) and Salmasnia, Maleki, and Mirzaei (2023), has shown that using Double Sampling strategy in designing control charts improves their detection ability without increasing the sample size.

In addition to the concern with the number of stages used to monitor a process, other practical factors must be considered. Generally, an assumption often made to simplify the application of control charts is that the data used to evaluate the process is accurate (MALEKI; SALMASNIA; YARMOHAMMADI SABER, 2022). However, errors due to either the measurement system or operators are inevitable. Even with highly advanced measuring systems, a difference between the actual quantities and the measured ones will always exist (MALEKI; AMIRI; CASTAGLIOLA, 2017).

The initial steps for applying control charts include measuring the process and analyzing the measurement data (SATO, 2006). Since the data used to monitor the process is collected using measurement systems, the effect of measurement errors on control charts' performance cannot be neglected. The measurement error can be present both in the data used to monitor the process and in the samples collected to calculate the control limits in case of unknown parameters.

Maravelakis (2003) highlighted that measurement error is a factor that can seriously affect the performance of a control chart. However, although in most cases the measurements

used for monitoring the process are not accurate many of the studies on control charts do not make such consideration. For Double Sampling control charts, for example, as can be seen in the literature review presented in Chapter 3, less than 5% of studies published in Journals investigate the effects of measurement errors on the performance of these charts. Another issue is that this small percentage of studies only investigated these effects on one type of Double Sampling control chart.

Considering the potential implications of neglecting measurement error effects on control charts performance, this Thesis aims to answer the following research question: How can the presence of measurement errors affect the performance of the DS S^2 control chart?

1.2. MOTIVATION

Control charts are still a widely used tool for monitoring industrial processes. In most process monitoring practical applications, in order to monitor it, its variables must be measured. Aware that no measurement system is perfect, some measurement errors will always be present. Neglecting them can directly impact the performance of the control charts and, consequently, the monitoring performed.

Modern production process monitoring involves an increasing number of sensors and measuring systems. Knowing that companies are constantly seeking to reduce costs, thinking about alternatives that enable the reduction of the number and size of samples collected for process monitoring is also an important issue. Thus, it is important to investigate the effects of measurement errors on the performance of control charts developed to reduce the sample size, such as the Double Sampling control chart.

Using Double Sampling control charts without considering the impacts of measurement errors on their performance can lead to incorrect results, affecting the decision-making capacity in their use and, consequently, the costs involved in the process. Based on searches in the main research databases (Scopus, Science Direct, SciELO and Engineering Village) and based on the recent Double Sampling literature review by Motsepa *et al.* (2021), as far as we know, no studies investigate the effect of measurement errors on the Double Sampling (DS) chart for process variance monitoring.

1.3. RESEARCH OBJECTIVES

The research objective is the formalization of the purpose of the work (MIGUEL *et al.*, 2010). This thesis has as general objective: Investigate the effects of measurement errors on the Double Sampling S² control chart.

For the general objective achievement, this thesis has the following specific objectives:

1. Review the available literature on Double Sampling control charts to highlight gaps in the literature;

2. Investigate how the effect of measurement errors can be considered in the Double Sampling S^2 control chart design;

3. Evaluate the Double Sampling S^2 control charts' performance under the effect of measurement errors;

4. Evaluate optimizing the control chart in the presence of measurement errors;

5. Propose suggestions for future studies to continue the work in order to contribute to the research field.

1.4. METHODOLOGICAL RELEASE

The proposed thesis is classified as normative axiomatic quantitative research using modeling and simulation. Axiomatic research yields knowledge about certain model variables' behavior based on assumptions about other model variables' behavior. Normative axiomatic quantitative research is intended to improve the existing literature results to find an optimal solution to a new problem or compare various strategies for addressing a specific issue. Mathematical simulation is special analytical modeling in which hypotheses about the model parameter values are made to test it (BERTRAND; FRANSOO, 2002; MEREDITH *et al.*, 1989).

The first step was a preliminary reading of papers on control charts to find gaps in the literature that needed to be studied. Papers that addressed Double Sampling control charts

were reviewed. The review aimed to identify what has already been done in the available literature and understand best practices, results, and limitations of existing studies. It was found that no studies considered the measurement error for the Double Sampling S^2 chart.

From the initial step, some decisions were made. It was assumed that the developed control chart is intended for use in normally distributed processes. The additive model is considered to represent the measurement error due to its wide application and ability to represent different practical situations. The measurement error is considered a random variable following a normal distribution, so the model must account for this randomness and extra variability.

Based on the available literature, parameters such as sample size, control limits range, shift size, and measurement error range were defined to evaluate the performance of the Double Sampling S^2 control chart under the effect of measurement error. Average run length and average sample size are used to evaluate the control charts' performance. Simulation studies were performed to analyze measurement error's effect on the control chart's performance. The implementation of computational solutions was done using the R programming language. The programming language choice is due to its wide use in statistical studies and because it is open source.

The optimization of the Double Sampling S^2 control chart is also proposed. To solve the optimization problem, the genetic algorithm (GA) method was chosen because of its effectiveness for optimizing nonlinear models. Genetic algorithms can be considered as a multi-directional search method to solve problems. GA is based on the principles of natural genetics and natural selection, because the essential aspects of natural genetics — reproduction, crossover, and mutation – are applied (ZAINUDDIN; ABD SAMAD, 2020).

According to Rao (2019), GAs differs from typical optimization approaches in the following ways:

1. Instead of a single design point, the procedure is started using a population of points (trial design vectors). When the number of design variables is n, the population size is commonly 2n to 4n. GAs are less prone to get trapped at a local optimum since numerous points are considered as candidate solutions;

2. GAs use only the values of the objective function;

3. In GAs the design variables are represented as strings of binary variables that correspond to the chromosomes in natural genetics. Thus, the search method is naturally

applicable for solving discrete and integer programming problems. For continuous design variables, the string length can be varied to achieve any desired resolution;

4. The objective function value corresponding to a design vector plays the role of fitness in natural genetics;

5. Each generation gives a fresh collection of strings based on randomized parent selection and crossover from the previous one. GAs effectively combines novel combinations with the available knowledge to discover a new generation with improved fitness or objective function value.

From the optimization study using a genetic algorithm, a table was created with the values of the optimized parameters. Finally, an illustrative simulation study is presented to demonstrate the use of optimized parameters.

1.5. THESIS STRUCTURE

This thesis is structured into six chapters. Figure 1 shows the proposed thesis' structure and the alignment of the chapters with the specific objectives of the Thesis.

Chapter 1 presents the contextualization and research question, research motivation, research objectives, and the methodological release.

Chapter 2 presents the relevant theoretical background. The fundamentals of control charts and measurement errors main concepts are presented. An overview of the literature on control charts for variability monitoring under the effect of measurement errors is also presented.

Chapter 3 presents the general procedure of the Double Sampling scheme and a Systematic Literature Review on Double Sampling control charts.

Chapter 4 details the implementation of the DS S^2 control chart in the presence of measurement errors. Details of the simulations conducted are also presented.

Chapter 5 presents the proposal for DS S^2 control chart optimization and an illustrative simulation example.

Finally, Chapter 6 summarize this thesis's main contributions and provide suggestions for further research involving related topics.

Figure 1 – Thesis' structure

Chapter 1 - Introduction

Chapter 2 – Theoretical Background

Contextualization

Chapter 3 – Systematic Literature Review

Specific Objective 1

Chapter 4 – Control chart Design

Specific Objectives 2 and 3

Chapter 5 – Control chart Optimization

Specific Objective 4

Chapter 6 – Conclusions

Specific Objective 5
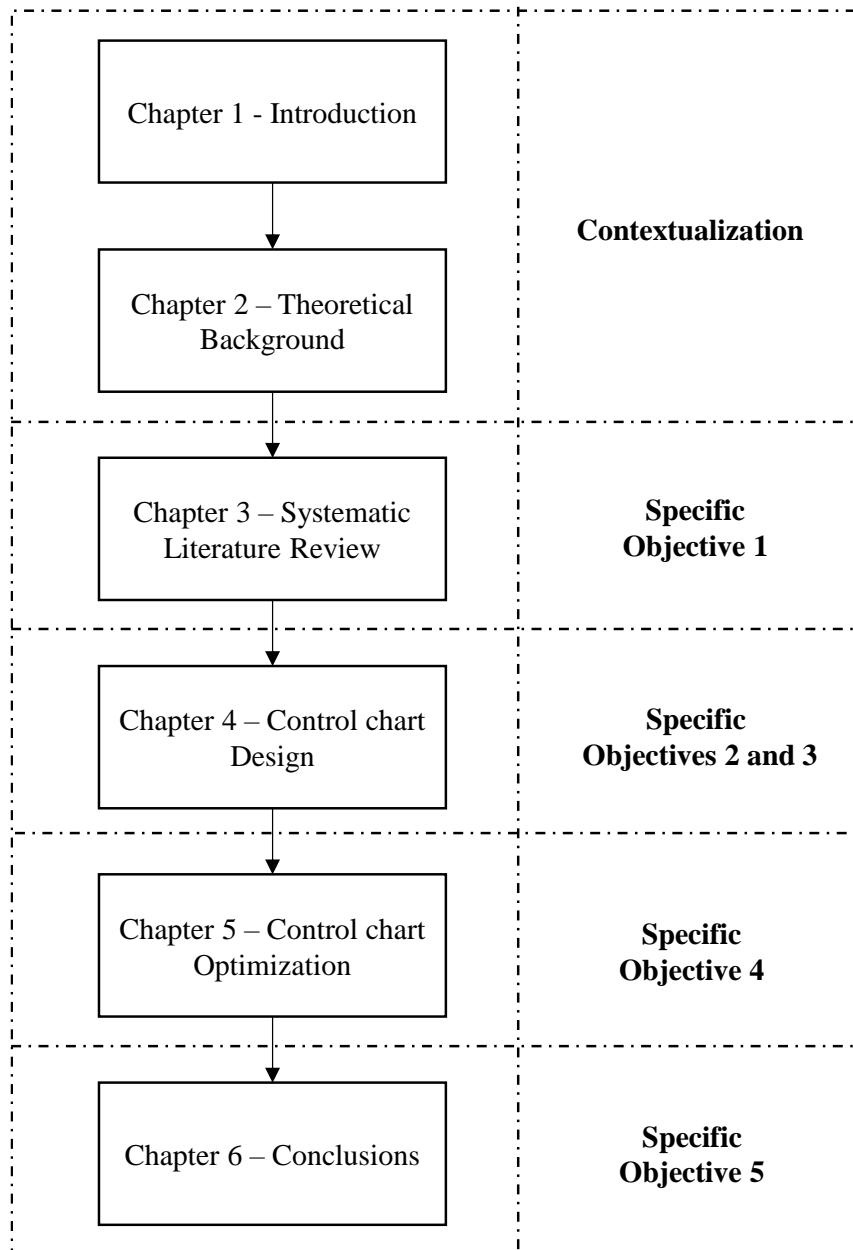
2. THEORETICAL BACKGROUND

This chapter presents the key concepts covered in the study. First, it presents the fundamental concepts about control charts and measurement errors and their importance for statistical quality control. Following, it presents the previous works on the effect of measurement error on control charts for process variability monitoring.

2.1. HISTORY AND FUNDAMENTALS OF CONTROL CHARTS

Control charts are one of the main techniques of statistical process control. Its primary objective is to evaluate the quality of a production process (MOYA-FERNÁNDEZ; ÁLVAREZ; SKALSKÁ, 2019). The first control chart was invented by Walter Andrew Shewhart in 1924 (WILEY, 2011).

Shewhart (1891–1967) received his bachelor's and master's degrees from the University of Illinois and a doctorate in physics from the University of California at Berkeley. He joined the Western Electric Company in 1918 to work on improving the quality of telephone hardware. The Western Electric Company's major plant was the Hawthorne Plant in Chicago. The Bell Telephone Company, which later changed its name to the American Telephone and Telegraph Company (AT&T), purchased hardware from Western Electric. Shewhart worked at Hawthorne Plant until 1925, when he moved to the Bell Telephone Research Laboratories, remaining until his retirement in 1956 (BEST; NEUHAUSER, 2006; WILEY, 2011).

Shewhart is known as the "father of statistical quality control" (XIE; MUKHERJEE, 2017). He gained notoriety in the statistical community after writing the report "Statistical Method from the Viewpoint of Quality Control" in 1937. He also published numerous articles while working at Bell Laboratories and the historic memorandum of May 16, 1924, in which he proposed the statistical control chart (AMERICAN SOCIETY FOR QUALITY, 2021).

The Shewhart control chart is a graphical plot used in the investigation of the process changes over time. The Shewhart chart, initially used to process mean monitoring, consists of three lines that are the lower control limit (LCL), upper control limit (UCL), and center line (CL). The LCL is typically plotted 3σ below the CL, while the UCL is typically plotted 3σ above the CL (KHOO, 2013).

Shewhart control charts visually represent the application of a sequential statistical significance test for an out-of-control condition, where control limits are confidence limits on the true process mean (NELSON, 1999). The basic structure of a Shewhart chart is shown in Figure 2.

Figure 2 – Shewhart control chart's general structure
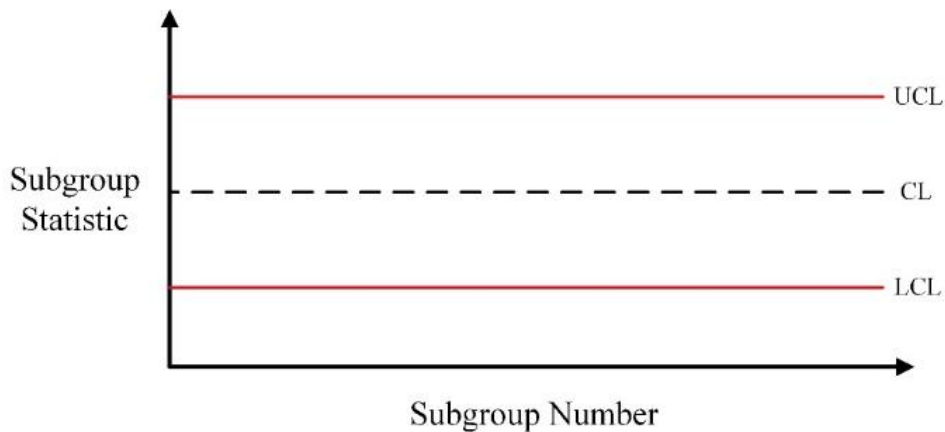
Shewhart control charts are used to identify the presence of causes that produce significant deviations from a process's stable operation. Shewhart (1930) and Deming (1986) referred to these causes as "assignable" causes and "special" causes, respectively. When the variability of the production process is exclusively produced by common causes, inherent in the work system, the process is said to be in-control. However, if the process' variability is produced by assignable causes, it is considered to be out-of-control (BAKIR, 2005; MOYA-FERNÁNDEZ; ÁLVAREZ; SKALSKÁ, 2019; NELSON, 1999).

About what can be considered a controlled process, Shewhart stated:

> "A phenomenon will be said to be controlled when, through the use of past experience, we can predict, at least within limits, how the phenomenon will be expected to vary in the future. Here it is understood that prediction within limits means that we can state, at least approximately, the probability that the observed phenomenon will fall within the given limits" (SHEWHART, 1930, pg. 367).

Shewhart X-bar, R, S^2, and S control charts are among the most popular control charts used to process monitoring (DIKO et al., 2017; GANGULY; PATEL, 2014).

2.2.1   X-BAR CHART

Consider that the true value of a quality characteristic is represented by a random sample X_{ij} of size $j = 1, 2, ..., n$ taken from a process at time $i = 1, 2, ..., m$. We can monitor this quality characteristic by its sample mean, given by Equation 1.

$$\bar{X}_j = \frac{\sum_{i=1}^{n} X_i}{n} , \qquad j = 1, 2, ..., m$$

Where $\bar{X}_j \sim N\left(\mu_0, \frac{\sigma_0}{\sqrt{n}}\right)$.

Assuming that X_{ij} is independent and identically distributed, and follows a normal distribution with known in-control process mean μ_0 and known standard deviation σ_0, the control limits of the k-sigma X-bar control chart with subgroups of size n are:

$$UCL_{\bar{X}} = \mu_0 + k\frac{\sigma_0}{\sqrt{n}}$$

$$CL_{\bar{X}} = \mu_0$$

$$LCL_{\bar{X}} = \mu_0 - k\frac{\sigma_0}{\sqrt{n}}$$

where UCL is the upper control limit, CL is the center line, LCL is the lower control limit, and k is a constant that represents the distance of the upper or lower control limit from the center line in terms of the standard deviation. k is typically assumed to be 3 or is chosen to provide a nominal in-control average run length such as 370 or 500.

In many practical cases, the process statistical parameters are not known. These parameters are estimated from samples or subgroups. In this case, the control limits would be given by:

$$\widehat{UCL}_{\bar{X}} = \hat{\mu} + k\frac{\hat{\sigma}}{\sqrt{n}} = \bar{\bar{X}} + k\frac{\hat{\sigma}}{\sqrt{n}}$$

$$\widehat{CL}_{\bar{X}} = \hat{\mu} = \bar{\bar{X}}$$

$$\widehat{LCL}_{\bar{X}} = \hat{\mu} - k\frac{\hat{\sigma}}{\sqrt{n}} = \bar{\bar{X}} - k\frac{\hat{\sigma}}{\sqrt{n}}$$

where $\bar{\bar{X}}$ is the grand average of all the $\bar{X}_j$ values used as an estimator of the process mean and $\hat{\sigma}$ is a chosen estimator of the process standard deviation.

Although the X-bar control chart is widely used for monitoring the mean of a process, as its control limits depend on the standard deviation, its application will only be useful if the process variability is also monitored. Therefore, it is recommended that together with the X-bar chart, a control chart be used to monitor the process variation. The R, S, and S^2 control charts are popular options.

2.2.2   R CONTROL CHART

The structure of the R control chart depends upon the sample statistic range (R), shown in Equation 8.

$$R = X_{max} - X_{min}$$

where X_{max} and X_{min} are the maximum and minimum order statistics for the values of the quality characteristic of interest, respectively.

Let $R_1, R_2, \ldots, R_m$ be the m samples' range. The average range is given by Equation 9.

$$\bar{R} = \frac{R_1 + R_2 + \cdots + R_m}{m}$$

There is a well-known relationship between a sample range and the standard deviation of a normal distribution given by Equation 10.

$$W = \frac{R}{\sigma}$$

The random variable W is called the relative range. The parameters of the distribution of W are functions of the sample size n and the mean of W is represented by d_2. Values of d_2 for various sample sizes can be found in Montgomery (2013). Thus, an estimator of $\hat{\sigma}$ is given by Equation 11.

$$\hat{\sigma} = \frac{R}{d_2}$$

So, if we use the average range of the m preliminary samples, we can use:

$$\hat{\sigma} = \frac{\bar{R}}{d_2}$$

as an unbiased estimator of σ.

To determine the control limits of the R control chart, we need an estimate of the standard deviation of R. Assuming that the quality characteristic is normally distributed, $\hat{\sigma}_R$ can be found from the distribution of the relative range. The standard deviation of W, named as d_3, is a known function of n (MONTGOMERY, 2013). Thus, since $W = R/\sigma$, $\hat{\sigma}_R$ is given by:

$$\hat{\sigma}_R = d_3 \frac{\bar{R}}{d_2}$$

Therefore, the control limits for the R control chart are:

$$\widehat{UCL}_R = \bar{R} + 3d_3 \frac{\bar{R}}{d_2} = \bar{R}\left(1 + 3\frac{d_3}{d_2}\right) = D_4\bar{R}$$

$$\widehat{CL}_R = \bar{R}$$

$$\widehat{LCL}_R = \bar{R} - 3d_3\frac{\bar{R}}{d_2} = \bar{R}\left(1 - 3\frac{d_3}{d_2}\right) = D_3\bar{R}$$

where $\bar{R}$ is the average range, σ_R is the standard deviation of R, and d_2, d_3, D_3, and D_4 are tabled constants that depend on the sample size and can be found in Montgomery (2013).

2.2.3 S² CONTROL CHART

Another way to monitor the process' variability is to control its variance, which can be done based on the unbiased estimator S^2. The resulting control chart is called S^2 chart. Consider that m samples are analyzed, each with size n, and their variances $S_1{}^2, S_2{}^2, ..., S_m{}^2$ are given by Equation 17.

$$S_j{}^2 = \frac{\sum_{i=1}^{n}(x_i - \bar{x})^2}{n-1}, j = 1,2,3,...,m$$

It follows that $\frac{(n-1)S^2}{\sigma^2} \sim \chi^2{}_{n-1}$, so the control limits for the S^2 control chart, for the known parameter case, are exact and given by:

$$UCL_{S^2} = \frac{\sigma^2}{n-1}\chi^2{}_{\alpha/2,n-1}$$

$$CL_{S^2} = \sigma^2$$

$$LCL_{S^2} = \frac{\sigma^2}{n-1}\chi^2{}_{1-(\alpha/2),n-1}$$

where $\chi^2{}_{\alpha/_2,n-1}$ and $\chi^2{}_{1-(\alpha/_2),n-1}$ denote the upper and lower $\alpha/_2$ percentage points of the chi-square distribution with $n-1$ degrees of freedom

Since $E(S^2) = \sigma^2$, S^2 is an unbiased estimator of σ^2 (MONTGOMERY, 2013). Therefore, the control limits for the S^2 control chart with estimated parameter are:

Equation 21

$$\widehat{UCL}_{S^2} = \frac{\bar{S}^2}{n-1}\chi^2{}_{\alpha/_2,n-1}$$

Equation 22

$$\widehat{CL}_{S^2} = \bar{S}^2$$

Equation 23

$$\widehat{LCL}_{S^2} = \frac{\bar{S}^2}{n-1}\chi^2{}_{1-(\alpha/_2),n-1}$$

where $\bar{S}^2$ is an average sample variance obtained from the analysis of preliminary data and given by Equation 24.

Equation 24

$$\bar{S}^2 = \frac{\sum_{j=1}^{m} S_j{}^2}{m}$$

2.2.4 S CONTROL CHART

Setting up the S control chart requires about the same sequence of steps as those for the range control chart, except that, for each sample, we must calculate the sample standard deviation. Although S^2 is an unbiased estimator of σ^2, S is not an unbiased estimator of σ. If the underlying distribution is normal, then S estimates $c_4\sigma$, where c_4 is a constant that depends on the sample size n. Furthermore, the standard deviation of S is $\sigma\sqrt{1-c_4{}^2}$ (MONTGOMERY, 2013). So, the three-sigma control limits for the S control chart are:

Equation 25

$$UCL_S = c_4\sigma + 3\sigma\sqrt{1-c_4{}^2}$$

Equation 26

$$CL_S = c_4\sigma$$

Equation 27

$$LCL_S = c_4\sigma - 3\sigma\sqrt{1 - c_4{}^2}$$

If σ is unknow, then it must be estimated by analyzing past data. Suppose that m preliminary samples are available, each of size n, and let S_i be the standard deviation of the ith sample. The average of the m standard deviations is given by Equation 28.

Equation 28

$$\bar{S} = \frac{\sum_{j=1}^{m} S_i}{m}$$

Then, the statistic $\bar{S}/c_4$ is an unbiased estimator of σ. Then, the control limits of the S chart are:

Equation 29

$$\widehat{UCL}_S = B_4\bar{S}$$

Equation 30

$$\widehat{CL}_S = \bar{S}$$

Equation 31

$$\widehat{LCL}_S = B_3\bar{S}$$

where B_3 and B_4 are given by Equation 32 and 33, respectively.

Equation 32

$$B_3 = 1 - \frac{3}{c_4}\sqrt{1 - c_4{}^2}$$

Equation 33

$$B_4 = 1 + \frac{3}{c_4}\sqrt{1 - c_4{}^2}$$

2.2. CONTROL CHARTS' CLASSIFICATION

As control charts' application spread among companies, new types of control charts were developed. Just as important as using control charts correctly is making the right choice on which control chart to use. Before deciding on the type of control chart, one must investigate several questions concerning the monitored process and collected data. Adams (2008) suggests asking the following questions:

- What type of data is available?

- How much data is available?

- Are data associated with long production runs or some other process environment such as batch processes or short production runs?

- Is a single-quality characteristic or multiple quality characteristics being considered? If multiple quality characteristics are important, are data values for the various key quality characteristics correlated with one another?

- Are data values for a given quality characteristic correlated over time (autocorrelated)?

- Are the distributional properties of the population reflected by the data?

- Are common probability distributions, such as the normal, binomial or Poisson distributions, useful approximations?

- Are key output quality characteristics driven by key process input variables? If so, do we have data on both inputs and outputs?

By answering the above questions, one can decide which control chart best suits one's monitoring needs. Table 1 shows the main control charts' classification.

The control charts' primary classifications can be made based on the type of data monitored and can be described as variable data, attribute data, profile data, and fuzzy data (MALEKI; AMIRI; CASTAGLIOLA, 2017). Variable-type data can be understood as measurable data, while attribute-type data can be understood as countable data (MONTGOMERY, 2013). Some of the main control charts for variable data are the Shewhart $\bar{X}$, R, S, and S^2 control charts (CHEN, 1998; GANGULY; PATEL, 2014). Some of the main attribute control charts are np, p, c and u charts (WU *et al.*, 2009).

Table 1 – Main control charts' classification

Classification	Type	Description
Data type	Attribute	Used for the non-measurable data, such as the number of failures or nonconformities.
	Variable	Used when the quality characteristics are measured, such as the workpiece's dimensions or mass.
	Profile	Used when the quality characteristic is better represented by a functional relationship between a response variable and one or more explanatory variables.
	Fuzzy	Used when the quality characteristic is characterized by some vagueness and ambiguity and expressed by fuzzy numbers or linguistic variables.
Design structure	Memoryless	Ignore past sample information, considering only current sample information.
	Memory-type	Consider recent and previous information in the given sample.
Number of variables monitored	Univariate	Used to monitor a single quality characteristic.
	Multivariate	Used to monitor several correlated quality characteristics.
Distribution	Parametric	Used when a distributional assumption is made regarding the process, such as normality.
	Non-parametric	Used when it is impossible or unjustified to make a distributional assumption.

Regarding profile monitoring, according to Maleki, Amiri, and Castagliola (2018) the main control charts developed use the linear regression model to represent the relationship between the response and the explanatory variable, but other types of profiles were also explored, such as the polynomial profiles, logistic regression profiles, and nonlinear profiles.

Regarding Fuzzy data monitoring, if there is uncertainty in the process or if quality characteristics are described by human subjectivity, then fuzzy set theory can be used to model the process data (PEKIN ALAKOC; APAYDIN, 2018). Fuzzy control charts can be subdivided into Type 1 and Type 2 (RAZALI *et al.*, 2020). These control charts are based on charts developed for other date types such as Shewhart-type, EWMA, and CUSUM control charts. In the Type 1 fuzzy sets, each element has a degree of membership function valued in the interval [0,1] and it is two-dimensional (ŞENTÜRK; ANTUCHEVICIENE, 2017). The Type 2 fuzzy set theory incorporates foot prints and high level uncertainty models to reflect ambiguity associated with the uncertainty of membership functions (RAZALI *et al.*, 2020).

Control charts can be also divided into memoryless and memory-type categories based on the mechanism of the design structure (ALI *et al.*, 2021). The memoryless charts focuses on the large shifts while the memory charts address the small shifts (RIAZ, 2015). The main memory-less control chart is the Shewhart control chart, proposed by W.A Shewhart (1924). The main memory-type control charts are the cumulative sum (CUSUM) control chart proposed by Page (1954) and the exponentially weighted moving average (EWMA) control chart proposed by Roberts (1959).

Another possible classification is based on the number of monitored variables. Control charts can be classified into univariate or multivariate charts when they monitor one or more process quality characteristics, respectively (ASLAM *et al.*, 2020; SAGHIR *et al.*, 2019). Some of the main univariate control charts are Shewhart-type charts, EWMA chart, and CUSUM chart and some of the main multivariate control charts are Hotelling's T², multivariate EWMA (MEWMA) and multivariate CUSUM (MCUSUM) (MALEKI; AMIRI; CASTAGLIOLA, 2018).

Moreover, control charts can be classified according to their distribution as parametric or non-parametric (CHAKRABORTI; GRAHAM, 2018). A nonparametric control chart is recommended when the distributional assumptions underlying a parametric control chart are violated. In this case, the control chart's performance frequently decreases in terms of the false alarm rate and its ability to detect a shift (BOONE; CHAKRABORTI, 2012).

Nonparametric control charts were developed for Shewhart-type, CUSUM-type, and EWMA-type, among others (CHAKRABORTI; GRAHAM, 2019).

2.3. CONSIDERATIONS FOR CONTROL CHARTS' PRACTICAL APPLICATION

Determining the control limits, the sample size, and the sampling frequency are among the most critical tasks in designing a control chart. Larger samples can help detect smaller shifts but are more costly and time-consuming, whereas smaller samples can be sufficient if the expected shift is large. In practice, 20 to 30 samples of size 5 are often used for variables charts. Also, data collection frequency will be impacted by conditions like time, costs, and expected shifts. Typically, to take smaller samples at shorter time intervals or larger samples at longer time intervals is preferable (CHAKRABORTI; GRAHAM, 2018).

Another factor that affects the amount of data collected is whether or not the process parameters are known. A fundamental premise for developing control charts is that the process parameters are known or estimated. When the parameters are known or specified, this is referred as the parameters known case or "Case K", and when parameters are unknown and need to be estimated, this is referred as the parameters unknown case or "Case U". (MCCRACKEN; CHAKRABORTI, 2013).

In practice, we rarely know the process parameters. In this case, estimating them from a Phase I data set is necessary, but the effect of parameter estimation on control chart properties should not be ignored (PATINO-RODRIGUEZ; PÉREZ; MANCO, 2021; TANG *et al.*, 2019). Several estimators can be used, the overall sample mean is the typical estimator for location, and the sample standard deviation and average range are common estimators for dispersion.

As Jensen *et al.* (2006) pointed out, when sufficient data are not available in Phase I, the resulting charts will often signal more frequently when the process is in control and have a reduced ability to detect process changes. To ensure adequate Phase II performance, many studies on different control charts recommend a number of Phase I samples much larger than previously suggested in the literature (CHENG; SUN; GUO, 2018; EPPRECHT; LOUREIRO; CHAKRABORTI, 2015; GHASEMI ESHKAFTAKI; ZEINAL HAMADANI; AHMADI YAZDI, 2021; MEIRA; OPRIME; MERGULHÃO, 2022).

Regardless of the control chart type, and whether the parameters are known or estimated, two main errors can occur in its analysis: the Type I error (α), when the process is in-control and the control chart signals the presence of an assignable cause, and the Type II error (β), when the process is out-of-control and the control chart cannot detect this status (AMIRI; MOSLEMI; DOROUDYAN, 2015; RAMLIE *et al.*, 2021).

In statistical design, the design variables, such as the sample size (n) and the width of control limits (k) are selected in such a way that the two statistical errors, Type I and Type II, are kept at minimum values (GANGULY, 2016; GHAFFAR; ALI; AHMED, 2021). In practical terms, if it is costly to produce a large number of nonconforming units, Type II error should be minimized. On the other hand, if it is more costly to stop the process for investigation, then Type I error should be minimized.

The sooner the control chart signals, the fewer nonconforming items would be manufactured. So, it is necessary to evaluate the performance of control charts in terms of identifying these signals. Several performance measures have been applied to evaluate the statistical properties of control charts. The most common method is to examine the control chart performance by evaluating its run length properties such as the average run length (ARL), the standard deviation run length (SDRL) or quantile-type metrics like median run length (MRL) (PERDIKIS *et al.*, 2021).

The run length is defined as the number of points plotted before a signaling event. A false alarm occurs when the process is declared out-of-control when, in fact, it is not, so the probability of a false alarm is referred to as the false alarm rate. ARL_0 measures the average time between false alarms when the process is in control, and ARL_1 measures the average time between alarms when the process is out-of-control. If the sample size varies from sample to sample, it is also important to evaluate control chart performance in terms of average sample size (ASS). If the process is out-of-control, the average sample size is called ASS_0, and if the process is out-of-control, the average sample size is called ASS_1. The control chart is better than the competitors if the ARL_1 (ASS_1) is smaller, considering the same shift, and the same ARL_0 and ASS_0 values for all control charts (CASTAGLIOLA; OPRIME; KHOO, 2017; MONTGOMERY, 2013).

When parameter estimators are used, one can refer to the unconditional run-length distribution, obtained by averaging its distributions for a given set of estimators over these estimators' distribution. The run-length distribution for a given set of estimators is called the conditional distribution. While the unconditional run-length properties are fixed and define

the control charts' average performance, the conditional run-length properties vary based on the values of the parameter estimators for a reference sample. As the conditional ARL shows the impact of parameter estimation based on the value of the estimator that the users have for their particular situation, it facilitates the practical evaluation of the control chart (CHAKRABORTI; GRAHAM, 2018; JARDIM; CHAKRABORTI; EPPRECHT, 2019).

Although ARL is the metric commonly used, an interpretation based on ARL alone could be misleading in evaluating the control charts' performance. Once the distribution of run length is geometric, run lengths' standard deviation is quite large, and the geometric distribution is very skewed. Thus, the mean of the distribution is not necessarily a very typical value of the run length (MONTGOMERY, 2013). Yeong *et al.* (2021) highlighted that for small shift sizes, the median is smaller than the mean, so more than fifty percent of the time, the false alarm will happen before what is indicated by the ARL_0. In this case, practitioners' confidence in the ARL_0 as a performance metric would be lowered. In this sense, some authors, such as Rozi *et al.* (2021), Teoh *et al.* (2014) and Yeong *et al.* (2021), recommend using the MRL as an alternative once it is less affected by the run length distribution skewness.

Another concern regarding the practical application of control charts is the distribution of monitored data. Many of the control charts proposed in the literature are developed considering the normality of the data due to its well-established theory. The control charting structures based on normality, or some other well-known distributional model, may be very efficient but not of high practical significance in many cases. In practice, not always the data distribution is known. When the data depart from normality, the performance of the many parametric control charts degrades considerably. When it happens, the need for non-parametric techniques emerges, such as distribution-free control charts, which are not dependent on the assumptions about the parent distribution (MABUDE; MALELA-MAJIKA; SHONGWE, 2020; RIAZ, 2015).

Finally, another practical consideration is that, in many applications, the monitored data are not accurate. A portion of error due to the measurement system used in data collection will always be present. Recent articles, such as those in the literature review developed by Maleki, Amiri, and Castagliola (2017), show that the presence of measurement errors degrade control charts' performance. As a result, assertiveness in decision-making is reduced in cases where the effects of measurement errors are neglected.

2.4. MEASUREMENT ERROR FUNDAMENTALS

The International Vocabulary of Metrology (VIM) defines measurement error as the measured quantity value minus a reference quantity value, and measurement uncertainty as the non-negative parameter characterizing the dispersion of the quantity values being attributed to a measurand, based on the information used (BIPM, 2012). Although these terms are not always applied correctly, their distinction is essential. Even when all error components are studied and their corrections are applied, uncertainty remains on the final measurement value, generating doubt on how well this result represents the quantity measured (HACK; TEN CATEN, 2012).

The Error Approach's objective is to estimate the true value that is as close as possible to that single true value. The deviation from the true value is composed of random and systematic errors. Systematic error is the component of measurement error that remains constant or varies predictably in replicate measurements. In contrast, random measurement error is the measurement error component that in replicate measurements varies unpredictably (BIPM, 2012). Random contributions and systematic errors tend to modify the quality characteristic value in two distinct ways. Random contributions increase the variance of the measured parameter but do not affect its mean value, while systematic errors displace the original data without altering the inherent variability of the process (MACII; CARBONE; PETRI, 2003).

A wide range of factors contributes to the presence of measurement errors. The main contributors are the metrological system characteristics, inspection method, imported uncertainties, operator skill, sampling concerns, and environmental conditions. Inaccurate and imprecise measurement can seriously decrease quality-oriented company profits because it affects process variability, leading to possible additional management costs. Consequently, the effect of measurement errors and uncertainty on process control techniques needs to be carefully investigated (SMITH, 2016).

Even though most statistical process monitoring research assumes that the measurements are accurate, this is a rare phenomenon in practice. The measurement errors can reduce monitoring schemes' performance in detecting out-of-control situations and increase the rate of false alarms. Even so, few studies have attempted to present remedial approaches to compensate for the effect of measurement errors (ANIS, 2008; MALEKI; AMIRI; CASTAGLIOLA, 2017). When measurement error is considered in the statistical

process monitoring literature, the prevailing measurement error model used is the additive model, shown in Equation 34.

$$Y = A + BX + \varepsilon$$

where X is the true value of the quality characteristic, ε is a random error term for measurement imprecision. A and B are two constants that are fixed, and Y is the observed result of some measurement operation. It is typically assumed for this model that Y follows a normal distribution with mean μ, and variance σ^2. The variance is partitioned into components corresponding to the variability in the quality characteristic and the error present. These components are usually denoted as $\sigma^2{}_p$ and $\sigma^2{}_m$, respectively.

The relationship between the actual and the observed values of the sampled units can also be expressed as a multiplicative model $Y = X\varepsilon$, where ε is an independent random variable with a mean value equal to 1 and a given variance. A recent consideration of the measurement error, named TCME model, is presented in the form of a two-component measurement error:

$$Y = A + BXe^{\eta} + \varepsilon$$

where A and B are the intercept and slope constants, ε and η are additive and multiplicative random disturbances, respectively, which are independently normally distributed variables with mean equal to zero and a given variance.

Additionally, Li and Huang (2009) presented a complete consideration of measurement errors in the form of a four-component measurement error model:

$$Y_j = b_j + s_j X_j + c_j{}^T V_j + \varepsilon_j$$

This model contains four types of measurement errors in a multivariate case with p correlated variables $\{X_1, \ldots, X_p\}$. Where b_j is the measurement error caused by sensor setup/calibration bias or drift when sensors are used in harsh environments; s_j is the

measurement sensitivity; c_j represents the relationship between observed and actual quantities, which also depends on the other variables (V_j), where $V_j \in \{X_1, \dots, X_p\}$ but $V_j \notin X_j$; and $\varepsilon_j \sim N(0, var(\varepsilon_j))$ denotes the sensor noise, the precision of the sensor is reflected by $var(\varepsilon_j)$.

In all these models, the error term is considered an independent random variable with a given variance. This variance can be assumed to be a constant value, namely $\sigma_\varepsilon{}^2$ or a linearly increasing variance. In this last case, ε is assumed to be a normally distributed variable with mean equal to zero and variance $C + D\mu_X$, where C and D are two other constants that are fixed. Hence, $Y \sim N(A + B\mu_X, B^2\sigma^2{}_X + C + D\mu_X)$.

2.5. SOME PREVIOUS WORKS ON THE EFFECT OF MEASUREMENT ERROR ON CONTROL CHARTS FOR PROCESS VARIABILITY MONITORING

In one of the first studies on the subject, Kanazuka (1986) evaluates the effect of measurement error on the $\bar{X}/R$ control chart for the case where the mean and variance change. They consider the additive error model and five measurement error values for seven mean shifts and three different variance shifts. They found that the $\bar{X}/R$ chart has a higher detecting power than when the charts are used separately. Also, the larger the measurement error, the smaller the detecting power. So, they suggest a large sample size to avoid this problem.

Mittag and Stemann (1998) also consider the additive measurement error model and use the control chart to monitor process location and spread simultaneously. They found that if the measurement error is present while the chart is set up, its sensitivity concerning process disturbances is reduced. In the case of the subsequent occurrence of measurement error, the specified upper bound for the false alarm probability could be lowered. So, they suggested ensuring gauge precision before and while applying any control chart.

Linna and Woodall (2001) considered the effect of measurement error on the performance of the S^2 chart using the additive measurement error model with a linear covariate between the observed value and the true one. They define the ratio η for σ_m^2 and B^2, where σ_m^2 represents the variability in the measurement system's error, and B is a constant of the linear covariates model. The chart with the lowest η value has the greatest power for detecting process variance shifts. Also, Shore (2004) developed equations for the S^2 chart that

prescribed allowable measurement error bias and standard deviation and investigated how to specify measurement error requirements to achieve desirable control chart performance.

Riaz (2014) investigated how the measurement error in Phase I for the S^2 chart influenced Phase II run length performance. He assumed a measurement error in Phase I and no measurement error in Phase II. They found that due to measurement error, the control limits expand and reduce the control chart detection ability. For a fixed value of shift, the ARL increases with the increase of the measurement error, and it is difficult to detect a particular shift magnitude.

Maleki, Maleki, and Dizabadi (2016) investigated the effect of measurement error on detecting and diagnosing the performance of the Maximum Exponentially Weighted Moving Average and Mean Squared Deviation (Max-EWMAMS) control chart in Phase II for simultaneous monitoring of the process mean and variability. They found that measurement errors can adversely affect the detecting performance while the effect on diagnosing performance is negligible for the Max-EWMAMS chart. Also, Javaid, Noor-Ul-Amin, and Hanif (2020) and Saemian, Maleki, and Salmasnia (2023) investigated the effect of measurement error on Max-EMWA and Max-HEWMAMS control charts, respectively, for simultaneous monitoring process mean and variability. They applied the covariate model and then the same model with multiple measurements to reduce the effects of measurement error.

Sabahno, Castagliola, and Amiri (2020) evaluated the effect of measurement errors on an adaptive multivariate control chart for simultaneous monitoring of the process mean and variability with measurement errors. They concluded that as the measurement errors increase, the chart performance worsens in terms of all the performance measures. They suggested that researchers may evaluate the effect of parameter estimation on the proposed chart's performance for future studies.

Thanwane *et al.* (2021a, 2021b) extended the study of the effect of measurement error on the HWMA monitoring scheme with estimated parameters by investigating its sensitivity through simulation and incorporating Fast Initial Response (FIR) features. They found that the FIR features improve the chart performance compared to the standard no FIR feature scheme.

Yang, Chen, and Lin (2023) proposed an approach to correct measurement error effects for monitoring process dispersion by applying the dispersion statistic of the sign chart to transform continuous random variables into discrete ones. They develop an exponentially weight-moving average variance control chart with measurement error correction to eliminate

error effects and provide more reliable control limits for monitoring process dispersion. They validated the development through a numerical example and found that the proposed control chart effectively handles moderate and large levels of measurement error.

3. SYSTEMATIC LITERATURE REVIEW ON DOUBLE SAMPLING CONTROL CHARTS

This chapter presents a systematic literature review on Double Sampling control charts. It presents a descriptive analysis of the articles reviewed and the previous works on the effect of measurement error on Double Sampling control charts.

3.1. DOUBLE SAMPLING CONTROL CHARTS

Double sampling schemes, proposed by Dodge and Romig (1929), are intended to be simple and cost-effective to use. The main goal of double sampling is to reduce, on average, the number of observations needed to make a decision. This scheme is particularly important in experiments involving an expensive inspection or a considerable waiting time between observations or inspections (BAR-LEV; BOUKAL, 2000).

Based on Double Sampling scheme, Croasdale (1974) proposed a monitoring procedure named Double Sampling (DS) $\bar{X}$ chart to offer better statistical efficiency in terms of the average run length than the Shewhart traditional chart. Two separate samples were used to create Croasdale's DS chart.

Later, Daudin (1992) modified the Croasdale's proposed chart by connecting the first and the second sample at the second stage. The procedure shown below is used for building the DS $\bar{X}$ chart. Figure 3 shows the DS control chart structure. This procedure can be extended to other control charts, such as the range, standard deviation, and variance control charts.

1) First, take a sample of size n_1 and compute the sample mean $\bar{X}_1$;
2) If $\bar{X}_1$ falls within the two interior limits of the stage one chart (-L1 and L1) the process is considered in-control;
3) If $\bar{X}_1$ falls outside the two outer limits of the stage one chart (-L2 and L2) the process is considered out-of-control;
4) If $\bar{X}_1$ falls between the limits -L1 and -L2 or between L1 and L2, a new sample of size n_2 is collected and the sample mean $\bar{X}_2$ is computed;

5) If $\bar{X}_2$ falls within the limits of stage two chart (-L3 and L3) the process is considered in-control, otherwise the process is considered out-of-control, and some action must be taken to investigate the special cause.

Figure 3 – Double sampling control chart structure
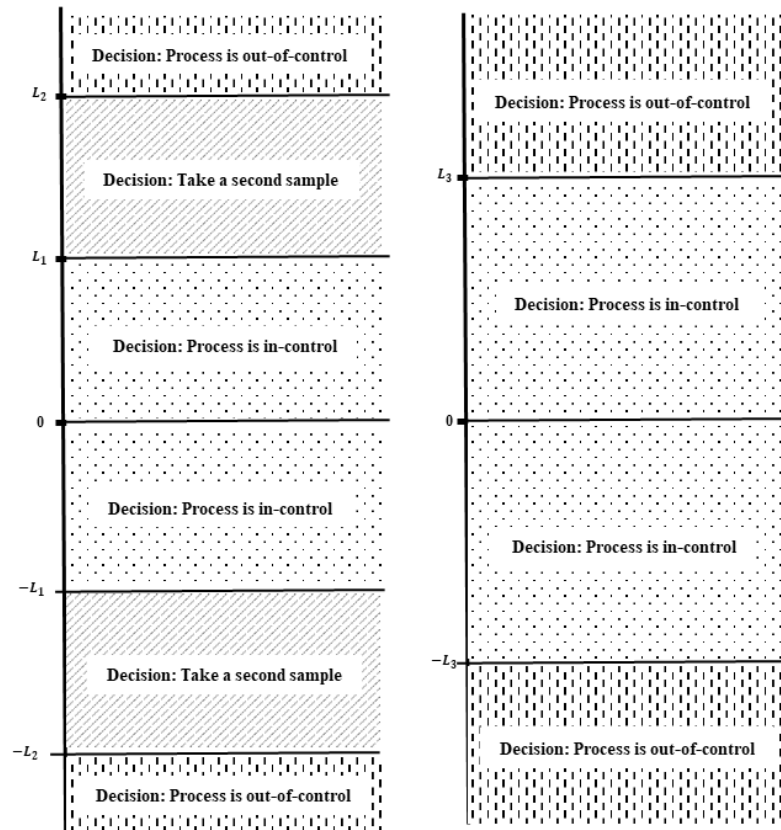
Recent researches has shown that using the double sampling scheme strategy in designing control charts improves their detection ability without increasing the sample size (SALMASNIA; MALEKI; MIRZAEI, 2023). Considering this, an SLR of studies on Double Sampling control charts is proposed and aims to answer the following research questions:

- How many studies on Double Sampling control charts have been proposed over the years? What are the characteristics of these studies?

- What types of Double Sampling control charts were studied?

- Which studies on Double Sampling control charts have considered the effects of measurement errors?

3.2. REVIEW METHODOLOGY

Systematic literature review (SLR) is a method for finding, evaluating, and synthesizing all available research relevant to a specific research question, topic, or phenomenon of interest. Is a reliable method to gain clear, accurate, and unbiased information on a research topic (VAN DINTER; TEKINERDOGAN; CATAL, 2021). The aim of an SLR is to systematically analyze existing literature to answer one or more research questions (HINDERKS *et al.*, 2020).

The PRISMA statement is used to operationalize the research (LIBERATI *et al.*, 2009). Using checklists like PRISMA enable improvement in the reporting quality and provides substantial transparency in the selection process of papers in a systematic review (KNOBLOCH; YOON; VOGT, 2011). The proposed research methodology framework is shown in Figure 4.

Figure 4 – Literature search overview
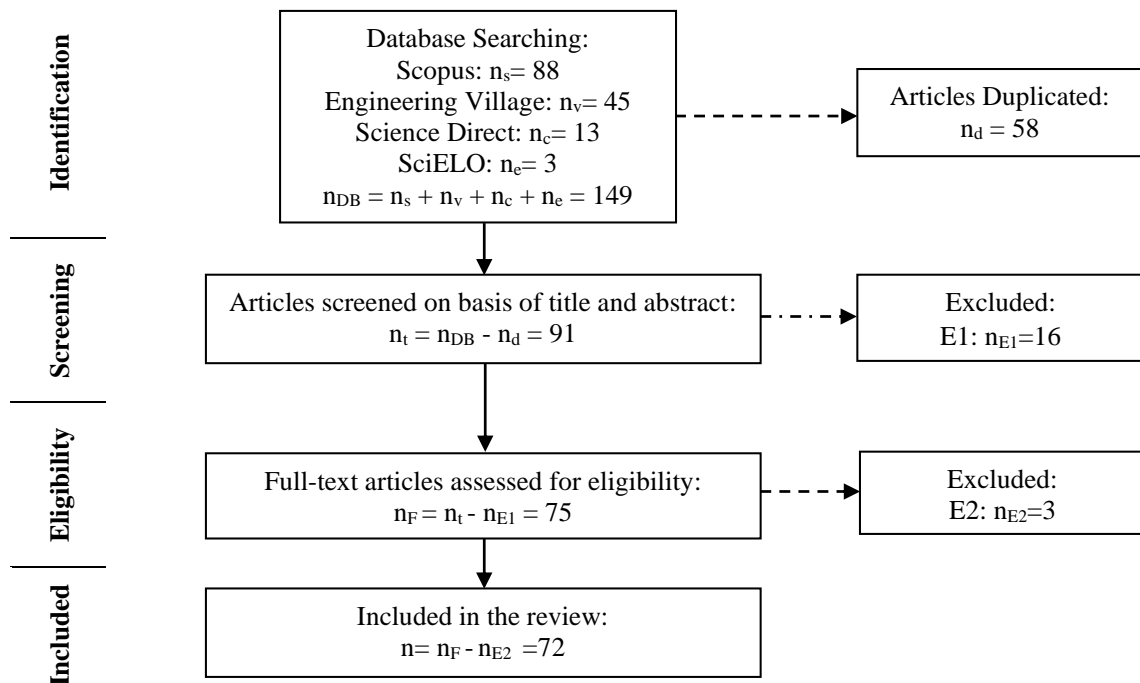
The identification phase includes the initial search in the selected databases. Scopus, Engineering Village, Science Direct and SciELO databases were considered in the search. Articles published in Journals in English and Portuguese were considered. There was no time

restriction for the search, the searches were updated until March 2023. The relevant papers are gathered via computerized search using the query strings including the terms "double sampling" and "control chart". The software StArt (FABBRI *et al.*, 2016) was used to remove duplicate articles.

In the screening the articles were filtered based on their titles and abstracts, 16 articles were excluded in this phase. In the Eligibility phase, a preliminary analysis of the articles was carried out to ensure that they were qualified for this SLR, using as an exclusion criterion the lack of adherence to the theme, for example, when dealing with double sampling but not specifically for the study of control charts. After the screening and eligibility phases, 72 articles were included for full-text review.

3.3. DESCRIPTIVE ANALYSIS

In order to analyze the relevance of the topic, the number of articles published on Double Sampling control charts over the years was analyzed. The Figure 5 shows the number of publications found in the search. The first study on the subject dates back to 1974. It can be seen from the analysis that the number of studies on the subject has been growing in the last decade. The year with the most publications was 2017, with ten publications. Considering that this review considered only the beginning of 2023, this number can be surpassed.

Figure 5 – Number of publications over time
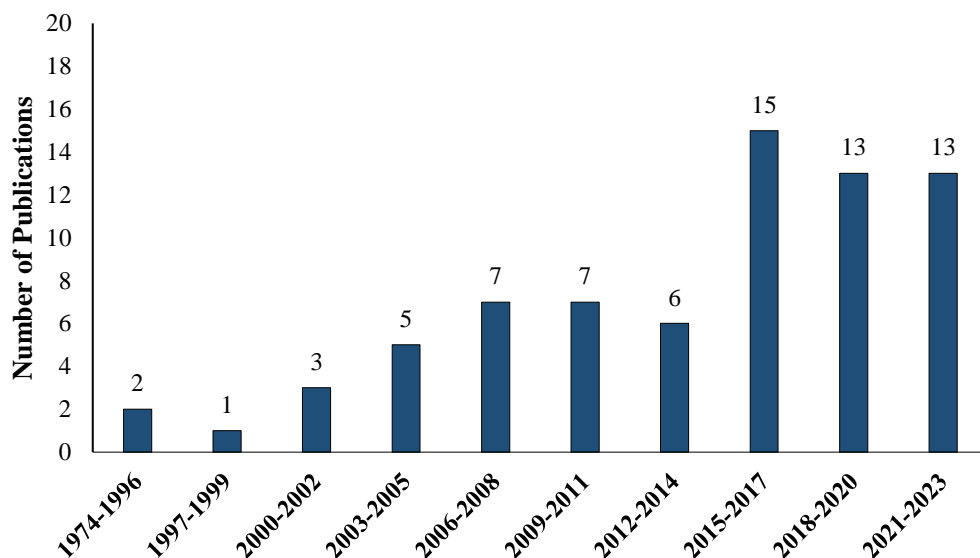
Figure 6 shows the participation of authors in publications. It is observed that there is a relevant collaboration between authors who study the subject, as several of them collaborated in three or more publications. The author with the highest number of participations is Michael Khoo Boon Chong, professor at the School of Mathematical Sciences, Universiti Sains Malaysia, with 17 participations in articles on the subject.

Figure 6 – Participations in articles per author
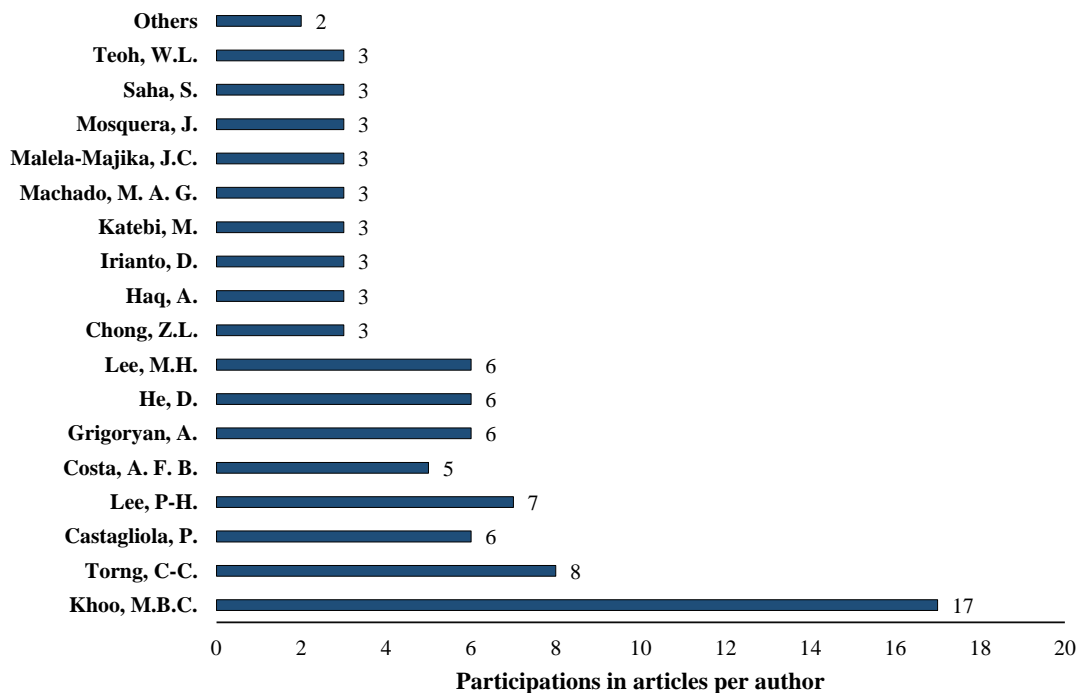
Research on control charts also proved to be relevant across different countries. Figure 7 shows the geographical distribution of the articles considering the place of work of the first author of each article. It is observed that there is a distribution of places of action across different continents. The country with the highest number of publications was Malaysia, with 21 publications, followed by the United States with 9 publications, Taiwan with 8, and Brazil and Iran with 6.

The Double Sampling scheme has been incorporated into many types of control charts. Figure 8 shows the most studied DS control charts, with three articles or more representing 49 of the 72 articles. The remaining 23 articles deal with control charts with two publications or fewer. Among the most studied types, the DS control chart based on the traditional Shewhart chart stands out, representing 49% of the articles with more than three

publications, followed by DS charts based on variable sampling interval (VSI-type) charts with 21%.

Figure 7 – Geographical distribution of the publications
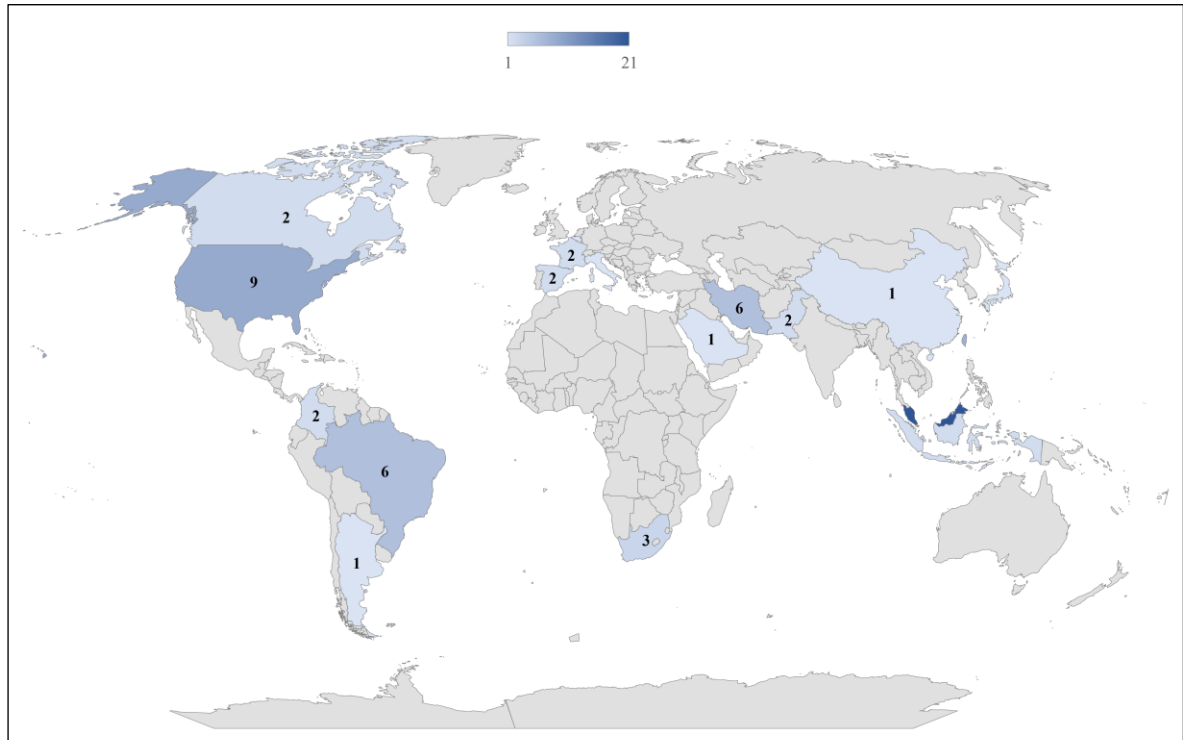
Figure 8 – Percentage of articles per DS chart type
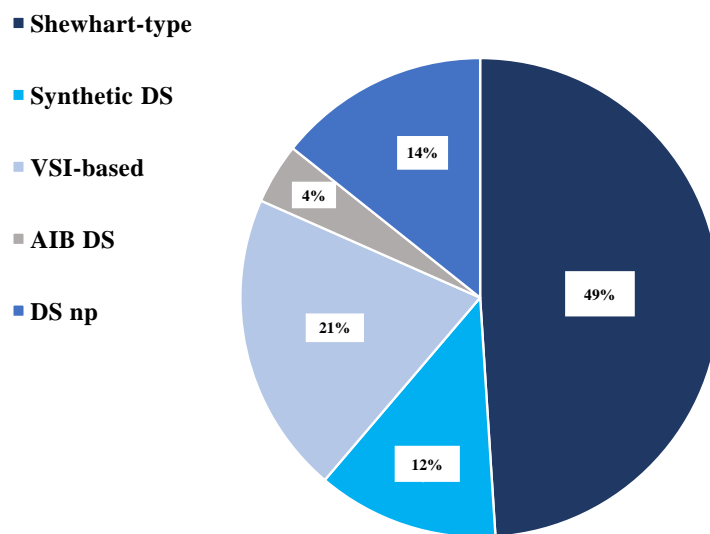
Regarding the sources of publications, it is noted that a wide variety of journals include publications on Double Sampling control charts. Table 2 shows the frequency of

publication in each journal. It is observed that the journals in which there is a higher frequency of publication are Quality and Reliability Engineering International, with 9 publications on the subject, and Communications in Statistics - Simulation and Computation and Communications in Statistics - Theory and Methods, with 7 articles each.

Table 2 – Publication Source

Journal	Frequency
Quality and Reliability Engineering International	9
Communications in Statistics - Simulation and Computation	7
Communications in Statistics - Theory and Methods	7
International Journal of Production Research	6
International Journal of Production Economics	5
Journal of Applied Statistics	3
Journal of Statistical Computation and Simulation	3
Computers & Industrial Engineering	2
European Journal of Industrial Engineering	2
Mathematics	2
International Journal of Industrial Engineering	1
Compusoft	1
European Journal of Operational Research	1
Expert Systems with Applications	1
Frontiers in Applied Mathematics and Statistics	1
IEEE Access	1
IIE Transactions	1
International Journal for Quality Research	1
International Journal of Advanced Manufacturing Technology	1
International Journal of Applied Engineering Research	1
International Journal of Difference Equations	1
International Journal of Pure and Applied Mathematics	1
Journal of Quality Technology	1
Journal of Engineering and Technological Sciences	1
Journal of Industrial and Production Engineering	1
Journal of Industrial Integration and Management	1
Journal of Probability and Statistics	1
Journal of Testing and Evaluation	1
Pesquisa Operacional	1
Quality Engineering	1
South African Journal of Industrial Engineering	1
Stat	1
Statistical Methodology	1
Stochastics and Quality Control	1
The International Journal of Advanced Manufacturing Technology	1
Transactions of the Institute of Measurement and Control	1

Table 3 shows the references per type of DS control chart. The main objectives of Table 3 are to highlight the number of studies per DS control chart, the variety of DS control charts studied, and the studies that were dedicated to investigating the effects of measurement errors and on what types of DS control charts this effect was investigated. In the first column of Table 3, we have the type of control chart/technique on which the DS chart is based. In the second column, we have the articles referring to the study of the respective control chart. In the third column, we have the studies found that investigate the effects of errors of measurement in this type of DS control chart.

Regarding the DS control chart type, we have the following: Double Sampling $\bar{X}$ chart (DS $\bar{X}$) for the process mean monitoring; Double Sampling S chart (DS S) for the standard-deviation monitoring; Double Sampling S^2 chart (DS S^2) for the variance monitoring; Double Sampling R chart (DS R) for the range monitoring; Double Sampling control chart for the joint monitoring of the process mean and standard-deviation (DS $\bar{X}$ and S); Double Sampling control chart based on the exponentially weighted moving average chart (DS EWMA); Double Sampling control chart for attribute monitoring (DS np and DS c); Double sampling chart based on Hotelling's T² chart (DS T²); Double Sampling control chart based on the sample generalized variance (DS $|S|$); Double Sampling chart based on variable sampling interval (DS VSI-based); Double Sampling control chart based on multivariate multiple sampling (MMS); Double Sampling control charts for bivariate processes (BDS); Double Sampling control chart for monitoring the slope of linear profiles under (DS $\hat{B}_1$); Auxiliary information based DS control chart (AIB DS); Side-sensitive modified group runs double sampling (SSMGRDS); Gauge-based Double Sampling control chart (wYSYL–DS); Double sampling control chart based on process capability index C_{pm} (DS C_{pm}); Distribution-free Double Sampling control chart (Nonparametric DS); Double sampling control chart for Coefficient of variation monitoring (DS CV); Double sampling attribute control chart for monitoring processes characterized by classifying the product characteristic into three discrete levels (DS three-level); Double Sampling Adaptive Thresholding LASSO (DSATL); and the Double Sampling chart based on the synthetic chart (Synthetic DS), which integrates the $\bar{X}$ and Conforming Run Length (CRL) charts.

Table 3 – Articles per DS control chart type

Control charts	Articles that do not consider measurement error	Articles that consider measurement error
DS $\bar{X}$-based	Croasdale (1974), Daudin (1992), Irianto and Shinozaki (1998), He, Grigoryan, and Sigh (2002), Hsu (2004), Claro, Costa, and Machado (2008), Costa and Claro (2008), Torng and Lee (2009a, 2009b), Torng et al. (2009), Irianto and Juliani (2010), Teoh et al. (2015, 2016), Iziy, Gildeh, and Monabbati (2017), Malela-majika, Motsepa, and Graham (2021), Khired, Aslam, and Dobbah (2021)	Lee et al. (2019), Khee Yong Si et al. (2021), Maleki et al. (2023)
DS S	He and Grigoryan (2002, 2003), Hsu (2007), Lee and Khoo (2018a)	-
DS S^2	Khoo (2004), Castagliola, Oprime, and Khoo (2017)	-
DS R	Costa (2017)	-
DS $\bar{X}$ and S	He and Grigoryan (2006)	-
DS EWMA	Yang and Wu (2017a, 2017b)	-
DS np	De Araújo Rodrigues, Epprecht, and De Magalhães (2011), Chong, Khoo, and Castagliola (2014), Zhou et al. (2017), Chong et al. (2017), Muñoz, Campuzano, and Mosquera (2022), Tuh et al. (2022, 2023)	-
DS c	Inghilleri, Lupo, and Passannanti (2015), Campuzano, Carrión, and Mosquera (2019)	-
DS T²	Champ and Aparisi (2008), Faraz, Heuchenne, and Saniga (2012)	-
DS $|S|$	Grigoryan and He (2005), Lee and Khoo (2018b)	-
DS VSI-based	Carot, Jabaloyes, and Carot (2002), Torng, Tseng, and Lee (2010), Lee, Chang, Torng (2012), Lee, Torng, Liao (2012), Torng, Chung, and Chen (2014), Noorossana, Shekary, and Deheshvar (2015), Joekes, Smrekar, and Barbosa (2015), Lee and Khoo (2017a), Katebi and Khoo (2021), Katebi and Moghadam (2022)	-
MMS	He and Grigoryan (2005)	-
BDS	Costa and Machado (2008), Machado and Costa (2008)	-
DS $\hat{B}_1$	Eizi, Sadeghpour Gildeh, and Ehsan Monabbati (2020)	-
AIB DS	Haq and Khoo (2018, 2019), Umar et al. (2020)	-
SSMGRDS	Saha et al. (2018)	-
wYSYL–DS	Mosquera and Aparisi (2020)	-
DS C_{pm}	Tomohiro, Arizono, and Takemoto (2020)	-
Nonparametric DS	Malela-Majika et al. (2021)	-
DS CV	Lee et al. (2021)	-
DS three-level	Katebi and Rahim (2022)	-
DSATL	Salmasnia, Maleki, and Mirzaei (2023)	-
Synthetic DS	Khoo et al. (2011, 2013a), Lee and Khoo (2017b), Woon (2017), You (2018), Malela-Majika and Rapoo (2019)	-

As can be seen from Table 3, only three articles have been focused on studying the effects of measurement errors on Double Sampling control charts, and all three have studied only the Double Sampling $\bar{X}$ control chart. Due to the focus of this Thesis, the synthesis of the articles made in this chapter deals only with the articles developed on the effect of measurement error on Double Sampling control charts. For more details on the other studies, the reader can refer to the articles cited above and to the review on DS control charts developed by Motsepa *et al.* (2021).

3.4. DS CONTROL CHARTS IN THE PRESENCE OF MEASUREMENT ERROR

Since most process monitoring techniques are based on collecting and analyzing measurements from the studied process, and some amount of error will always be present in the measurements, several researchers have focused on studying the impact of measurement errors on control charts' performance (MALEKI; AMIRI; CASTAGLIOLA, 2017).

Lee *et al.* (2019) investigated the effect of measurement error ratio, the effect of the B coefficient in the linear covariate error model, and the effect of multiple measurements on the performance of the DS $\bar{X}$ chart. For the performance comparison, they consider that the control charts have the same in-control performance (i.e., $ARL_0 = 370$ and $n = 5$ or 10) and the control chart with the smaller out-of-control average run length (ARL_1) performs better. They compared the ARL_1 in terms of different measurement error ratios $\gamma^2 = 0$, 0.1, 0.5, and 1. Where γ^2 is the ratio between the variance corresponding to the portion of error present in the measurement and the variance corresponding to the variability in the quality characteristic. By comparing the performance results, they found that the ARL_1 values without considering the measurement errors are smaller than those with measurement errors and that the DS $\bar{X}$ control chart performs better with the smaller measurement error ratio. They also find that the negative effect of measurement errors on the performance of the DS $\bar{X}$ control chart decreases with the increase of the value in B and the value of with the increase in the number of samples. They finished the study with an illustrative example of a solar wafer manufacturing process, with the quality characteristic being maximum open-circuit voltage. This illustrative example showed that the out-of-control signal is detected for the case without measurement errors. In contrast, there is no out-of-control signal when measurement errors exist. Thus, they stated that in the presence of measurement errors, the DS $\bar{X}$ chart is slower in detecting shifts in the process mean than the case without measurement errors.

Khee Yong Si *et al.* (2021) investigate the economic design of the DS $\bar{X}$ chart with measurement errors by using the linear covariate error model. The optimal design parameters are proposed through the minimization of the cost function. They concluded that the measurement error ratio and coefficient *B* in the linear covariate error model affect the sampling interval, the number of multiple measurements per item, the in-control average run length, and the expected cost per hour. They suggested that the negative effect of measurement errors can be economically reduced (i.e., the lower expected cost per hour) by a smaller measurement error ratio value or a larger *B* value.

Maleki *et al.* (2023) investigated the effect of measurement errors on the performance of the DS $\bar{X}$ chart, with both constant and linearly increasing variance. They compared the performance of the DS $\bar{X}$ chart and the classical $\bar{X}$ chart regarding average run length (ARL) and standard deviation of run length (SDRL). They assumed that the measurement error component is a normal variable $N(0, \sigma_\varepsilon^2)$. For the performance evaluation, they select three values for the variance of the error component, $\sigma_\varepsilon^2 = 0.1$, 0.2, and 0.3. The control limits were selected such that $ARL_0 = 370$. The magnitude of mean shift was considered as $\delta \in \{0, 0.25, 0.5, 0.75, 1, 1.5\}$, and the out-of-control average run length (ARL_1) values were computed based on 25000 simulations. As a result, they found that the DS $\bar{X}$ chart outperforms the classical one in all out-of-control scenarios. They also stated that taking several measurements on each item can effectively reduce the undesired impact of the error on the chart's performance. For future studies, they suggested simultaneous monitoring of the process mean and variability in the presence of measurement errors using the double sampling strategy.

3.5. REVIEW FINAL CONSIDERATIONS

The present review systematically collects studies on double sampling control charts. Its main aim is to assess the current state of the research topic and possible opportunities for future studies. From a total of 149 articles, 72 were selected by following the PRISMA methodology. The articles' analysis allowed the identification of the control charts employed in each case and the frequency of publications on each chart.

As a result, the study contributes to the knowledge of the double sampling control chart scheme. The outcomes showed that there are still many opportunities to study the application of double sampling control charts since most of the articles focused on the

applying traditional control charts, such as Shewhart-based charts, and most consider that the data monitored is accurate. The articles on the effect of measurement errors on the DS charts were only carried out to monitor the process mean. Therefore, further studies are needed to investigate the effect of the errors on other control charts, such as the range, standard-deviation, and variance monitoring.

The review's main limitations are that it only considers articles written in Portuguese and English that are also indexed in Scopus, Engineering Village, SciELO, and Science Direct databases. A study covering other languages and other databases is encouraged.

4. DS S² CONTROL CHART DESIGN

As far as we know and based on the literature review presented, no studies investigate the effects of measurement errors on the Double Sampling S² control chart. This chapter presents the Double Sampling S^2 control chart in the presence of measurement error.

4.1. DOUBLE SAMPLING S² CHART WITH MEASUREMENT ERROR

Assume that when the process is in-control the quality characteristic of interest X can be described as a normal random variable with mean μ and variance $\sigma_p{}^2$. As it is not possible to know the exact value of a measured variable, we consider the linear covariate model to express the measured values of the quality characteristic, as shown in Equation 37.

Equation 37

$$Y_{ij} = A + BX_{ij} + \varepsilon_{ij}$$

where A and B are two constant values, with $B \geq 1$, and ε_{ij} is the measurement error term which is assumed to be independent from X_{ij} and follow a normal distribution $N(0, \sigma_m{}^2)$. Y_{ij} and X_{ij} are, respectively, the observed and the true values for the jth observation of the ith sample. The measured quantity Y, is then distributed as normal with mean $A + B\mu$ and variance $B^2\sigma_p{}^2 + \sigma_m{}^2$, i.e., $Y_{ij} \sim N(A + B\mu, B^2\sigma_p{}^2 + \sigma_m{}^2)$.

Given Y as the observed value of the quality characteristic, we will demonstrate that $S_Y{}^2$ is an unbiased estimator for the variance of Y. Equation 38 and 39 show, respectively, the expected value and the variance of Y.

Equation 38

$$E[Y] = A + B\mu$$

Equation 39

$$V[Y] = B^2\sigma_p{}^2 + \sigma_m{}^2$$

Knowing that the variance for a random variable is the expected value for the squared deviations, we will use the following auxiliary results in the demonstration:

$$V[Y] = E[(Y - (A + B\mu))^2]$$

Rewriting Equation 40 considering the expected value of Y, we have:

$$V[Y] = E[Y^2] - (E[Y])^2$$

$$V[Y] = E[Y^2] - (A + B\mu)^2$$

Rearranging the terms of Equation 42:

$$E[Y^2] = V[Y] + (A + B\mu)^2$$

Substituting the variance of Y given by Equation 39, we have:

$$E[Y^2] = (B^2\sigma_p{}^2 + \sigma_m{}^2) + (A + B\mu)^2$$

Considering that the variance of the average value of Y can be written by Equations 45 and 46:

$$V[\bar{Y}] = E[\bar{Y}^2] - (E[\bar{Y}])^2$$

$$V[\bar{Y}] = E[\bar{Y}^2] - (A + B\mu)^2$$

We can find the expected value of the square of the mean value of Y as:

$$E[\bar{Y}^2] = V[\bar{Y}] + (A + B\mu)^2$$

Considering the variance of the average value of Y can also be found by:

$$V[\bar{Y}] = \frac{B^2\sigma_p{}^2 + \sigma_m{}^2}{n}$$

Substituting Equation 48 in Equation 47 we have:

$$E[\bar{Y}^2] = \frac{B^2\sigma_p{}^2 + \sigma_m{}^2}{n} + (A + B\mu)^2$$

The above considerations assist in determining the expected value for the squared deviations around the population mean (ZIBETTI, [s.d.]).

Thus,

$$E\left[\sum_{j=1}^{n}(Y_j - (A + B\mu))^2\right] = \sum_{j=1}^{n} E[(Y_j - (A + B\mu))^2]$$

$$= \sum_{j=1}^{n} E[Y_j{}^2 - 2Y_j(A + B\mu) + (A + B\mu)^2]$$

$$= \sum_{j=1}^{n} E[Y_j{}^2] - 2(A + B\mu)\sum_{j=1}^{n} E[Y_j] + \sum_{j=1}^{n} E[(A + B\mu)^2]$$

Making the substitutions considering the auxiliary results above, we have:

Equation 51

$$\sum_{j=1}^{n} E[Y_j{}^2] - 2(A + B\mu) \sum_{j=1}^{n} E[Y_j] + \sum_{j=1}^{n} E[(A + B\mu)^2]$$

$$= n\big[(B^2\sigma_p{}^2 + \sigma_m{}^2) + (A + B\mu)^2\big] - 2n(A + B\mu)^2 + n(A + B\mu)^2$$

So, we can rewrite Equation 50 as:

Equation 52

$$E\left[\sum_{j=1}^{n}(Y_j - (A + B\mu))^2\right] = n\big[(B^2\sigma_p{}^2 + \sigma_m{}^2) + (A + B\mu)^2\big] - 2n(A + B\mu)^2 + n(A + B\mu)^2$$

$$= n(B^2\sigma_p{}^2 + \sigma_m{}^2) + n(A + B\mu)^2 - 2n(A + B\mu)^2 + n(A + B\mu)^2$$

$$= n(B^2\sigma_p{}^2 + \sigma_m{}^2)$$

Dividing Equation 52 by n, we have:

Equation 53

$$E\left[\frac{\sum_{j=1}^{n}(Y_j - (A + B\mu))^2}{n}\right] = (B^2\sigma_p{}^2 + \sigma_m{}^2)$$

Using the sample mean $\bar{Y}$ as an estimator for the population mean, we have that:

Equation 54

$$\bar{Y} = \frac{\sum_{j=1}^{n} Y_j}{n} \qquad \therefore \quad \sum_{j=1}^{n} Y_j = n\bar{Y}$$

We also consider that:

Equation 55

$$E\left[\sum_{j=1}^{n}(Y_j - \bar{Y})^2\right] = \sum_{j=1}^{n} E[Y_j^2 - 2Y_j\bar{Y} + \bar{Y}^2]$$

$$= E\left[\sum_{j=1}^{n} Y_j^2 - 2\bar{Y}\sum_{j=1}^{n} Y_j + \sum_{j=1}^{n}\bar{Y}^2\right]$$

$$= E\left[\sum_{j=1}^{n} Y_j^2 - 2\bar{Y}\sum_{j=1}^{n} Y_j + n\bar{Y}^2\right]$$

$$= E\left[\sum_{j=1}^{n} Y_j^2 - 2\bar{Y}(n\bar{Y}) + n\bar{Y}^2\right]$$

$$= E\left[\sum_{j=1}^{n} Y_j^2 - n\bar{Y}^2\right]$$

Thus, we can rewrite equation 55 as:

Equation 56

$$E\left[\sum_{j=1}^{n}(Y_j - \bar{Y})^2\right] = \sum_{j=1}^{n} E[Y_j^2] - nE[\bar{Y}^2]$$

Making the substitutions in Equation 56 considering the auxiliary results shown above, we have:

Equation 57

$$E\left[\sum_{j=1}^{n}(Y_j - \bar{Y})^2\right] = n\left[(B^2\sigma_p{}^2 + \sigma_m{}^2) + (A + B\mu)^2\right] - n\left[\frac{B^2\sigma_p{}^2 + \sigma_m{}^2}{n} + (A + B\mu)^2\right]$$

$$= n(B^2\sigma_p{}^2 + \sigma_m{}^2) + n(A + B\mu)^2 - (B^2\sigma_p{}^2 + \sigma_m{}^2) - n(A + B\mu)^2$$

$$= n(B^2\sigma_p{}^2 + \sigma_m{}^2) - (B^2\sigma_p{}^2 + \sigma_m{}^2)$$

Thus, Equation 57 can be rewritten as:

$$E\left[\sum_{j=1}^{n}(Y_j - \bar{Y})^2\right] = (n-1)\left(B^2\sigma_p{}^2 + \sigma_m{}^2\right)$$

Dividing Equation 58 by $(n-1)$, we have:

$$E\left[\frac{\sum_{j=1}^{n}(Y_j - \bar{Y})^2}{(n-1)}\right] = B^2\sigma_p{}^2 + \sigma_m{}^2$$

Therefore,

$$S_Y{}^2 = \frac{\sum_{j=1}^{n}(Y_j - \bar{Y})^2}{n-1}$$

is an unbiased estimator for the variance of Y.

For the Double Sampling S^2 chart procedure, considering the measurement error, we first take a sample of size n_1 and compute the sample variance as:

$$S_{Y_1}{}^2 = \frac{\sum_{j=1}^{n_1}(Y_{1j} - \bar{Y}_1)^2}{n_1 - 1}$$

where $S_{Y_1}{}^2$ indicates that the sample variance was calculated for the observed values at the first stage (Y_{1j}) and $\bar{Y}_1$ is the sample mean of these observed values.

There are three possibilities during the first stage. The first possibility is that $S_{Y_1}^2 \leq L_1$, so the process is in-control (IC). The second possibility is that $S_{Y_1}^2 > L_2$, so the process is considered out-of-control (OOC). The third possibility is that $L_1 < S_{Y_1}^2 \leq L_2$. If it happens, a second sample of size n_2 is taken, and the sample variance is computed as:

Equation 62

$$S_{Y_2}^2 = \frac{\sum_{j=1}^{n_2}(Y_{2j} - \overline{Y}_2)^2}{n_2 - 1}$$

where $S_{Y_2}^2$ indicates that the sample variance was calculated for the observed values at the second stage (Y_{2j}) and $\overline{Y}_2$ is the sample mean for these observed values. Then, the pooled sample variance S_{Yp}^2 is computed as:

Equation 63

$$S_{Yp}^2 = \frac{(n_1 - 1)S_{Y_1}^2 + (n_2 - 1)S_{Y_2}^2}{n_1 + n_2 - 2}$$

Decisions at the second stage are based on S_{Yp}^2. There are two possibilities during the second stage. The first possibility is that $S_{Yp}^2 \leq L_3$, so the process is in-control (IC), and the second possibility is that $S_{Yp}^2 > L_3$, so the process is considered out-of-control (OOC).

Considering the presence of measurement error, it will be considered as control limits of the first stage:

Equation 64

$$L_1 = k_1(B^2\sigma_p^2 + \sigma_m^2)$$

and

Equation 65

$$L_2 = k_2(B^2\sigma_p^2 + \sigma_m^2)$$

And as control limit of the second stage, we have:

$$L_3 = k_3(B^2 \sigma_p{}^2 + \sigma_m{}^2)$$

where k_1, k_2 and k_3 are constants such that $0 < k_1 < k_2$ and $k_3 \geq 0$, and the decisions are made based on the following intervals:

- $\Omega_1 = [0, L_1]$

- $\Omega_2 = (L_1, L_2]$

- $\Omega_3 = (L_2, \infty)$

- $\Omega_4 = [0, L_3]$

- $\Omega_5 = (L_3, \infty)$

Figure 9 shows an example of the DS S^2 control chart, where we can see the decision-making areas between the control limits. In Figure 9, the stages are represented in separate charts, where the chart in Figure 9 (a) represents Stage 1, and the chart in Figure 9 (b) represents Stage 2. It can be noted that, in this example, most of the points fell within the interval Ω_1. Also, it can be observed that when a point falls in the interval Ω_2, it is automatically plotted in the interval Ω_4. This scheme continues until a point fall in the interval Ω_5, as shown in Figure 9 (b).

Plotting both stages on a single control chart may be preferred for practical use. Figure 10 shows a DS S^2 control chart with both stages represented in the same chart. In this case, the green and red lines represent the Stage 1 control limits, and the black dashed line represents the Stage 2 control limit. A black dot is plotted when a value falls between the green and red lines, representing L_1 and L_2, respectively.

In the example of Figure 9, an out-of-control value was identified in the second stage. However, in an alternative scenario, an out-of-control situation could have been found even in the first stage if the value was greater than L_2, as shown in the example of Figure 10.

Figure 9 – DS S² chart simulation example for stages in separate charts

(a)   (b)
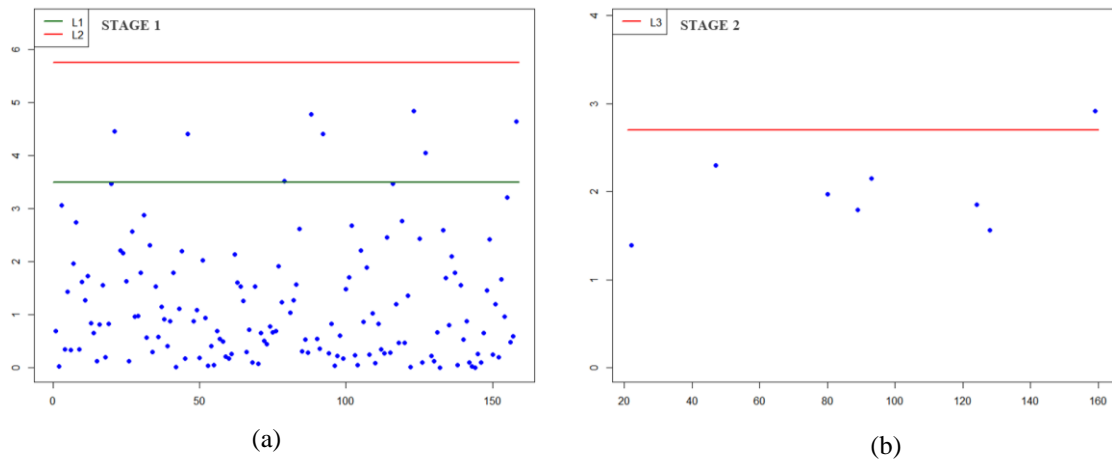
Figure 10 – DS S² chart simulation example for both stages in the same chart
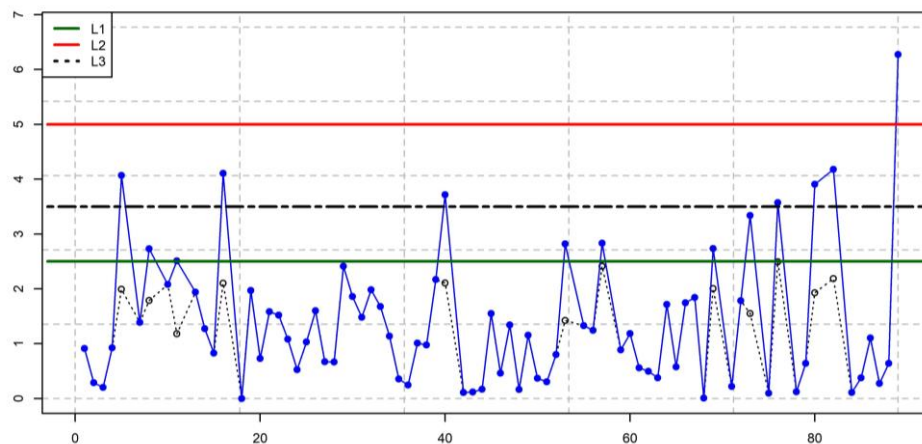
4.2. SIMULATION STUDY FOR THE DS S² CONTROL CHART IN THE PRESENCE OF MEASUREMENT ERROR

This section shows a simulation study to evaluate the effects of measurement errors on the DS S^2 control chart. The DS S^2 control chart is analyzed via the run-length distribution and the average sample size. Computational simulations were made with the statistical language programming R. Figure 11 shows the simulation flowchart.

According to Chakraborti and Graham (2019), raising the simulation size sufficiently can reduce the inaccuracy of a run-length characteristic. Table 4 shows the ARL value and time of simulation for different simulation amounts.
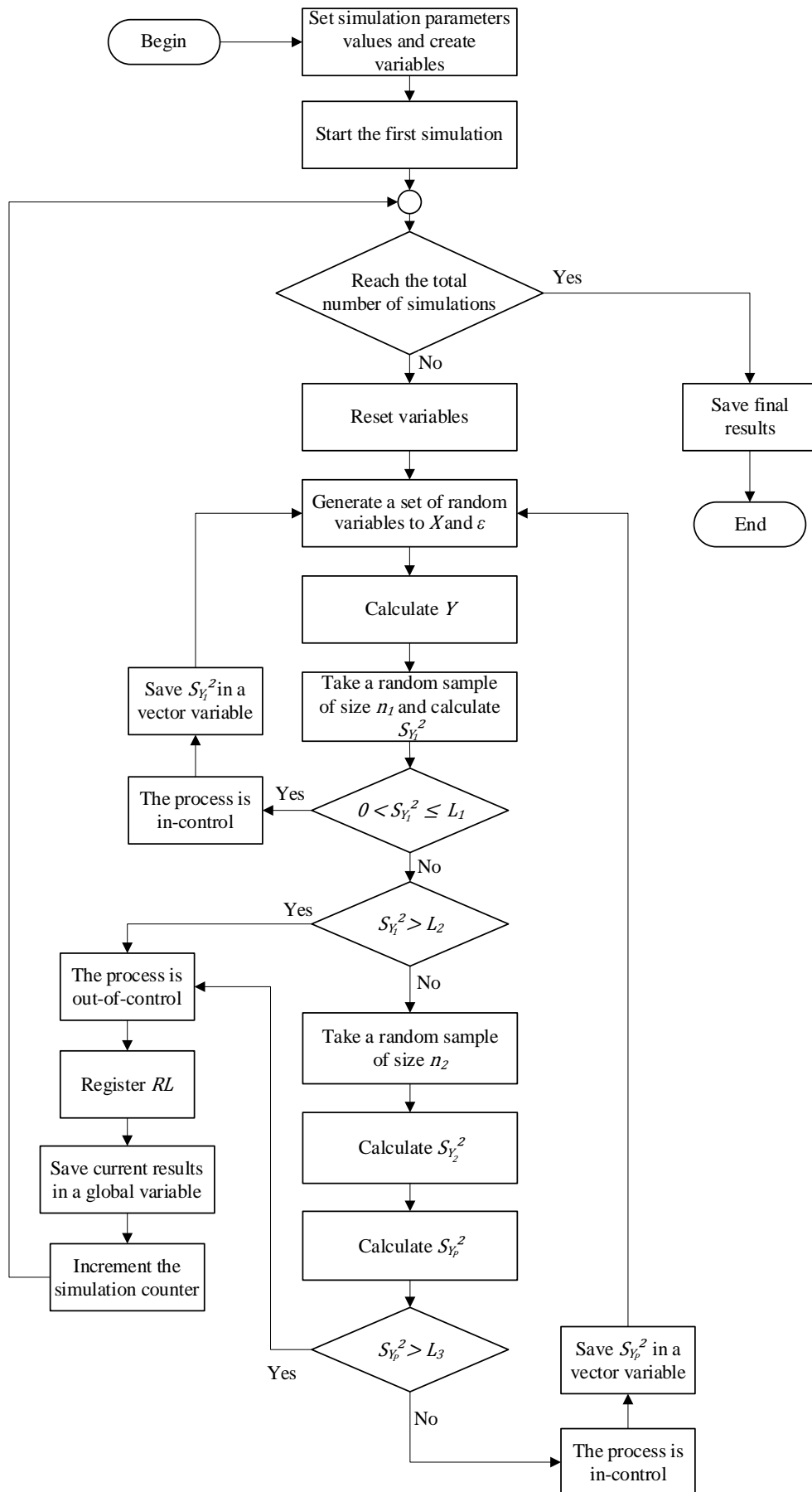
Figure 11 – Simulation flowchart

Table 4 – Impact of the number of simulations

Simulation characteristics	Simulation quantity	ARL	SDRL	Simulation time (s)
S² chart	10	160.70	210.36	0.42
δ=1	100	192.12	202.87	3.33
n = 5	1000	198.37	200.47	27.94
$ARL_0 = 200$	10000	202.52	201.27	395.56
	100000	203.34	204.49	3065.91

In this work, we use 10,000 simulations. This choice was due to the average simulation time. It is worth noting that this time may vary due to the limitations of the computer used. A laptop with Windows 10 operating system, 8 GB RAM, and Intel Core i7 8th Gen processor was used.

The first step to the simulation study was choose DS S^2 control chart parameters. Based on the work of Khoo (2004), we initially set the parameters of DS S^2 chart as $n_1 = 3$, $n_2 = 6$, $L_1 = 3.5$, $L_2 = 5.75$, and $L_3 = 2.7$, chosen by Khoo (2004) for comparison with a traditional S^2 chart for the condition of n = 5 and $ARL_0 = 200$.

In the study, 10.000 in-control observations are generated from a normal distribution, $N(\mu, \sigma_p^2)$, $\mu = 0$ and $\sigma_p^2 = 1$. The error term is considered a normal distributed variable, $N(0, \sigma_m^2)$. To generate the out-of-control samples, we consider $\sigma_p' = \delta\sigma_p$, where δ denotes the shift magnitude. The DS S^2 control chart with and without the influence of measurement error is evaluated for $\delta \in \{1.0, 1.1, 1.5\}$ and $\sigma_m \in \{0, 0.1, 0.3, 0.5, 1.0, 1.5\}$. Table 5 presents the simulation results of the DS S² control chart's evaluation in the presence of measurement error for fixed limits and $\delta = 1.0$.

Table 5 – DS S² control chart's evaluation (δ=1.0)

δ	σ_m	DS S^2	
		ARL	ASS
1.0	0	202.96	3.19
	0.1	188.31	3.19
	0.3	118.62	3.25
	0.5	57.22	3.37
	1.0	9.33	3.76
	1.5	3.09	3.21

From Table 5 we can see that the ARL value decreases as the magnitude of the σ_m increases. Considering that for an in-control process, the higher the ARL value the better, this result indicates that the performance of the DS S^2 chart is reduced as the measurement error increases. Appendix B presents some RL distribution results.

Figures 12 to 17 show some DS S^2 control charts simulation results for δ=1.0 and σ_m= (0, 0.1, 0.3, 0.5, 1.0, 1.5), respectively. Through the plotted control charts, the impact of the measurement error on the number of plotted points can be verified. The increase in the use of the second stage of the DS S^2 control chart can also be noted as the measurement error increases.

Figure 12 – DS S² control chart for δ=1.0 and σ_m= 0

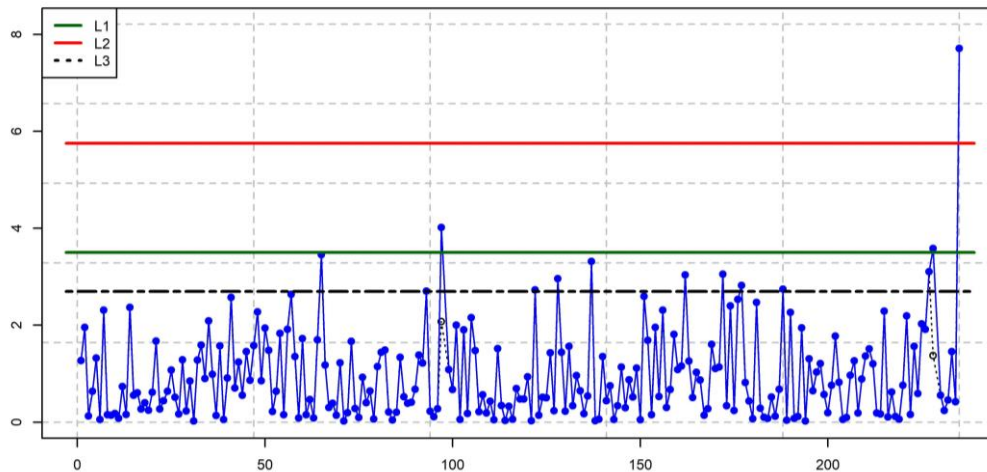Figure 13 – DS S² control chart for δ=1.0 and σ_m= 0.1
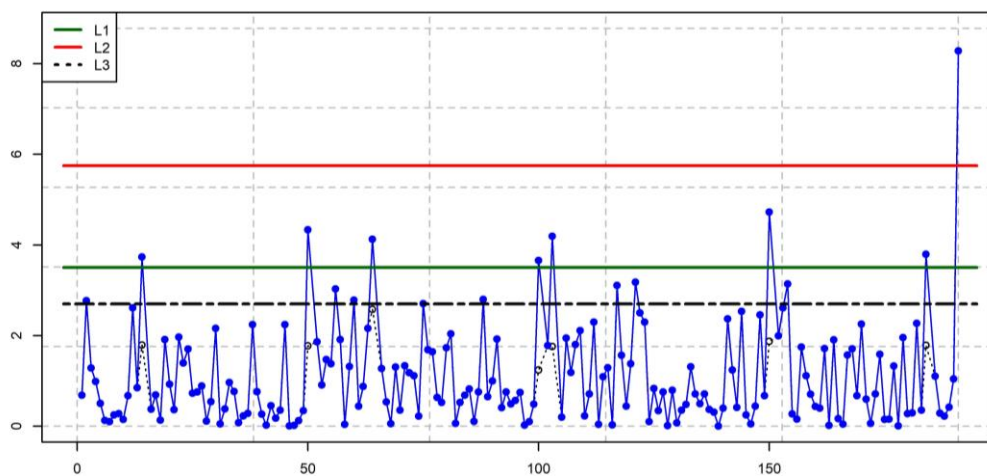
Figure 14 – DS S² control chart for δ=1.0 and σ_m= 0.3
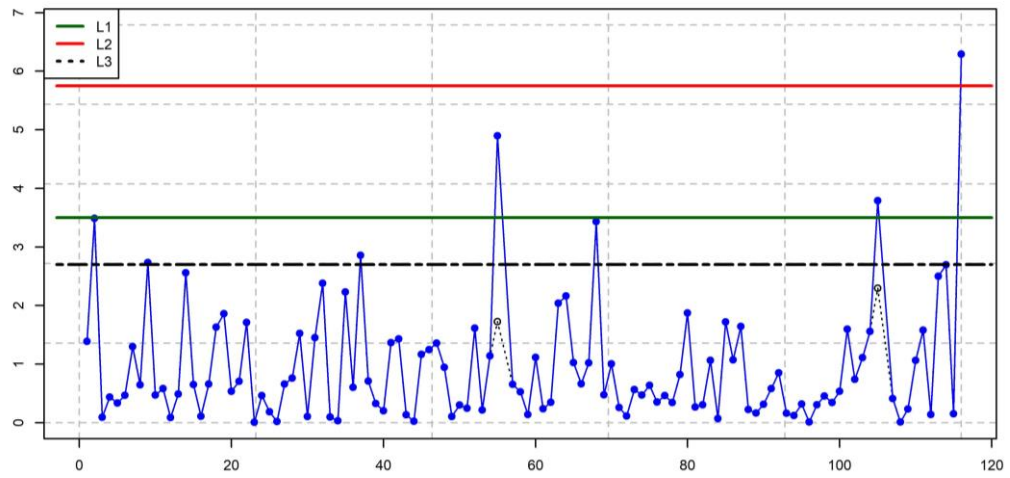
Figure 15 – DS S² control chart for δ=1.0 and σ_m= 0.5
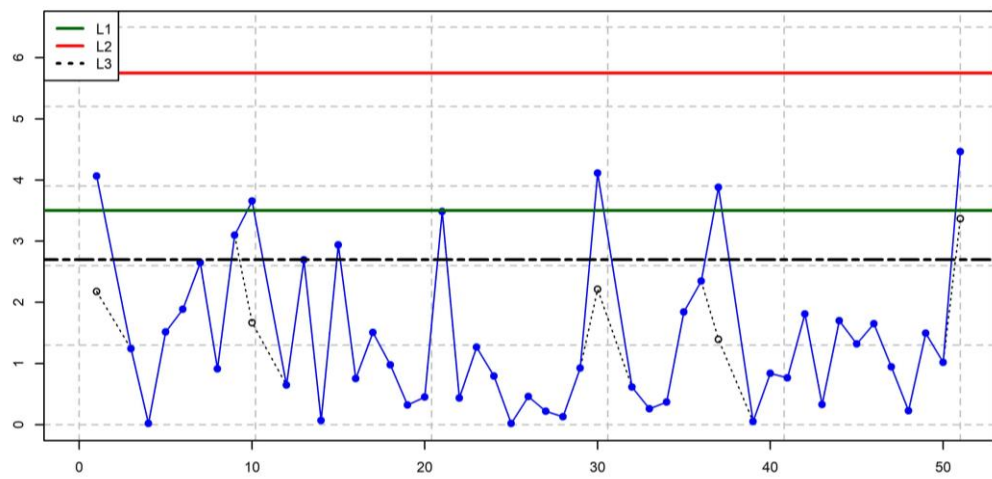
Figure 16 – DS S² control chart for δ=1.0 and σ_m= 1.0
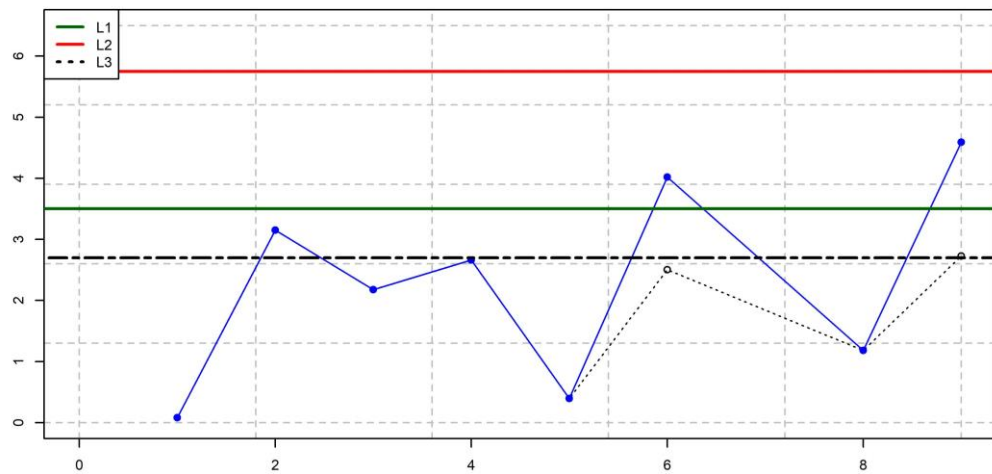
Figure 17 – DS S² control chart for δ=1.0 and σ_m= 1.5

Table 6 shows the DS S^2 control chart's evaluation considering δ =1.1, $n_1 = 3$, $n_2 = 6$, $L_1 = 3.5$, $L_2 = 5.75$, and $L_3 = 2.7$.

Table 6 – DS S² control chart's evaluation (δ=1.1)

δ	σ_m	DS S^2	
		ARL	ASS
	0	69.51	3.33
	0.1	64.31	3.36
	0.3	48.69	3.40
1.1	0.5	28.50	3.51
	1.0	7.30	3.80
	1.5	2.75	3.90

From Table 6, we can see that the ARL values decrease compared to the values in Table 5, indicating its detection ability. It can be seen that the presence of the measurement error can mask the chart's performance since, for the same shift value, it presents a considerable difference for the ARL as the measurement error increases. In addition, the average sample size increases as the error magnitude increases. This sample size increase may indicate that, in the presence of measurement error, the DS S^2 chart consults the chart's second stage more often before indicating that the process is out-of-control.

Figures 18 to 23 show some DS S^2 control charts simulation results for δ=1.1 and σ_m= (0, 0.1, 0.3, 0.5, 1.0, 1.5), respectively.

Figure 18 – DS S² control chart for δ=1.1 and $\sigma_m = 0$

Figure 19 – DS S² control chart for δ=1.1 and $\sigma_m = 0.1$
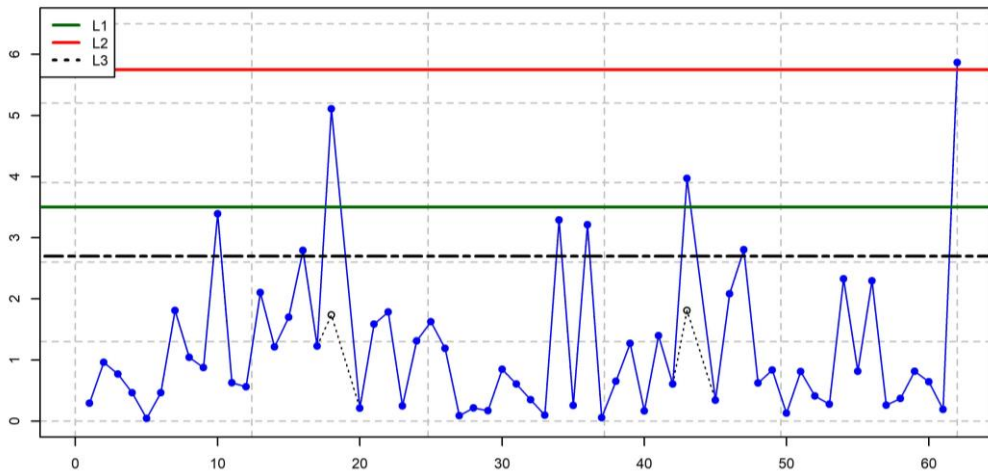
Figure 20 – DS S² control chart for δ=1.1 and $\sigma_m = 0.3$
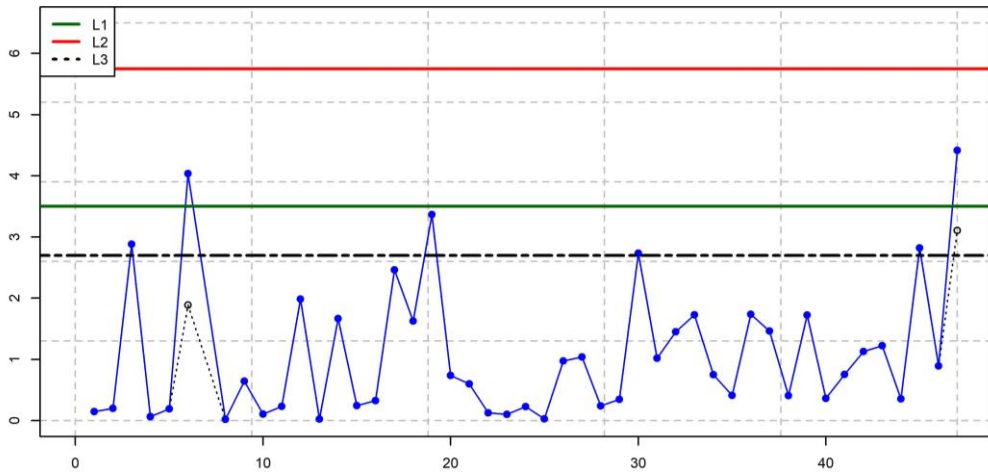
Figure 21 – DS S² control chart for δ=1.1 and σ_m= 0.5
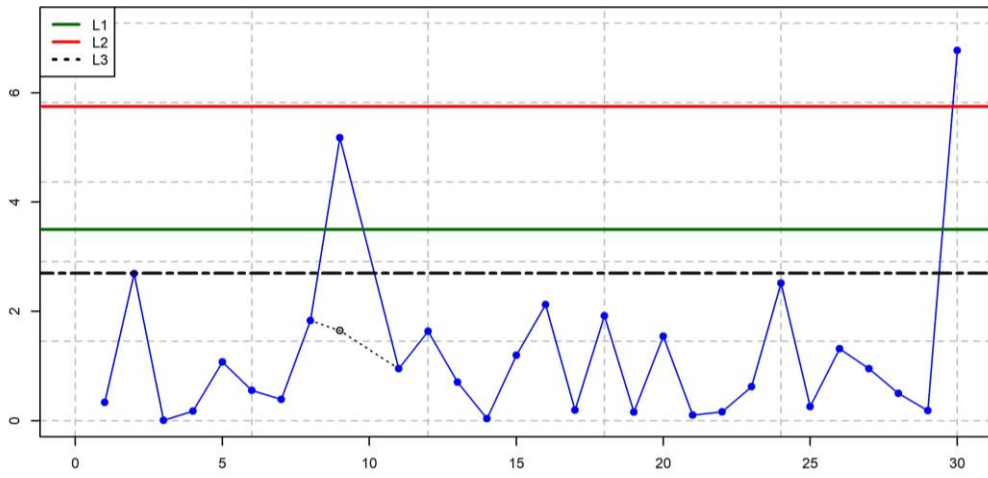
Figure 22 – DS S² control chart for δ=1.1 and σ_m= 1.0
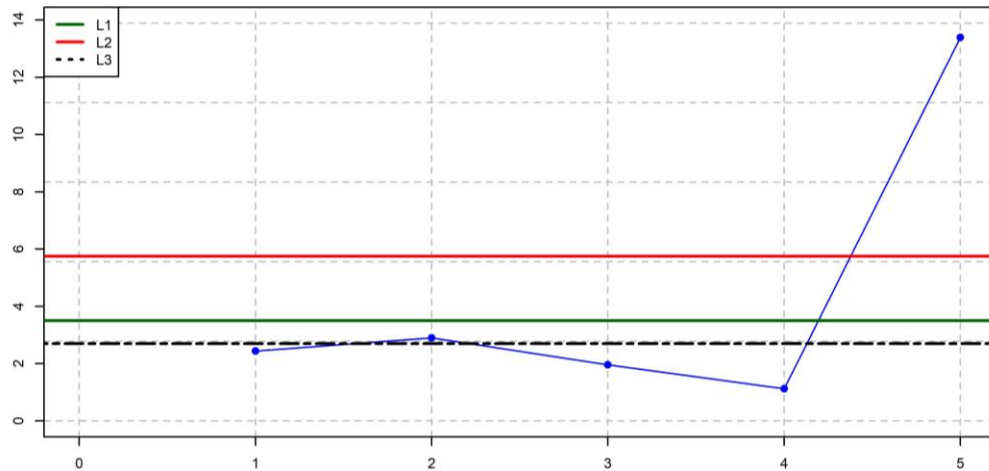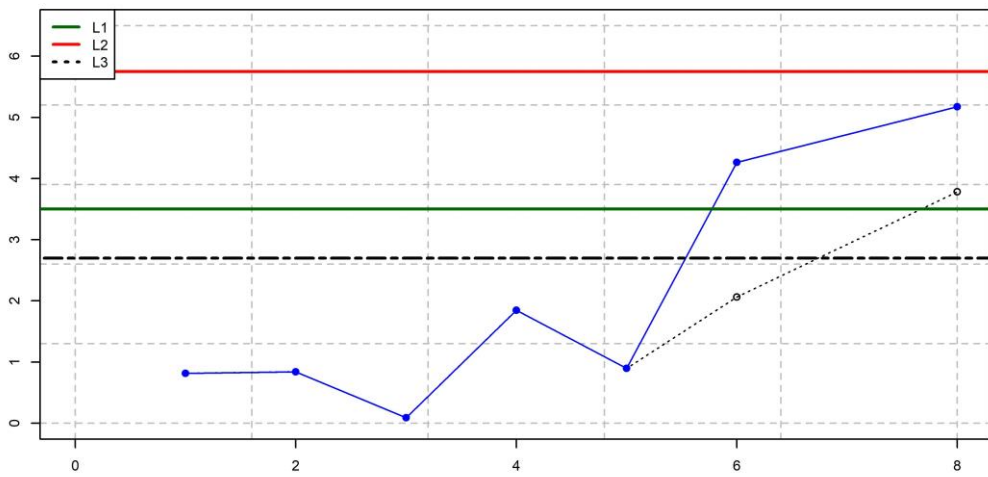

Figure 23 – DS S² control chart for δ=1.1 and σ_m= 1.5
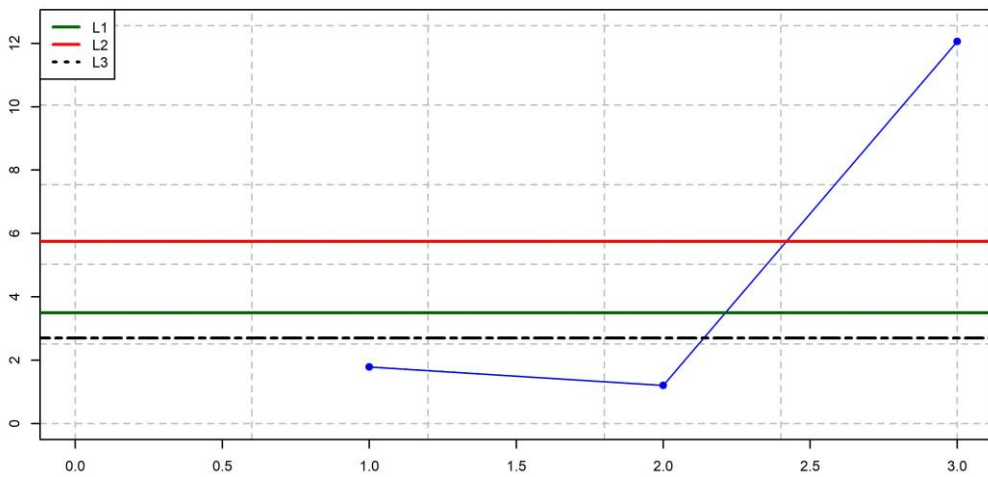
Table 7 shows the DS S^2 control chart's evaluation considering δ =1.5, $n_1 = 3$, $n_2 = 6$, $L_1 = 3.5$, $L_2 = 5.75$, and $L_3 = 2.7$.

Table 7 – DS S² control chart's evaluation (δ=1.5)

δ	σ_m	DS S^2	
		ARL	ASS
1.5	0	7.23	3.82
	0.1	6.77	3.81
	0.3	6.20	3.83
	0.5	5.30	3.86
	1.0	3.03	3.91
	1.5	1.78	3.94

Comparing results in Tables 6 and 7 we can see that the measurement error has a greater impact on the ARL value for δ =1.1 than for δ =1.5. However, the average sample size values are larger for δ =1.5. than for δ =1.1 for all σ_m values. Figures 24 to 29 show some DS S^2 control charts simulation results for δ=1.5 and σ_m= (0, 0.1, 0.3, 0.5, 1.0, 1.5), respectively.

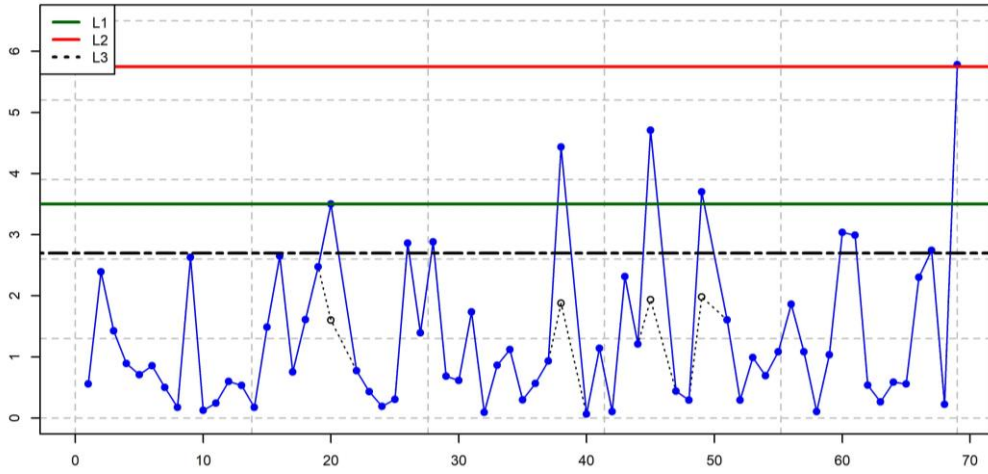Figure 24 – DS S² control chart for δ=1.5 and σ_m= 0
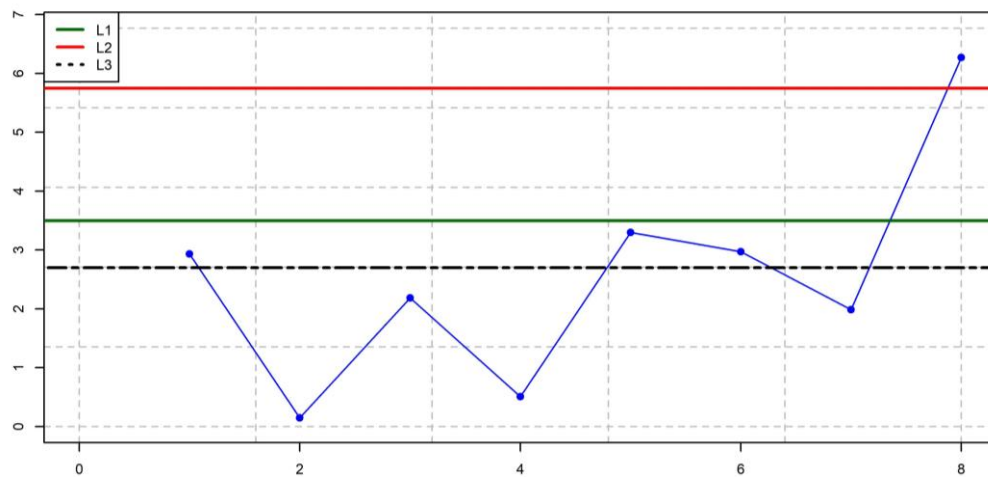
Figure 25 – DS S² control chart for δ=1.5 and σ_m= 0.1
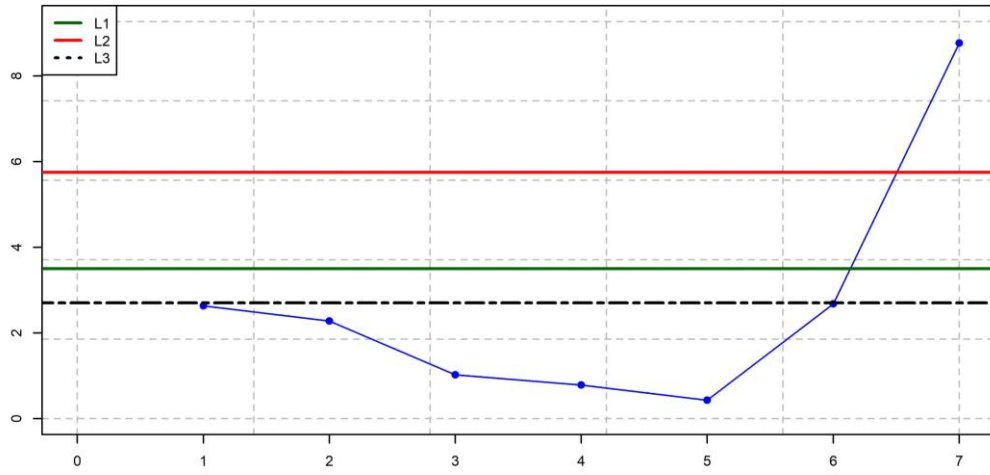
Figure 26 – DS S² control chart for δ=1.5 and σ_m= 0.3
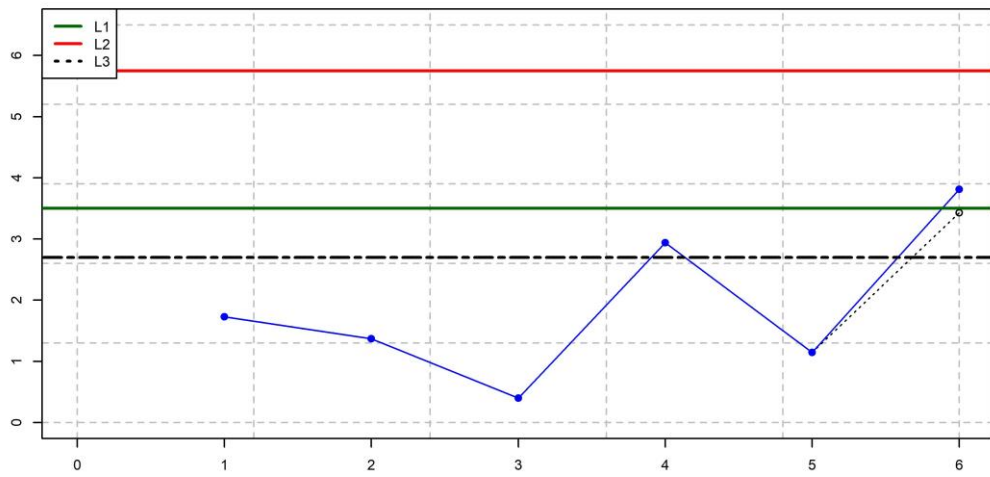
Figure 27 – DS S² control chart for δ=1.5 and σ_m= 0.5
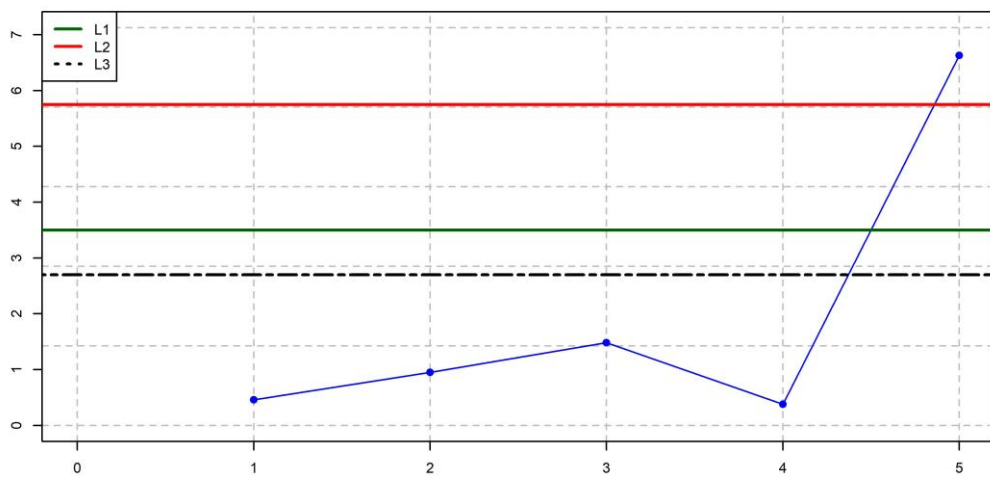
Figure 28 – DS S² control chart for δ=1.5 and σ_m= 1.0
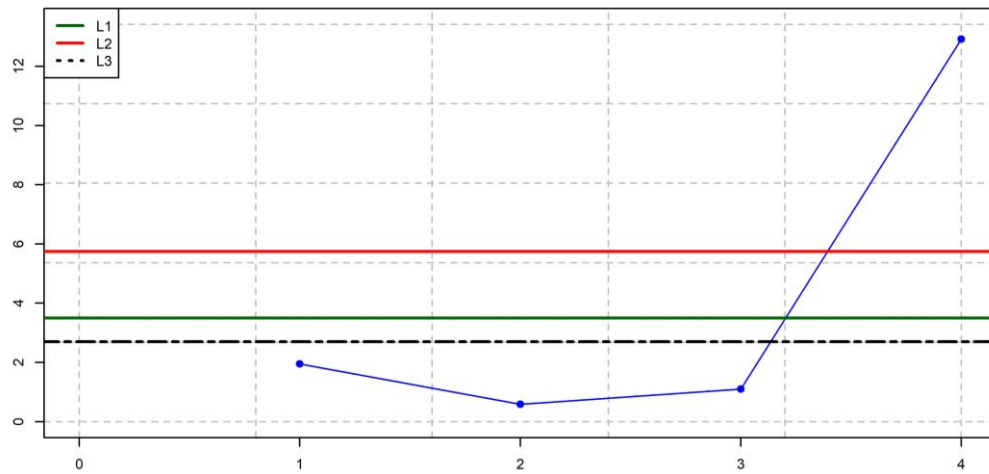
Figure 29 – DS S² control chart for δ=1.5 and σ_m= 1.5
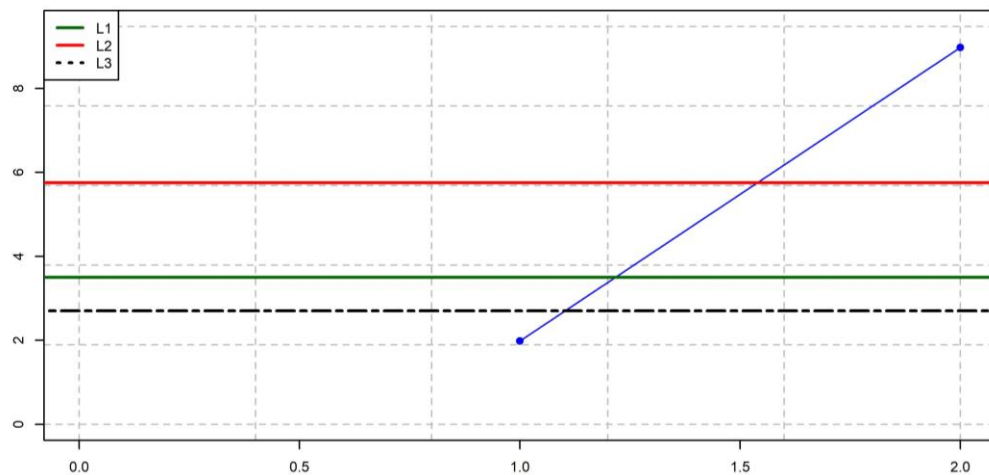
Figure 30 presents the ARL percentage difference in relation to the condition without the measurement error $\sigma_m = 0$. Results in Figure 30 demonstrate the effect of measurement errors on the DS S^2 control chart performance. We can notice that the greater the measurement error, the greater the percentage difference in the ARL value in relation to the condition without the presence of the measurement error. We can also notice that this percentage difference is greater for the δ=1.0 and δ=1.1. Considering that most processes are expected to operate under control conditions or with low shifts, the effect of measurement error is even greater in this condition.

Figure 30 – ARL percentage difference for $\delta \in \{1.0, 1.1, 1.5, 2.0\}$ and $\sigma_m \in \{0.1, 0.3, 0.5, 1.0, 1.5\}$
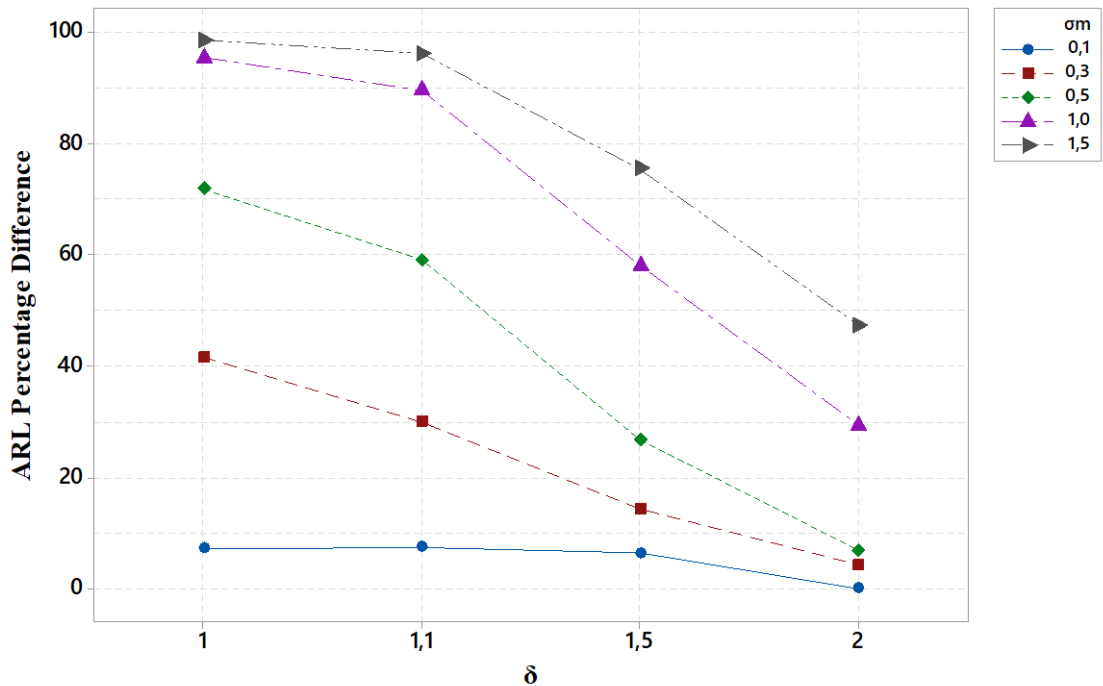
It is worth mentioning that for the evaluations presented in Tables 5, 6, and 7 the parameters n_1, n_2, L_1, L_2, and L_3, necessary to use the DS S^2 control chart, were chosen by Khoo (2004) considering the following conditions: L_2 must be higher than the upper control limit of a classical S^2 chart; L_1, must be lower than the classical upper control limit of a classical S^2 chart; and the ratio between n_2 and n_1 is about $n_2 = 2n_1$ or $n_2 = 3n_1$. As a result, different settings for the same parameters may result in different performance outcomes.

Table 8 shows the ARL and ASS results obtained by changing some of the control chart parameters. The first comparison is made by changing only the n_2 value from 6 (Setting 1) to 4 (Setting 2). For this change, it is observed that the control chart's performance decrease in terms of ARL when the process is under control (δ=1) but gains detection ability in the case of δ=1.1. It is observed that the difference in the chart's ARLs of Setting 1 to that of Setting 2 diminishes for measurement errors of greater magnitude (σ_m=1.0 and σ_m=1.5).

In the last columns of Table 8, we have Setting 3, in which there is a change in n_2 value to 5 and in the L_2 limit to 6. With the Setting 3, we can observe that the ARL values are better than for the Setting 1 for δ=1.1 without experiencing a substantial decline in performance in the case where δ=1.

Table 8 – DS S² control chart's evaluation on different simulation settings

δ	σ_m	Setting 1 n_1, n_2, L_1, L_2, L_3 3, 6, 3.5, 5.75, 2.7		Setting 2 n_1, n_2, L_1, L_2, L_3 3, 4, 3.5, 5.75, 2.7		Setting 3 n_1, n_2, L_1, L_2, L_3 3, 5, 3.5, 6, 2.7	
		ARL	ASS	ARL	ASS	ARL	ASS
1.0	0	202.95	3.19	121.76	3.15	179.91	3.18
	0.1	188.31	3.20	115.20	3.16	165.45	3.19
	0.3	118.62	3.25	77.42	3.21	107.82	3.23
	0.5	57.22	3.37	41.45	3.28	52.28	3.34
	1.0	9.33	3.76	8.62	3.52	9.46	3.69
	1.5	3.09	3.21	3.00	3.61	3.11	3.80
1.1	0	69.51	3.33	48.12	3.26	61.84	3.32
	0.1	64.32	3.36	46.58	3.27	59.39	3.32
	0.3	48.69	3.40	34.64	3.31	43.97	3.38
	0.5	28.50	3.51	22.29	3.38	26.46	3.47
	1.0	7.30	3.80	6.51	3.56	7.16	3.74
	1.5	2.75	3.90	2.78	3.59	2.78	3.79

Table 9 adds to the results presented in Table 8 the values found for the ARL of the traditional S^2 control chart for $\delta \in \{1.0, 1.1\}$ and $\sigma_m \in \{0, 0.1, 0.3, 0.5, 1.0, 1.5\}$. From Table 9, comparing the results of the "Setting 1" DS S^2 chart with those of the traditional S^2 chart, it is observed that the ARL values found for DS S^2 chart are better for $\delta = 1$. However, the "Setting 1" DS S^2 chart presented worse ARL values for $\delta = 1.1$ than the S^2 chart.

Comparing the results for the "Setting 2" DS S^2 chart the ARL results for $\delta = 1.1$ are better than for the traditional chart. However, in this case, there is a significant performance loss compared to the traditional control chart for $\delta = 1$.

Regarding "Setting 3" DS S^2 chart, the ARL results are better than the traditional chart $\delta = 1.1$ for lower measurement error and worse for higher measurement error values (σ_m=0.5 to σ_m=1.5). However, the "Setting 3" chart performed better for larger error values than the S^2 chart for $\delta = 1$. It is worth mentioning that the average sample size for all DS chart settings was less than 4, while the traditional chart worked with $n = 5$.

Table 9 – S² control chart and DS S² control chart's evaluation on different simulation settings

δ	σ_m	Setting 1 n_1, n_2, L_1, L_2, L_3 3, 6, 3.5, 5.75, 2.7		Setting 2 n_1, n_2, L_1, L_2, L_3 3, 4, 3.5, 5.75, 2.7		Setting 3 n_1, n_2, L_1, L_2, L_3 3, 5, 3.5, 6, 2.7		S^2 chart n, ARL_0 5, 200
		ARL	ASS	ARL	ASS	ARL	ASS	ARL
1.0	0	202.96	3.19	121.76	3.16	179.91	3.18	201.20
	0.1	188.31	3.20	115.19	3.16	165.46	3.19	189.18
	0.3	118.62	3.25	77.42	3.21	107.82	3.23	115.28
	0.5	57.21	3.37	41.45	3.28	52.28	3.34	53.32
	1.0	9.33	3.76	8.62	3.52	9.47	3.69	7.59
	1.5	3.09	3.21	3.00	3.61	3.11	3.80	1.96
1.1	0	69.51	3.33	48.12	3.26	61.85	3.32	66.55
	0.1	64.31	3.36	46.58	3.27	59.39	3.32	59.68
	0.3	48.68	3.40	34.64	3.31	43.97	3.38	45.14
	0.5	28.50	3.51	22.29	3.38	26.46	3.47	25.19
	1.0	7.29	3.80	6.51	3.56	7.16	3.74	5.61
	1.5	2.75	3.90	2.78	3.59	2.78	3.78	1.71

Figures 31 and 32 show the ARL percentage difference for the S^2 control chart and the DS S^2 control (Setting 1, Setting 2, and Setting 3), for $\delta = 1$ and $\delta = 1.1$, respectively.

Figure 31 – ARL percentage difference for DS S² control chart and S² chart ($\delta = 1$)
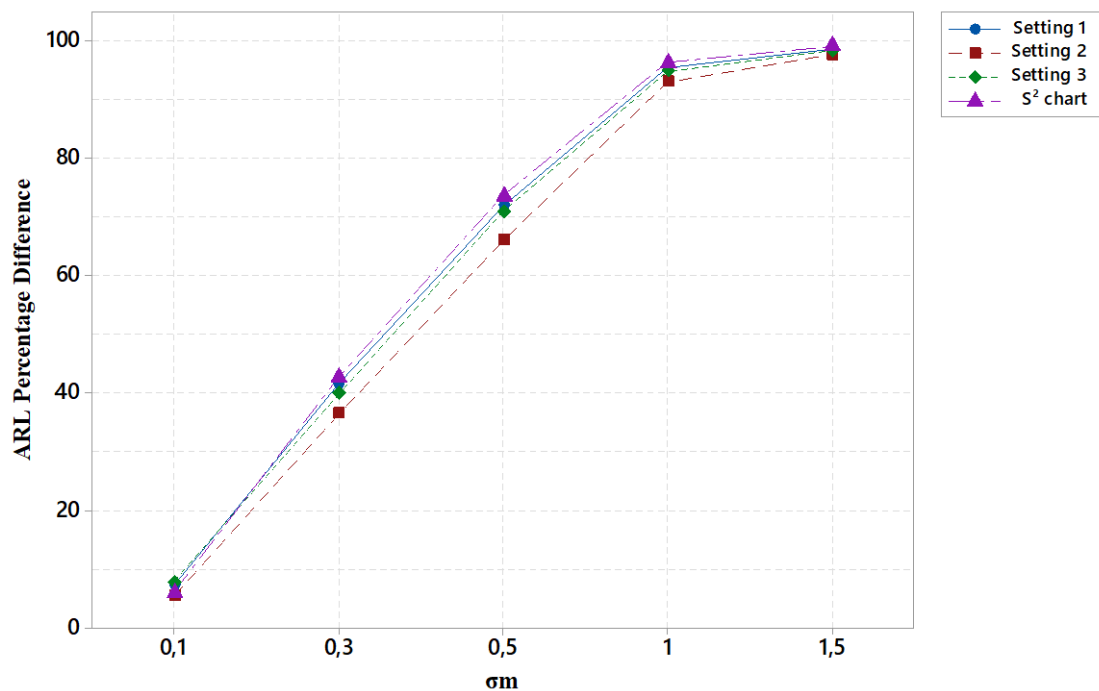
Figure 32 – ARL percentage difference for DS S² control chart and S² chart ($\delta = 1.1$)
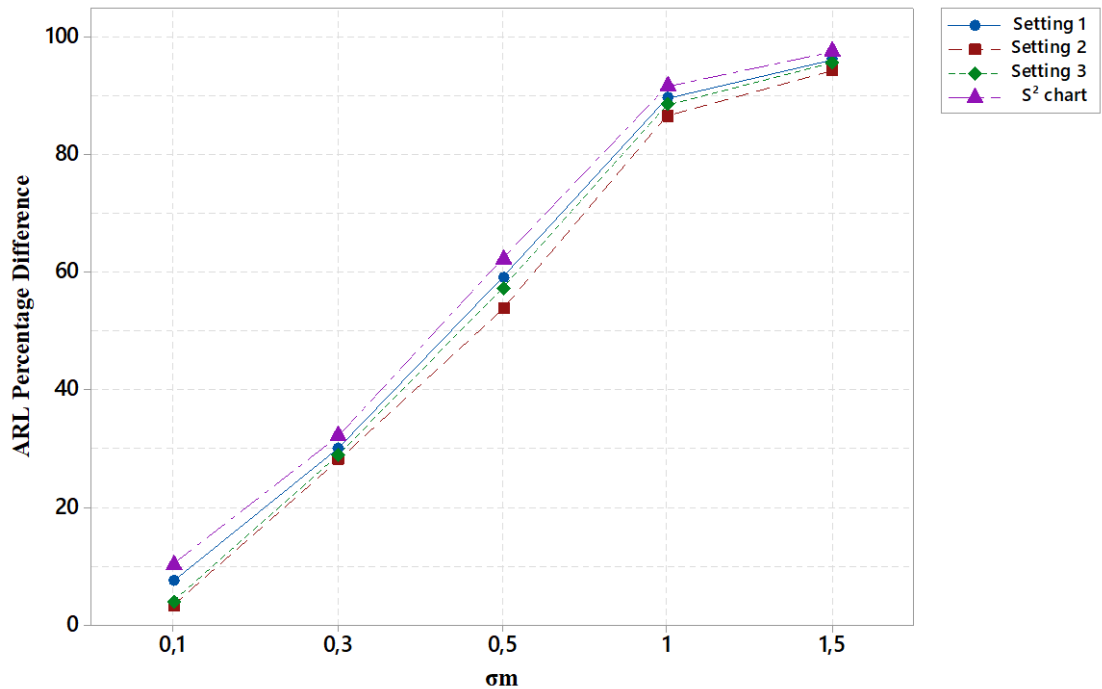
The ARL percentage differences presented in Figures 31 and 32 represent the effects of measurement errors on the ARL values. The percentage difference is calculated by comparing the ARL results to those without measurement errors ($\sigma_m=0$). It is observed that the DS S^2 control chart was more robust to the presence of measurement errors, showing a smaller percentage difference for almost all magnitudes of error, both for $\delta = 1$ and $\delta = 1.1$.

The difference between the impact of measurement errors on ARL values is even greater when comparing the results from S^2 chart with those from the "Setting 2 DS S^2 chart".

The results in Tables 8 and 9 and Figures 31 and 32 highlight that the DS S^2 chart's ARL varies considerably depending on the parameters used. Thus, investigations that optimize the charts' parameters are necessary to improve the DS S^2 chart application.

5. DOUBLE SAMPLING S² CONTROL CHART OPTIMIZATION

The optimization process proposed in this chapter is based on the work of Castagliola, Oprime, and Khoo (2017), He and Grigoryan (2002), Khoo (2004), and Torng and Lee (2009b).

Suppose that the process monitored is an in-control state, but $S_{Y_1}^2 > L_2$ or $S_{Yp}^2 > L_3$. So, it will be concluded that a Type I error occurred. Its probability can be calculated by Equation 67.

Equation 67

$$\alpha = Pr\left(S_{Y_1}^2 > L_2\right) + Pr\left(L_1 < S_{Y_1}^2 \leq L_2\right) \times Pr\left(S_{Yp}^2 > L_3\right)$$

Starting by analyzing the first term of Equation 67, considering that $\frac{(n_1-1)S_{Y_1}^2}{B^2\sigma_p^2+\sigma_m^2} \sim \chi_{(n_1-1)}^2$ (demonstration in Appendix A), we have that:

Equation 68

$$Pr\left(S_{Y_1}^2 > L_2\right) = 1 - Pr\left(S_{Y_1}^2 \leq L_2\right)$$

$$= 1 - Pr\left(S_{Y_1}^2 \leq L_2\right) = 1 - Pr\left(\left(\frac{n_1-1}{B^2\sigma_p^2+\sigma_m^2}\right)S_{Y_1}^2 \leq \left(\frac{n_1-1}{B^2\sigma_p^2+\sigma_m^2}\right)L_2\right)$$

$$= 1 - F_{n_1-1}\left[\left(\frac{n_1-1}{B^2\sigma_p^2+\sigma_m^2}\right)L_2\right] = 1 - F_{n_1-1}[(n_1-1)k_2]$$

where $F_{n_1-1}[.]$ is the chi-square distribution function with $n_1 - 1$ degrees of freedom.

Now, analyzing the second term of Equation 67:

Equation 69

$$Pr\left(L_1 < S_{Y_1}^2 \leq L_2\right) \times Pr\left(S_{Yp}^2 > L_3\right) = Pr\left(L_1 < S_{Y_1}^2 \leq L_2\right) \times \left[1 - Pr\left(S_{Yp}^2 \leq L_3\right)\right]$$

Thus,

Equation 70

$$Pr\left(L_1 < S_{Y_1}^2 \leq L_2\right) \times \left[1 - Pr\left(S_{Yp}^2 \leq L_3\right)\right] = \int_{\Omega_2^*} \left[1 - Pr\left(S_{Yp}^2 \leq L_3 \middle| S_{Y_1}^2 = z\right)\right] f(z)\, dz$$

where $f(.)$ is the probability density function of $S_{Y_1}^2$ and $\Omega_2^* = ((n_1 - 1)k_1, (n_1 - 1)k_2]$. The derivation of Ω_2^* can be seen in Appendix C.

First, we must find $Pr\left(S_{Yp}^2 \leq L_3 \middle| S_{Y_1}^2 = z\right)$. Since $S_{Y_1}^2$ and $S_{Y_2}^2$ are independent, we have that:

Equation 71

$$Pr\left(S_{Yp}^2 \leq L_3\right) = Pr\left[\frac{(n_1 - 1)S_{Y_1}^2 + (n_2 - 1)S_{Y_2}^2}{n_1 + n_2 - 2} \leq L_3\right]$$

$$= Pr\left[(n_1 - 1)S_{Y_1}^2 + (n_2 - 1)S_{Y_2}^2 \leq (n_1 + n_2 - 2)L_3\right]$$

Given $S_{Y_1}^2 = z$, so

Equation 72

$$Pr\left(S_{Yp}^2 \leq L_3 \middle| S_{Y_1}^2 = z\right) = Pr\left[(n_2 - 1)S_{Y_2}^2 \leq (n_1 + n_2 - 2)L_3 - (n_1 - 1)z\right]$$

$$= Pr\left[\frac{(n_2 - 1)S_{Y_2}^2}{B^2\sigma_p^2 + \sigma_m^2} \leq \frac{(n_1 + n_2 - 2)L_3 - (n_1 - 1)z}{B^2\sigma_p^2 + \sigma_m^2}\right]$$

$$= F_{n_2-1}\left[\frac{(n_1 + n_2 - 2)L_3 - (n_1 - 1)z}{B^2\sigma_p^2 + \sigma_m^2}\right]$$

$$= F_{n_2-1}\left[(n_1 + n_2 - 2)k_3 - \frac{(n_1 - 1)z}{B^2\sigma_p^2 + \sigma_m^2}\right]$$

where $F_{n_2-1}(.)$ is the chi-square distribution function with $n_2 - 1$ degrees of freedom.

Thus, naming Equation 70 as P_{a2}, give us:

$$P_{a2} = \int_{\Omega_2^*} \left\{ 1 - F_{n_2-1} \left[(n_1 + n_2 - 2)k_3 - \frac{(n_1 - 1)z}{B^2\sigma_p{}^2 + \sigma_m{}^2} \right] \right\} f(z)\, dz$$

Then, considering the density function of a continuous random variable that follows a chi-square distribution, we get:

$$P_{a2} = \int_{\Omega_2^*} \left[1 - \int_0^{\left[(n_1+n_2-2)k_3 - \frac{(n_1-1)z}{B^2\sigma_p{}^2+\sigma_m{}^2} \right]} \frac{1}{\Gamma\left(\frac{n_2-1}{2}\right)} \left(\frac{1}{2}\right)^{\left(\frac{n_2-1}{2}\right)} t^{\left(\frac{n_2-1}{2}\right)-1} e^{-\frac{t}{2}}\, dt \right] f(z)\, dz$$

To find $f(z)$, we consider that Q is a random variable, so that

$$Q = \frac{(n_1 - 1)S_{Y_1}^2}{B^2\sigma_p{}^2 + \sigma_m{}^2} \sim \chi^2_{(n_1-1)}$$

where Q follows a chi-square distribution with $(n_1 - 1)$ degrees of freedom and density function $h(q)$, so:

$$h(q) = \frac{1}{\Gamma\left(\frac{n_1-1}{2}\right)} \left(\frac{1}{2}\right)^{\left(\frac{n_1-1}{2}\right)} q^{\left(\frac{n_1-1}{2}\right)-1} e^{-\frac{q}{2}}$$

Besides, we consider that

$$S_{Y_1}^2 = g(q) = \frac{(B^2\sigma_p{}^2 + \sigma_m{}^2)Q}{(n_1 - 1)}$$

So, given that $S_{Y_1}^2 = z$, we get

Equation 78

$$Q = g^{-1}\left(S_{Y_1}^2\right) = g^{-1}(z) = \frac{(n_1 - 1)z}{B^2\sigma_p{}^2 + \sigma_m{}^2}$$

We can use the Jacobian transformation for determining the density function of a random variable that is a function of another random variable with known probability distribution. Knowing that Q is a random variable that follows a chi-square distribution with density function $h(q)$, and $S_{Y_1}^2 = z = g(q)$, so:

Equation 79

$$f(z) = f\left(S_{Y_1}^2 = z\right) = h[g^{-1}(z)]\left|\frac{d}{dz}g^{-1}(z)\right| = h\left[\frac{(n_1 - 1)z}{B^2\sigma_p{}^2 + \sigma_m{}^2}\right]\left|\frac{d}{dz}\frac{(n_1 - 1)z}{B^2\sigma_p{}^2 + \sigma_m{}^2}\right|$$

So, considering $h(.)$ given by Equation 76, we have

Equation 80

$$f(z) = \frac{1}{\Gamma\left(\frac{n_1 - 1}{2}\right)}\left(\frac{1}{2}\right)^{\left(\frac{n_1-1}{2}\right)}\left(\frac{(n_1 - 1)z}{B^2\sigma_p{}^2 + \sigma_m{}^2}\right)^{\left(\frac{n_1-1}{2}\right)-1}e^{-\frac{1}{2}\left(\frac{(n_1-1)z}{B^2\sigma_p{}^2+\sigma_m{}^2}\right)}\left(\frac{(n_1 - 1)}{B^2\sigma_p{}^2 + \sigma_m{}^2}\right)$$

Therefore,

Equation 81

$$P_{a2}$$
$$= \int_{\Omega_2{}^*}\left\{\left[1 - \int_0^{\left[(n_1+n_2-2)k_3-\frac{(n_1-1)z}{B^2\sigma_p{}^2+\sigma_m{}^2}\right]}\frac{1}{\Gamma\left(\frac{n_2 - 1}{2}\right)}\left(\frac{1}{2}\right)^{\left(\frac{n_2-1}{2}\right)}t^{\left(\frac{n_2-1}{2}\right)-1}e^{-\frac{t}{2}}dt\right]\right.$$
$$\left.\times\frac{1}{\Gamma\left(\frac{n_1 - 1}{2}\right)}\left(\frac{1}{2}\right)^{\left(\frac{n_1-1}{2}\right)}\left(\frac{(n_1 - 1)}{B^2\sigma_p{}^2 + \sigma_m{}^2}\right)^{\left(\frac{n_1-1}{2}\right)-1}z^{\left(\frac{n_1-1}{2}\right)-1}e^{-\frac{1}{2}\left(\frac{(n_1-1)z}{B^2\sigma_p{}^2+\sigma_m{}^2}\right)}\left(\frac{(n_1 - 1)}{B^2\sigma_p{}^2 + \sigma_m{}^2}\right)\right\}dz$$

Thus, from Equation 67, Equation 68, and Equation 81 we have that

Equation 82

$$\alpha$$

$$= 1 - F_{n_1-1}[(n_1 - 1)k_2]$$

$$+ \int_{\Omega_2^*} \left\{ \left[1 - \int_0^{\left[(n_1+n_2-2)k_3 - \frac{(n_1-1)z}{B^2\sigma_p^2+\sigma_m^2} \right]} \frac{1}{\Gamma\left(\frac{n_2-1}{2}\right)} \left(\frac{1}{2}\right)^{\left(\frac{n_2-1}{2}\right)} t^{\left(\frac{n_2-1}{2}\right)-1} e^{-\frac{t}{2}} dt \right] \right.$$

$$\left. \times \frac{1}{\Gamma\left(\frac{n_1-1}{2}\right)} \left(\frac{1}{2}\right)^{\left(\frac{n_1-1}{2}\right)} \left(\frac{(n_1-1)}{B^2\sigma_p^2+\sigma_m^2}\right)^{\left(\frac{n_1-1}{2}\right)-1} z^{\left(\frac{n_1-1}{2}\right)-1} e^{-\frac{1}{2}\left(\frac{(n_1-1)z}{B^2\sigma_p^2+\sigma_m^2}\right)} \left(\frac{(n_1-1)}{B^2\sigma_p^2+\sigma_m^2}\right) \right\} dz$$

Simplifying Equation 82, we get:

Equation 83

$$\alpha$$

$$= 1 - F_{n_1-1}[(n_1 - 1)k_2]$$

$$+ c_1 \int_{\Omega_2^*} \left\{ \left[1 - c_2 \int_0^{\left[(n_1+n_2-2)k_3 - \frac{(n_1-1)z}{B^2\sigma_p^2+\sigma_m^2} \right]} t^{\left(\frac{n_2-1}{2}\right)-1} e^{-\frac{t}{2}} dt \right] z^{\left(\frac{n_1-1}{2}\right)-1} e^{-\frac{1}{2}\left(\frac{(n_1-1)z}{B^2\sigma_p^2+\sigma_m^2}\right)} \right\} dz$$

where c_1 and c_2 are given by Equations 84 and 85.

Equation 84

$$c_1 = \frac{1}{\Gamma\left(\frac{n_1-1}{2}\right)} \left(\frac{1}{2}\right)^{\left(\frac{n_1-1}{2}\right)} \left(\frac{(n_1-1)}{B^2\sigma_p^2+\sigma_m^2}\right)^{\left(\frac{n_1-1}{2}\right)}$$

Equation 85

$$c_2 = \frac{1}{\Gamma\left(\frac{n_2-1}{2}\right)} \left(\frac{1}{2}\right)^{\left(\frac{n_2-1}{2}\right)}$$

In case of the process is out-of-control, we consider that the process shifts to a certain value $\sigma_p' = \delta\sigma_p$, where δ denotes the shift magnitude. Supposing that the process is

out-of-control, but $S_{Y_1}^2 \le L_1$ or $S_{Yp}^2 \le L_3$, it will be concluded that a Type II error occurred, and its probability can be calculated by

$$\beta_\delta = Pr\left(S_{Y_1}^2 \le L_1\right) + Pr\left(L_1 < S_{Y_1}^2 \le L_2\right) \times Pr\left(S_{Yp}^2 \le L_3\right)$$

Similar to what was demonstrated before, but now considering that the process is out-of-control, we get:

$$\beta_\delta = F_{n_1-1}\left[\frac{(n_1-1)k_1(B^2\sigma_p{}^2+\sigma_m{}^2)}{B^2\delta^2\sigma_p{}^2+\sigma_m{}^2}\right]$$

$$+ c_3 \int_{\Omega_2^{**}} \left\{ \left[c_2 \int_0^{\left[\frac{(n_1+n_2-2)(B^2\sigma_p{}^2+\sigma_m{}^2)k_3-(n_1-1)z}{B^2\delta^2\sigma_p{}^2+\sigma_m{}^2}\right]} t^{\left(\frac{n_2-1}{2}\right)-1} e^{-\frac{t}{2}} dt \right] \right.$$

$$\left. \times z^{\left(\frac{n_1-1}{2}\right)-1} e^{-\frac{1}{2}\left(\frac{(n_1-1)z}{B^2\delta^2\sigma_p{}^2+\sigma_m{}^2}\right)} \right\} dz$$

where $\Omega_2^{**} = \left(\frac{(n_1-1)k_1(B^2\sigma_p{}^2+\sigma_m{}^2)}{B^2\delta^2\sigma_p{}^2+\sigma_m{}^2}, \frac{(n_1-1)k_2(B^2\sigma_p{}^2+\sigma_m{}^2)}{B^2\delta^2\sigma_p{}^2+\sigma_m{}^2}\right)$. The derivation of Ω_2^{**} can be seen in Appendix C. And c_3 is given by Equation 88.

$$c_3 = \frac{1}{\Gamma\left(\frac{n_1-1}{2}\right)} \left(\frac{1}{2}\right)^{\left(\frac{n_1-1}{2}\right)} \left(\frac{(n_1-1)}{B^2\delta^2\sigma_p{}^2+\sigma_m{}^2}\right)^{\left(\frac{n_1-1}{2}\right)}$$

As seen in the analysis in Chapter 4, the DS S^2 control chart's performance will depend on the values chosen for its parameters. Thus, it is necessary to use mechanisms that seek to optimize these parameters for different scenarios. Optimal design of the DS S^2 control

chart involves determining the following parameters: sample size of the first stage (n_1), sample size of the second stage (n_2), the limits L_1 and L_2 on the first stage, and the limit L_3 on the second stage. To find these parameters, we consider the design as an optimization problem.

For the purpose of optimization, we want to minimize the average sample size. As pointed out by Torng and Lee (2009), in Double Sampling control charts it is not consequential to add a sample of size n_2 for each sampling. So, considering the probability of addition a second sample of size n_2 we can estimate the expected sample size $E_0(n)$ of the DS S^2 control chart under in-control processes. $E_0(n)$ is given by:

Equation 89

$$E_0(n) = n_1 + n_2 Pr\left(L_1 < S_{Y_1}^2 \leq L_2\right)$$

$$= n_1 + n_2 \left\{ F_{n_1-1}\left[\frac{(n_1-1)L_2}{B^2\sigma_p{}^2 + \sigma_m{}^2}\right] - F_{n_1-1}\left[\frac{(n_1-1)L_1}{B^2\sigma_p{}^2 + \sigma_m{}^2}\right] \right\}$$

Thus, we can rewrite the expected sample size of the DS S^2 control chart under in-control processes as:

Equation 90

$$E_0(n) = n_1 + n_2\left\{ F_{n_1-1}[(n_1-1)k_2] - F_{n_1-1}[(n_1-1)k_1] \right\}$$

Moreover, the expected sample size under an out-of-control process $E_\delta(n)$ for a shift size of δ is:

Equation 91

$$E_\delta(n) = n_1 + n_2 \left\{ F_{n_1-1}\left[\frac{(n_1-1)k_2(B^2\sigma_p{}^2 + \sigma_m{}^2)}{B^2\delta^2\sigma_p{}^2 + \sigma_m{}^2}\right] \right.$$
$$\left. - F_{n_1-1}\left[\frac{(n_1-1)k_1(B^2\sigma_p{}^2 + \sigma_m{}^2)}{B^2\delta^2\sigma_p{}^2 + \sigma_m{}^2}\right] \right\}$$

Therefore, based on Torng and Lee (2009), which used the weight method proposed by Zadeh (1963), a multi-objective programming method is used for statistical design of the DS S^2 control chart. This multi-objective method was chosen because, as pointed out by Hsu (2007), the average sample size when the process is in control should not be used as a sole criterion for control charts' performance evaluation.

It's also crucial to consider the average number of samples to detect a process shift, the process shift probability from an in-control to an out-of-control state, and its shift magnitude. Thus, we consider the objective to minimize both $E_0(n)$ and $E_\delta(n)$. The combined objective function will be given by

Equation 92

$$\min_{n_1,n_2,k_1,k_2,k_3} U[E_0(n)] + (1-U)[E_\delta(n)]$$

where U represents the weight value, which represents the importance degree of the objective function, so that the sum of weights of all objective functions will be equal to 1.

The next step is to define the constraints of the problem. The average run length (ARL) is commonly used to assess the statistical performance of control charts. For in-control process, the average run length is written as $ARL_0 = 1/\alpha$.

When the process is out-of-control, with a shift size of δ, the necessary average sampling times for detecting the process shift can be expressed as $ARL_1 = 1/(1 - \beta_\delta)$. So, the objective function is subject to two main constraints: the probability of concluding that an in-control process is out-of-control is less than α (Type I error), and the probability of considering that an out-of-control process is in control is less than β (Type II error). These two constraints can be rewritten as

Equation 93

$$ARL_0 \geq ARL_0{}^*$$

Equation 94

$$ARL_1 \leq ARL_1{}^*$$

where $ARL_0{}^*$ is a specified minimal value of the in-control average run length (ARL_0), aiming at a tolerable occurrence of false alarms, and $ARL_1{}^*$ is a maximum value specified of the out-of-control average run length (ARL_1), aiming the faster detecting when process shift has occurred.

In addition to the constraints in Equation 93 and Equation 94, lower and upper bounds for the charts' limits are set up. Lower and upper bounds are imposed on n_1, n_2, k_1, k_2 and k_3 as lower = (3, 3, 0, 0, 0) and upper = $(n, n+1, 10, 10, 10)$, respectively. The bounds for k_1, k_2 and k_3 were chosen based on the minimum and maximum values found by Castagliola, Oprime, and Khoo (2017). Because it is desirable in practical applications to use moderately small sample sizes, we restrict the possible outcomes for n_1 and n_2 such that $3 \leq n_1 \leq n$ and $3 \leq n_2 \leq n + 1$, where n is some value chosen for the maximum number of observations desired for each sample.

To solve the optimization problem, the genetic algorithm (GA) optimization technique was chosen, because of its effectiveness for optimizing nonlinear models. GA optimization method has been widely used in recent studies for control chart design, examples include the works of Jafarian-Namin *et al.* (2019), Yang *et al.* (2021), Yu and Zhang (2021), Mirabi, Fatemi Ghomi, and Jolai (2022), and Quintero-Arteaga *et al.* (2022). The flowchart with the optimization procedure can be seen in Figure 33.

This work proposes an optimization routine using the R programming language. The R language was chosen for its wide range of statistical materials and open-source packages. The genetic algorithm package "GA" proposed by Scrucca (2013) was used. The integrations in Equation 74 and Equation 78 are computed with numerical integration using Simpson's rule (GERALD; WHEATLEY, 1989; HE; GRIGORYAN, 2003). For validation of the integration method used, the results were compared to those found by the mathematical software WolframAlpha.

Table 10 presents the optimal combinations of n_1, n_2, k_1, k_2, k_3, for different combinations of $\delta \in \{1.0, 1.1, 1.2, 1.3, 1.5, 1.7, 2.0, 2.5\}$ and $\sigma_m \in \{0, 0.1, 0.3, 0.5, 0.7\}$, considering $ARL_0{}^* = 370.4$, $U = 0.5$, and $n = 5$. The values of δ and σ_m used for the optimization will from now on be named as δ_{opt} and $\sigma_{m_{opt}}$, respectively.

Figure 33 – Optimization procedure


```
                           ┌─────────┐
                           │  Begin  │
                           └─────────┘
                                │
              ┌─────────────────────────────────┐
              │ Set simulation parameters       │
              │ values and create               │
              │ variables                       │
              └─────────────────────────────────┘
                                │
              ┌─────────────────────────────────┐
              │ Set the objective function      │
              │ and constraints                 │
              └─────────────────────────────────┘
                                │
              ┌─────────────────────────────────┐
              │ Set GA object and limits        │
              │ of the search domain            │
              └─────────────────────────────────┘
                                │
              ┌─────────────────────────────────┐
              │ Generate initial                │
              │ population                       │
              └─────────────────────────────────┘
                                │
              ┌─────────────────────────────────┐
              │ Starting at the first           │
              │ chromosome of the initial       │
              │ population                       │
              └─────────────────────────────────┘
```
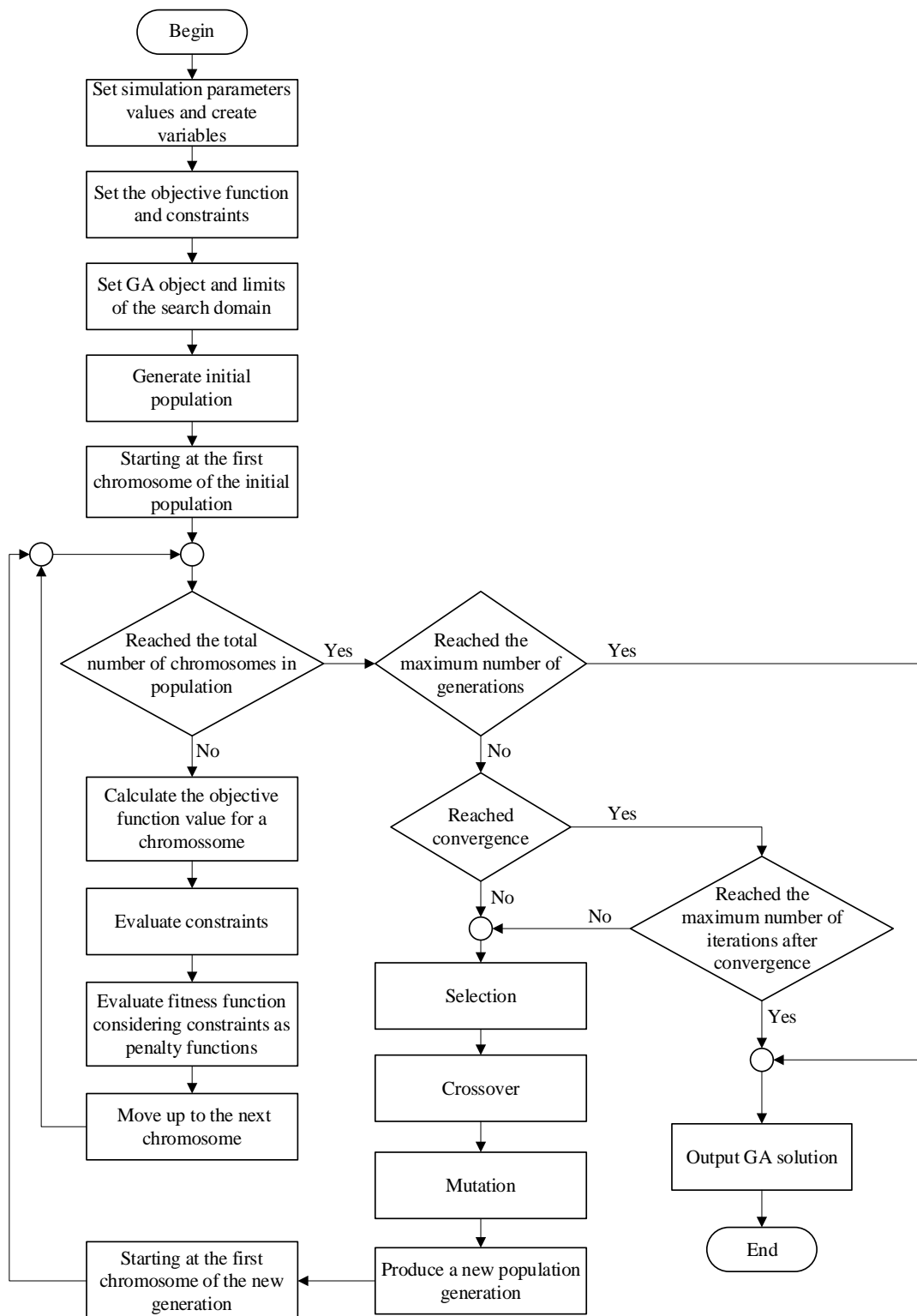
Table 10 – DS S^2 control chart's optimized parameters

δ_{opt}	$\sigma_{m_{opt}}$	n_1	n_2	k_1	k_2	k_3
1	0	5	6	0.595	4.063	4.808
1	0.1	5	5	0.598	4.063	4.966
1	0.3	5	5	0.622	4.063	5.290
1	0.5	5	5	0.670	4.063	5.470
1	0.7	5	5	0.737	4.063	5.158
1.1	0	5	6	0.812	4.093	3.759
1.1	0.1	5	5	0.793	4.044	4.158
1.1	0.3	5	5	0.811	4.022	3.882
1.1	0.5	5	5	0.854	3.980	3.483
1.1	0.7	5	5	0.908	4.022	3.121
1.2	0	5	6	1.131	5.177	1.375
1.2	0.1	5	6	1.133	6.309	1.401
1.2	0.3	5	5	1.040	3.844	3.496
1.2	0.5	5	5	1.056	3.853	3.302
1.2	0.7	5	5	1.112	3.901	3.027
1.3	0	5	6	1.137	5.398	1.077
1.3	0.1	5	6	1.143	5.106	1.188
1.3	0.3	5	6	1.198	5.869	0.498
1.3	0.5	5	6	1.382	5.756	1.264
1.3	0.7	5	6	1.632	5.965	1.030
1.5	0	5	6	1.099	5.473	0.565
1.5	0.1	5	6	1.142	5.096	0.947
1.5	0.3	5	6	1.218	5.574	0.897
1.5	0.5	5	6	1.382	5.665	0.975
1.5	0.7	5	6	1.619	8.828	0.977
1.7	0	5	6	1.134	5.030	0.689
1.7	0.1	5	6	1.152	4.892	0.753
1.7	0.3	5	6	1.215	5.958	0.675
1.7	0.5	5	6	1.383	5.625	0.526
1.7	0.7	5	6	1.631	5.918	0.840
2	0	4	5	0.440	4.319	2.720
2	0.1	5	6	1.535	4.087	0.479
2	0.3	5	6	1.451	4.167	0.702
2	0.5	5	6	1.383	5.623	0.540
2	0.7	4	5	0.603	4.740	2.036
2.5	0	4	5	1.586	4.474	3.182
2.5	0.1	4	5	1.579	4.452	3.142
2.5	0.3	5	6	2.248	4.065	0.899
2.5	0.5	4	5	1.205	4.728	2.721
2.5	0.7	5	5	1.448	3.137	2.462

5.1. SIMULATION EXAMPLE

To verify the use of the Double Sampling S^2 control chart with the optimized parameters, a simulation example is proposed.

In this example, 100 thousand data of $X \sim N(0, \sigma_p{}')$ and $\varepsilon \sim N(0, \sigma_m)$ were simulated, and the observed values of the quality characteristic was calculated using Equation 34. For the DS S^2 chart, samples for n_1 and n_2 were collected from this database according to the process listed in the flowchart in Figure 11. For comparison, the S^2 chart was considered for $n = 5$ and $ARL_0 = 370.4$.

First, the DS S^2 chart optimized for $\delta_{opt}=1$ and $\sigma_{m\,opt}= 0$ is studied. The ARL and E(n) results obtained are presented in Table 11 for the cases with $\delta \in \{1.0, 1.1, 1.5, 2.0\}$ and $\sigma_m \in \{0, 0.5, 1.0\}$.

Table 11 – DS S² control chart with parameters optimized for $\delta_{opt} = 1$ and $\sigma_{m\,opt}= 0$

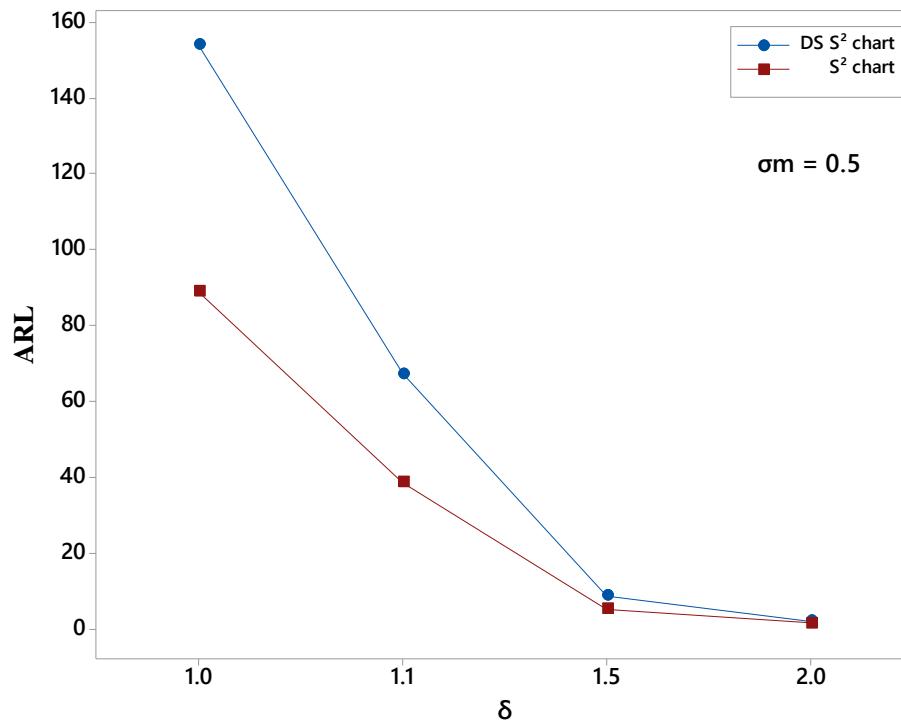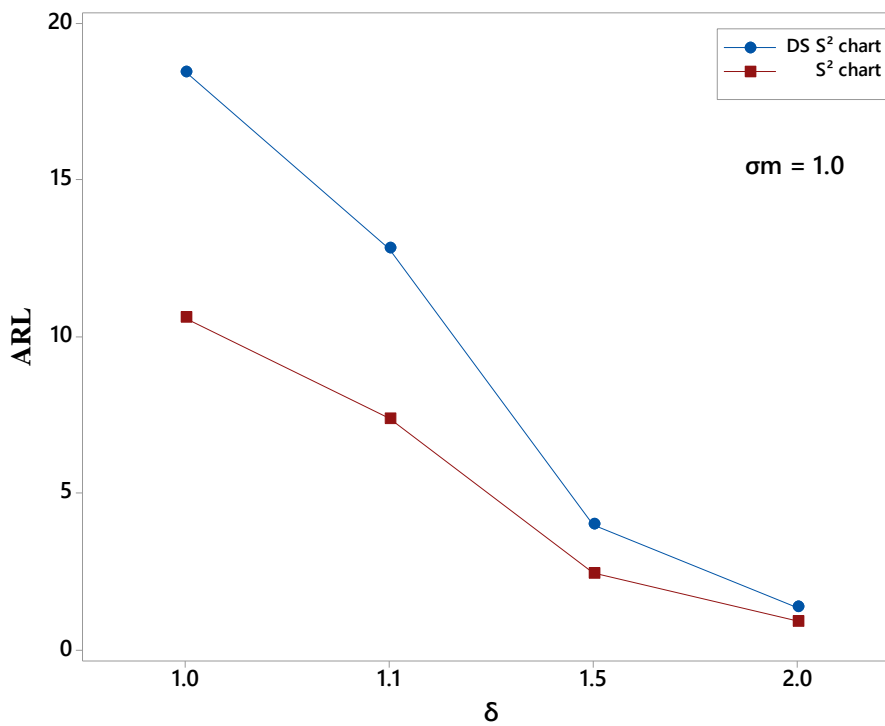|		DS S² chart		S² chart
δ	σ_m	n_1, n_2, k_1, k, k_3 5, 6, 0.595, 4.063, 4.808		$n=5$
		ARL	E(n)	ARL
	0	633.87	6.98	385.10
1.0	0.5	153.97	7.06	88.86
	1.0	18.44	6.90	10.58
	0	187.18	7.05	108.50
1.1	0.5	67.14	7.05	38.52
	1.0	12.80	6.81	7.36
	0	12.50	6.81	7.08
1.5	0.5	8.61	6.70	5.02
	1.0	3.99	6.42	2.44
	0	2.34	6.18	1.53
2.0	0.5	1.95	6.11	1.32
	1.0	1.34	5.94	0.90

Table 11 shows that the DS S² chart expected value for the sample size varied between 6 and 7. From the ARL results, the DS S^2 control chart performed better (highest ARL value) for δ = 1 in all evaluated measurement errors, even though it has been optimized for $\sigma_{m_{opt}}$= 0. However, for the cases in which δ = 1.1, 1.5, and 2.0, the S^2 control chart operated with a better (lower) ARL in most cases.

Figures 34, 35, and 36 shows the ARL results of the S^2 and DS S^2 charts for σ_m = 0.0, σ_m = 0.5, and σ_m = 1.0, respectively.

Figure 34 – ARL for the S² and DS S² control charts (σ_m = 0.0)
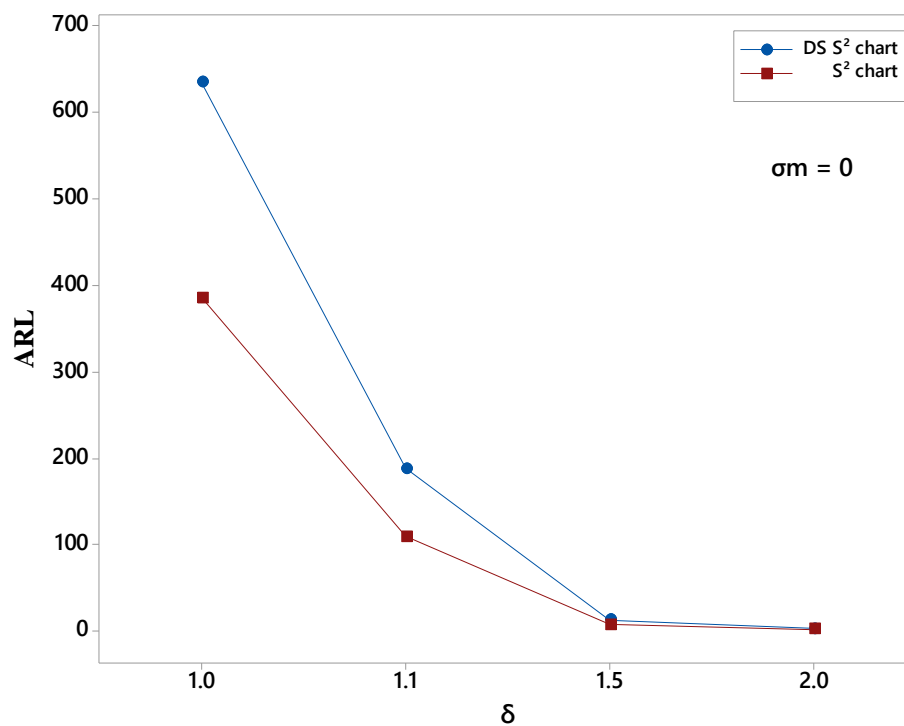
Figures 34, 35, and 36 shows that the most significant difference occurs for δ = 1.0, which is aligned with what is expected since the DS S^2 chart, in this case, was optimized with δ_{opt} = 1. It can be seen that the S^2 control chart outperforms the DS S^2 chart for δ = 1.1 and that the difference in performance between the two control charts reduces when δ = 1.5 and δ =2.0.

Figure 35 – ARL for the S² and DS S² control charts ($\sigma_m = 0.5$)

Figure 36 – ARL for the S² and DS S² control charts ($\sigma_m = 1.0$)

Figures 37 and 38 presents the ARL percentage difference of ARL in relation to the condition without the measurement error ($\sigma_m = 0$) for the DS S^2 control chart and the S^2 chart.

Figure 37 – ARL percentage difference for the DS S² and S² control charts ($\sigma_m = 0.5$)
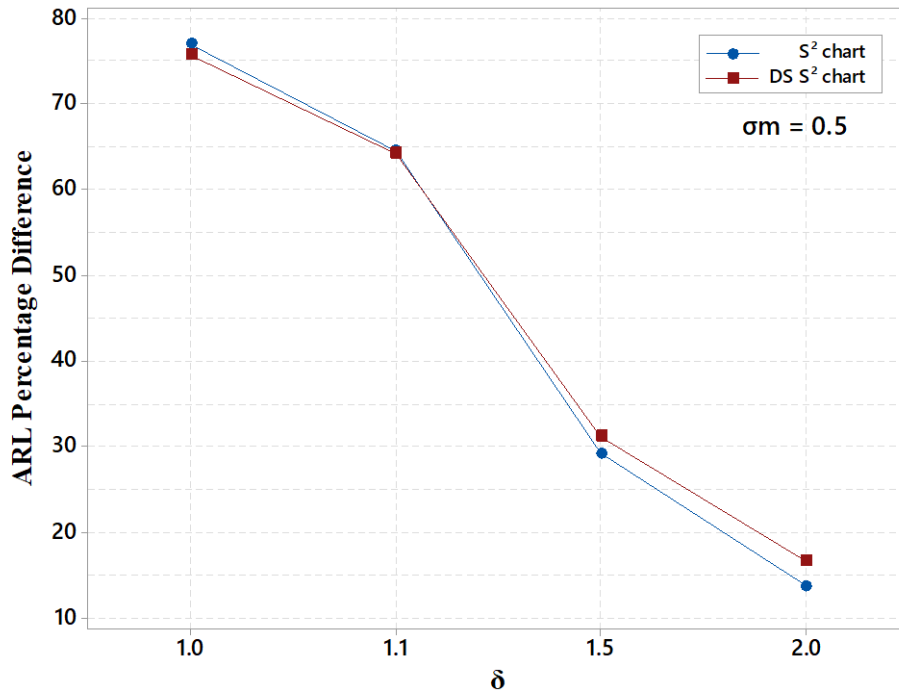
Figure 38 – ARL percentage difference for the DS S² and S² control charts ($\sigma_m = 1.0$)
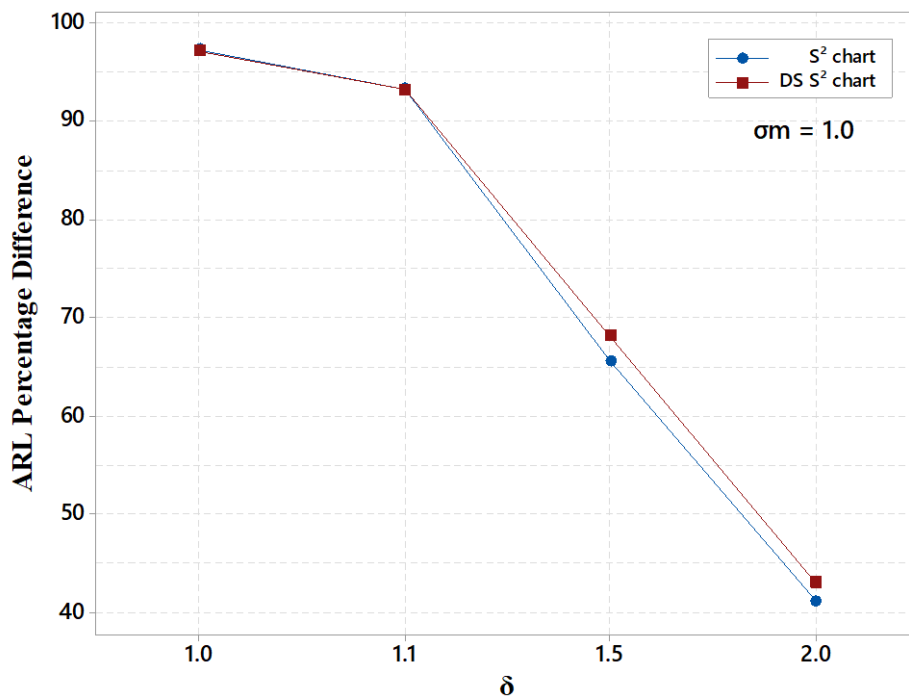
From Figure 37, for the case where $\sigma_m = 0.5$, the percentage differences were similar for the DS S^2 and S^2 charts. For $\delta = 1.0$, the impact of the measurement inaccuracy seems slightly smaller on the DS S^2 chart. As for $\delta = 1.5$ and $\delta = 2.0$, the S^2 chart suffers slightly

less from the error effect. From Figure 38, for the case where $\sigma_m = 1.0$, both control charts perform very similarly for $\delta = 1.0$ and $\delta = 1.1$. The impact of the measurement errors seems slightly smaller on the S^2 chart as the shift increases.

We can also notice from Figures 37 and 38 that the measurement error has a larger effect on the performance of the two control charts when the process is in control, the impact (ARL percentage difference) becomes smaller as that the magnitude of the shift increases.

Table 12 shows the comparison of ARL results for the S^2 control chart and three settings of the DS S^2 chart:

- Setting 1: $\delta_{opt} = 1.0$ and $\sigma_{m_{opt}} = 0.5$;
- Setting 2: $\delta_{opt} = 1.1$ and $\sigma_{m_{opt}} = 0.1$;
- Setting 3: $\delta_{opt} = 1.1$ and $\sigma_{m_{opt}} = 0.5$.

The optimal parameters ($\delta_{opt} = 1.0$, $\delta_{opt} = 1.1$, $\sigma_{m_{opt}} = 0.1$, and $\sigma_{m_{opt}} = 0.5$) were chosen for this example because, in most practical applications, measurement errors are expected to be low and the process is expected to be in an in-control state, or near to it. To verify the influence of measurement error, the optimal DS chart S^2 parameters for these settings were used.

Table 12 shows the ARL and E(n) values for the three DS S^2 chart settings. We can see that both for the case when the process is in control ($\delta = 1.0$) and when the process shifts ($\delta = 1.1$, $\delta = 1.5$, and $\delta = 2.0$), the ARL value decreases as the measurement error increases, which indicates the occurrence of more false alarms. However, for $\delta = 1.0$, the DS S^2 control charts optimized for Settings 1 and 3 suffer much less impact (lower percentage of ARL reduction) for measurement errors up to $\sigma_m = 0.5$ (value for which they were optimized) than when the S^2 control chart is used. This outcome can be seen in Figures 39, 40, and 41, which show the ARL percentage difference (for $\sigma_m = 0.5$) compared to the S^2 chart for the DS S^2 chart with Settings 1, 2, and 3, respectively.

From Table 12 it is observed that the DS S^2 chart with Setting 2 has the best performance (among the charts tested in the example) since it is close to the values obtained for the S^2 chart when operating with shifts 1.1, 1.5, and 2.0 (for all values of σ_m) and performs considerably better for $\delta = 1.0$ (state in which the process is expected to operate most

of the time). In this case (δ =1.0), for the DS S^2 chart we have ARL= 608.759, 143.959, and 16.564, for σ_m=0, 0.5, and 1.0, respectively, versus ARL = 385.104, 88.860, and 10.576 of the S^2 chart.

Table 12 – ARL results for DS S² control chart with parameters optimized for the effects of measurement error

δ	σ_m	Setting 1 n_1, n_2, k_1, k, k_3 5, 5, 0.670, 4.063, 5.470		Setting 2 n_1, n_2, k_1, k, k_3 5, 5, 0.793, 4.044, 4.158		Setting 3 n_1, n_2, k_1, k, k_3 5, 5, 0.854, 3.980, 3.483		S² chart n=5
		ARL	E(n)	ARL	E(n)	ARL	E(n)	ARL
1.0	0	791.97	6.67	608.76	6.70	837.5	6.35	385.10
	0.5	611.87	6.88	143.96	6.86	443.44	6.62	88.86
	1.0	45.82	6.97	16.56	6.82	29.43	6.84	10.58
1.1	0	791.33	6.84	179.46	6.84	579.73	6.58	108.50
	0.5	209.33	6.96	62.63	6.89	153.95	6.75	38.52
	1.0	45.44	6.98	11.49	6.76	19.34	6.82	7.369
1.5	0	28.19	6.92	11.08	6.74	18.27	6.82	7.08
	0.5	19.17	6.86	7.73	6.65	11.82	6.78	5.02
	1.0	8.22	6.63	3.50	6.40	4.89	6.60	2.44
2.0	0	4.48	6.39	2.02	6.18	2.72	6.41	1.53
	0.5	3.84	6.32	1.70	6.11	2.33	6.34	1.32
	1.0	2.46	6.13	1.20	5.97	1.54	6.18	0.90

Figures 42, 43, and 44 show the ARL percentage difference (for σ_m =1.0) for the S^2 chart and the DS S^2 chart with Settings 1, 2, and 3, respectively. Even though the measurement error effect for σ_m = 0.5 is lower in Settings 1 and 3 when the process is under control (Figures 39 and 41), for cases in which the process shifts, the DS S^2 control charts with Setting 1 and 3 show more vulnerability to the effects of measurement error than the S^2 chart. This result also holds for larger measurement errors (σ_m =1.0), as shown in Figures 42 and 44.
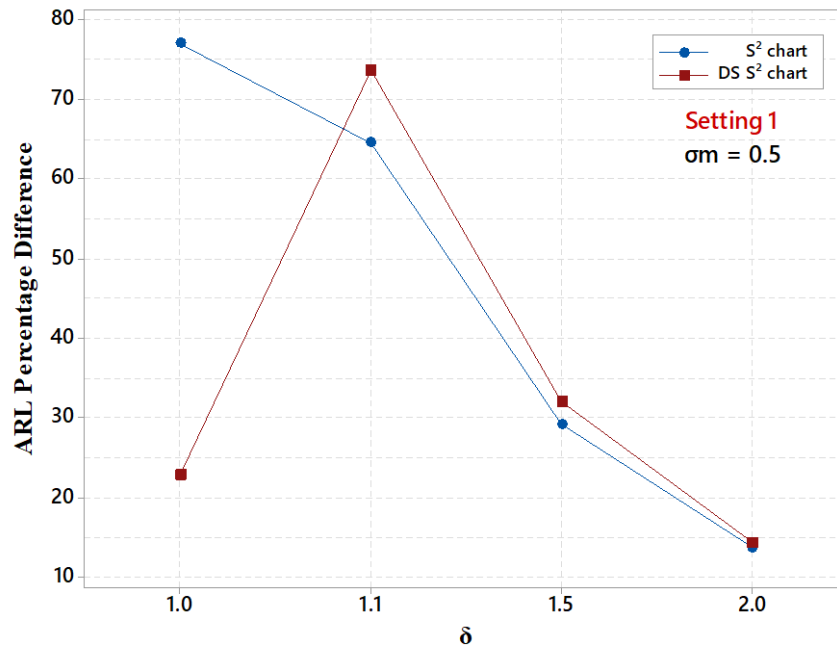
Figure 39 – ARL percentage difference for the S² and DS S² charts (Setting 1: $\sigma_m = 0.5$)

Figure 40 – ARL percentage difference for the S² and DS S² charts (Setting 2: $\sigma_m = 0.5$)

Figure 41 – ARL percentage difference for the S² and DS S² charts (Setting 3: $\sigma_m = 0.5$)

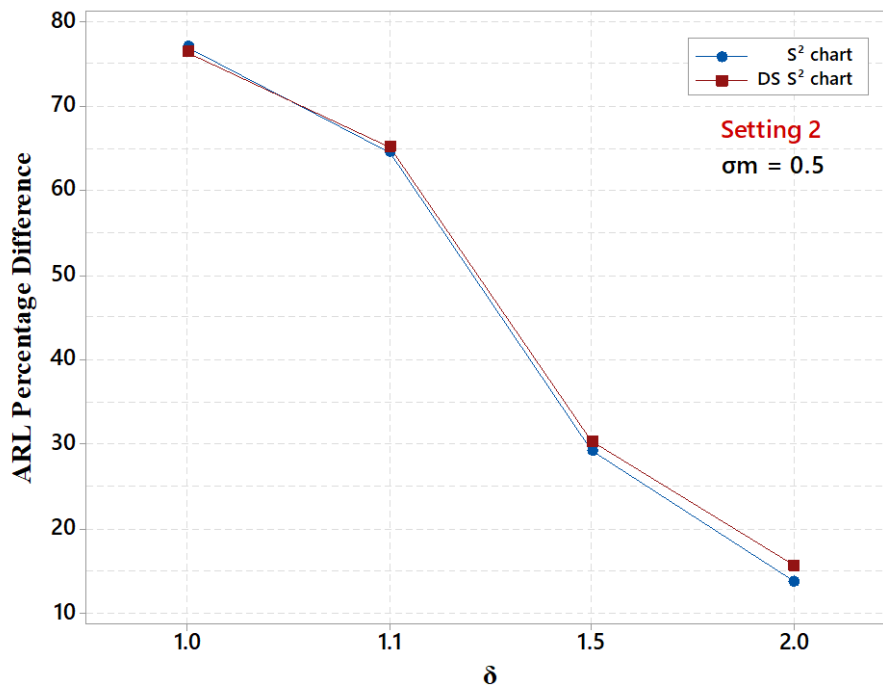

Figure 42 – ARL percentage difference for the S² and DS S² charts (Setting 1: $\sigma_m = 1.0$)

Figure 43 – ARL percentage difference for the S² and DS S² charts (Setting 2: $\sigma_m = 1.0$)

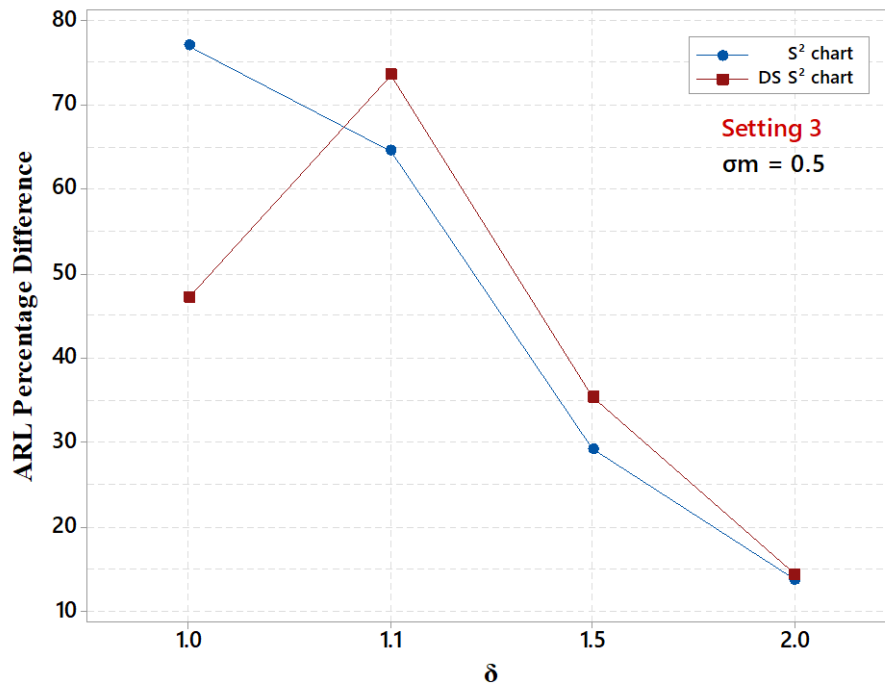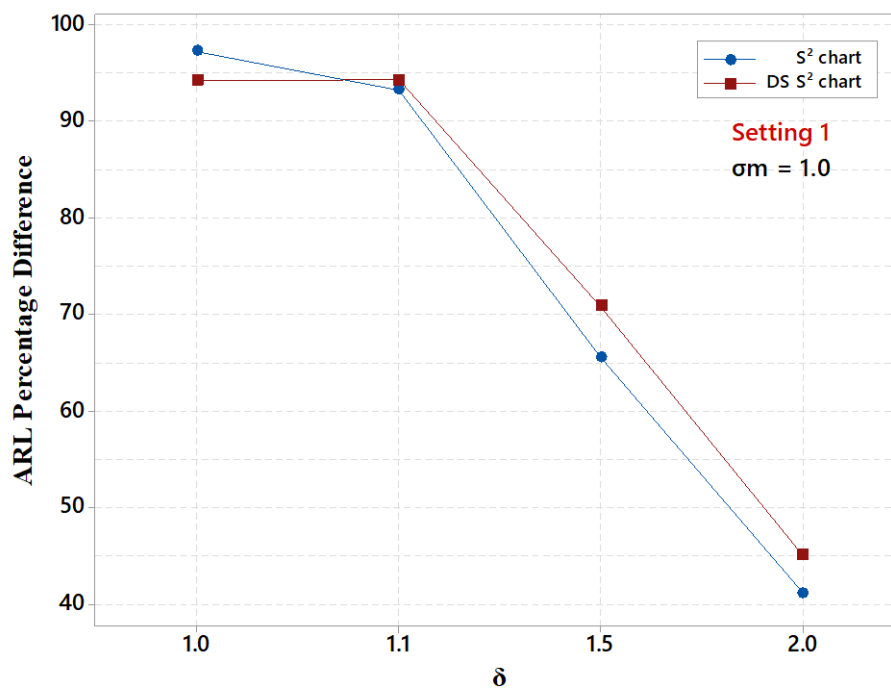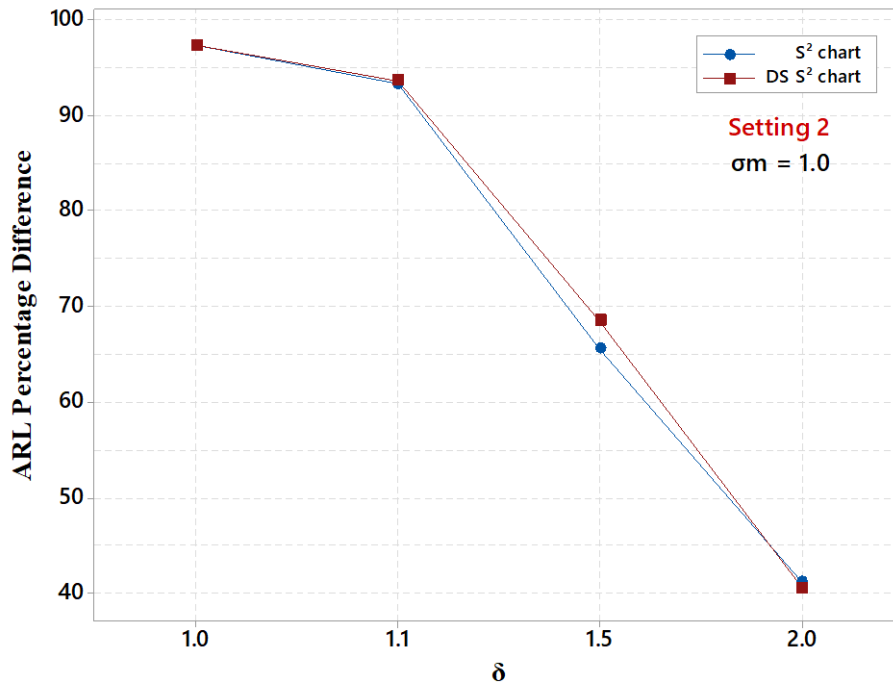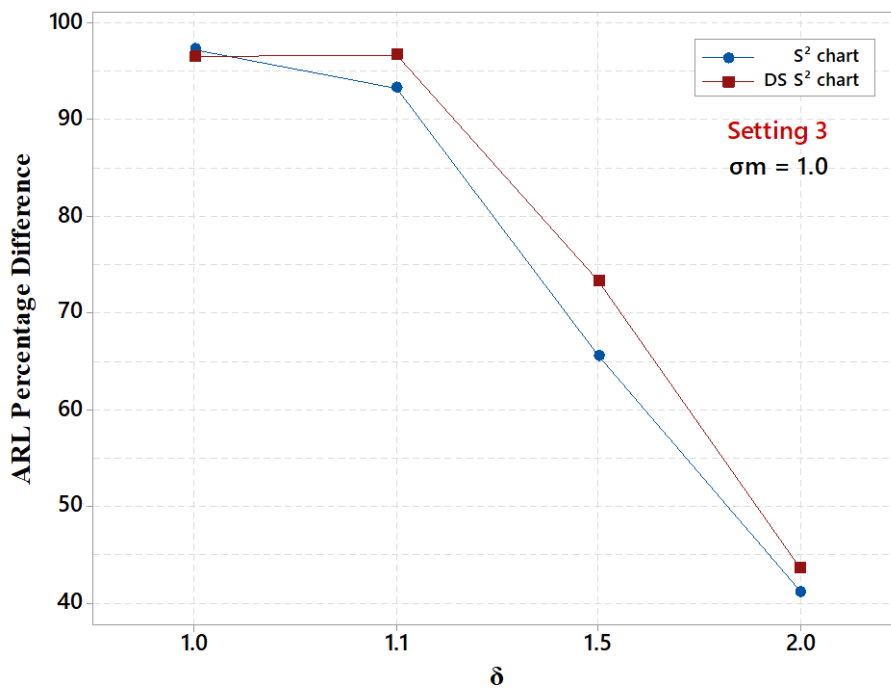

Figure 44 – ARL percentage difference for the S² and DS S² charts (Setting 3: $\sigma_m = 1.0$)

Considering that in practical applications, it may be necessary to monitor a process in which data is collected using a measurement system with larger measurement error, an example is now proposed that considers the use of a measurement system with $\sigma_m = 0.7$.

Table 13 show the ARL results considering the use of the S^2 control chart, the DS S^2 control chart optimized for $\delta_{opt} = 1.0$ and $\sigma_{m_{opt}}=0$ (Setting 0), and the DS S^2 control chart optimized for $\delta_{opt} = 1.0$ and $\sigma_{m_{opt}} = 0.7$ (Setting 4).

Table 13 – ARL results for S^2 chart and DS S² control chart ($\sigma_{m_{opt}} = 0.7$)

δ	σ_m	Setting 0		Setting 4		S² chart
		n_1, n_2, k_1, k, k_3 5, 6, 0.595, 4.063, 4.808		n_1, n_2, k_1, k, k_3 5,5,0.737,4.063,5.158		$n=5$
		ARL	E(n)	ARL	E(n)	ARL
1.0	0.7	63.32	7.47	589.23	6.78	22.90
	1.0	18.44	6.90	99.68	6.94	10.58
1.1	0.7	35.50	7.41	247.96	6.88	13.81
	1.0	12.80	6.81	61.75	6.94	7.37
1.5	0.7	6.70	6.93	25.92	6.88	3.08
	1.0	3.99	6.42	13.59	6.76	2.44
2.0	0.7	1.73	6.30	5.11	6.44	1.29
	1.0	1.34	5.95	3.77	6.32	0.90

Figures 45, 46, and 47 show the DS S^2 chart (Setting 0), the S² chart (Setting 4), and the S^2 chart when process' data have $\delta = 1.0$ and $\sigma_m = 0.7$. Figures 48, 49, and 50 show the DS S^2 chart (Setting 0), the S^2 chart (Setting 4), and the S^2 chart when process' data have $\delta = 1.1$ and $\sigma_m = 0.7$. Figures 51, 52, and 53 show the DS S^2 chart (Setting 0), the S^2 chart (Setting 4), and the S^2 chart when process' data have $\delta = 1.5$ and $\sigma_m = 0.7$. Figures 54, 55, and 56 show the DS S^2 chart (Setting 0), the S^2 chart (Setting 4), and the S^2 chart when process' data have $\delta = 2.0$ and $\sigma_m = 0.7$.

From the results in Table 13 and figures 45 to 56, we can clearly see the impact of larger measurement errors on the control charts. When the process is in control, both the DS S^2 chart optimized to operate without measurement errors and the traditional S^2 control chart show much lower ARL results than the DS S^2 control chart optimized $\sigma_{m_{opt}} = 0.7$ (Setting 4). For $\delta = 1.1$, 1.5, and 2.0, the Setting 4 DS S^2 control chart shows good detection ability. Although the S^2 and DS S^2 charts present lower ARL values for $\delta = 1.1$, 1.5, and 2.0, the cost of false alarms when operating in control makes them an unfavorable choice for larger measurement error scenarios.

Figure 45 – DS S² chart (Setting 0: $\delta = 1.0$, $\sigma_m = 0.7$)

Figure 46 – DS S² chart (Setting 4: $\delta = 1.0$, $\sigma_m = 0.7$)

Figure 47 – S² chart (δ = 1.0, σ_m = 0.7)

Figure 48 – DS S² chart (Setting 0: δ = 1.1, σ_m = 0.7)

Figure 49 – DS S² chart (Setting 4: δ = 1.1, σ_m = 0.7)

Figure 50 – S² chart (δ = 1.1, σ_m = 0.7)
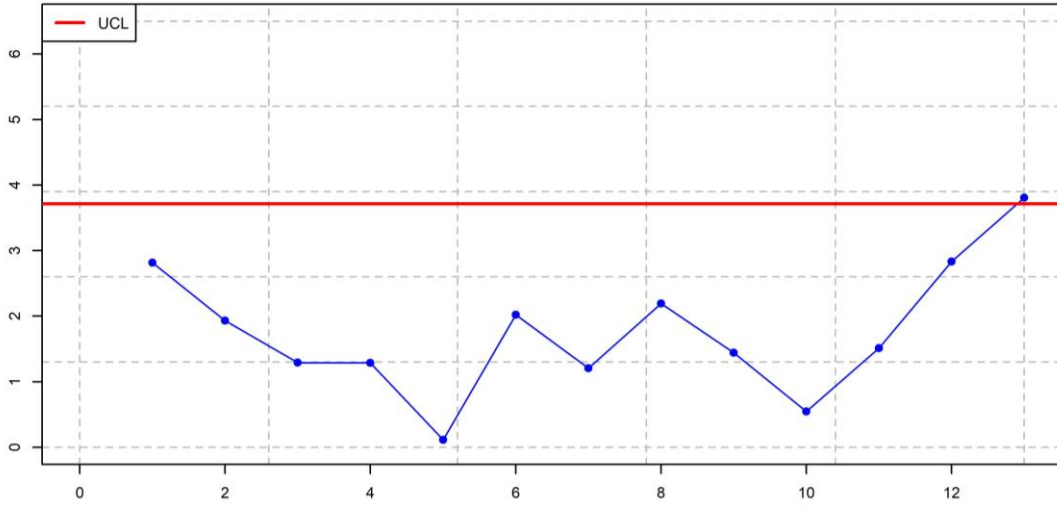
Figure 51 – DS S² chart (Setting 0: δ = 1.5, σ_m = 0.7)
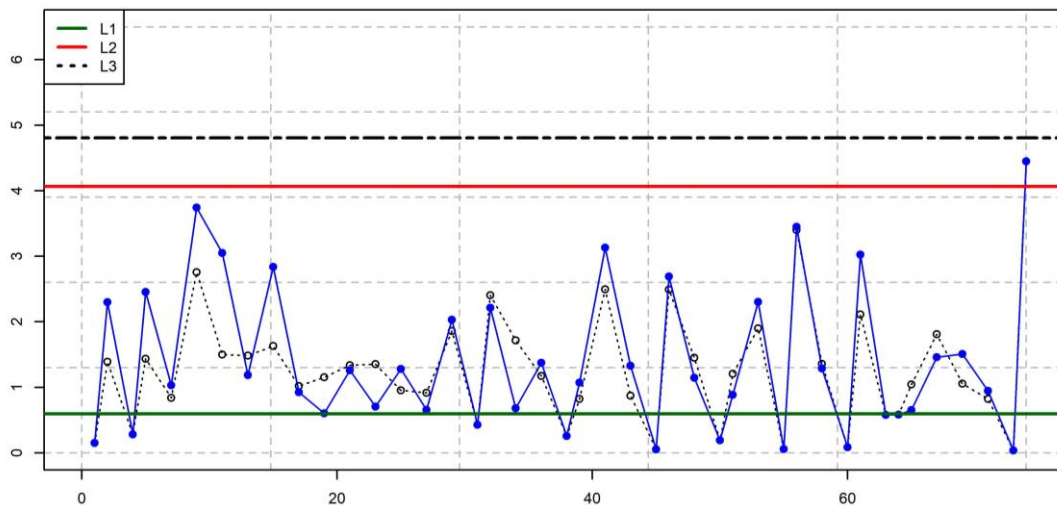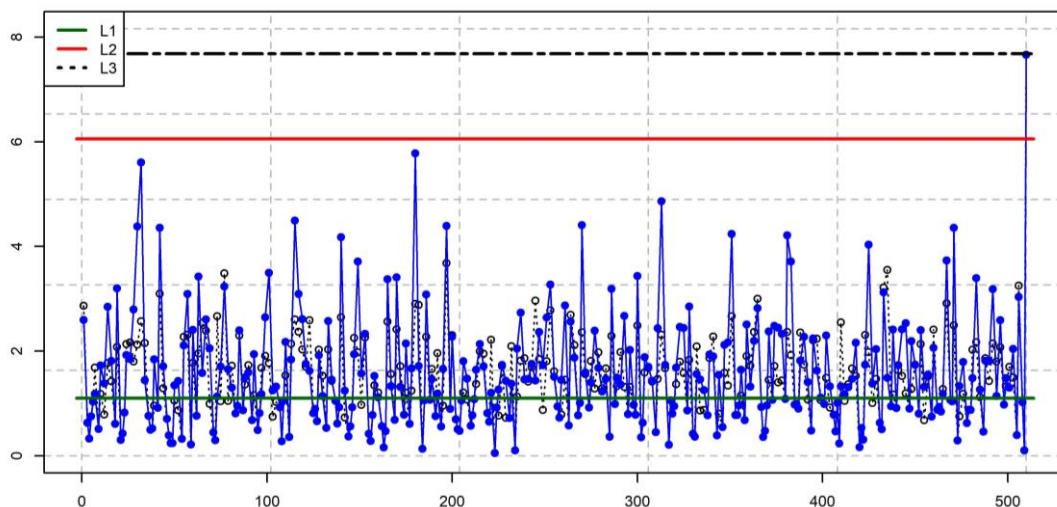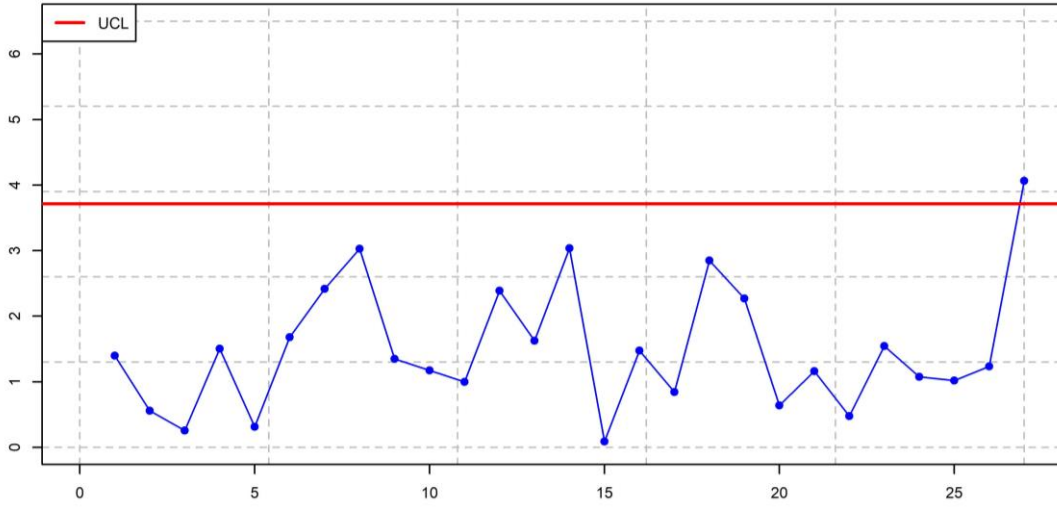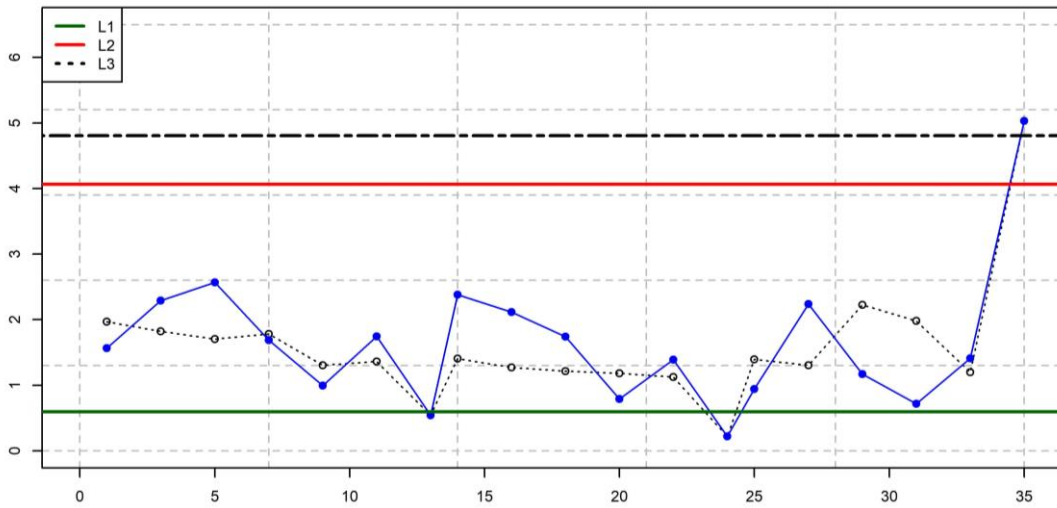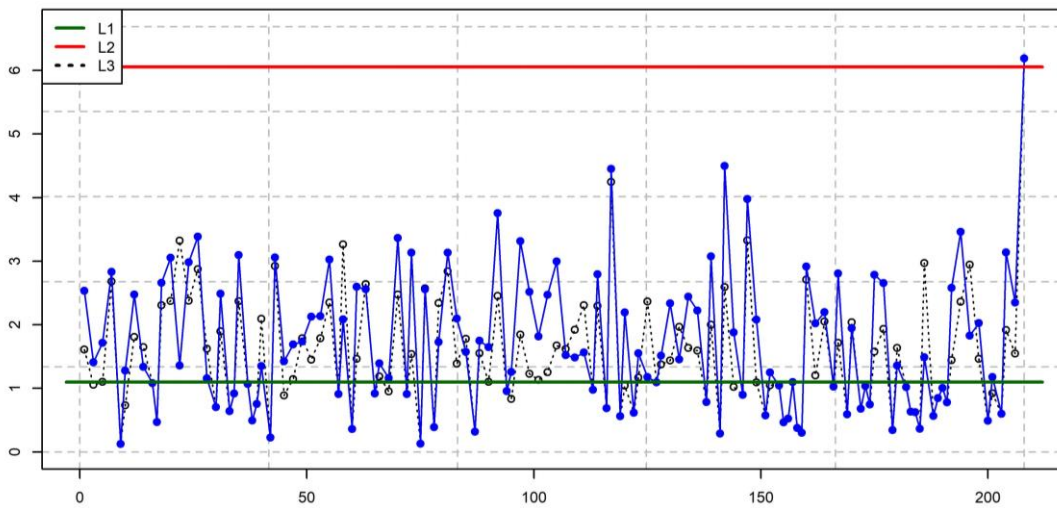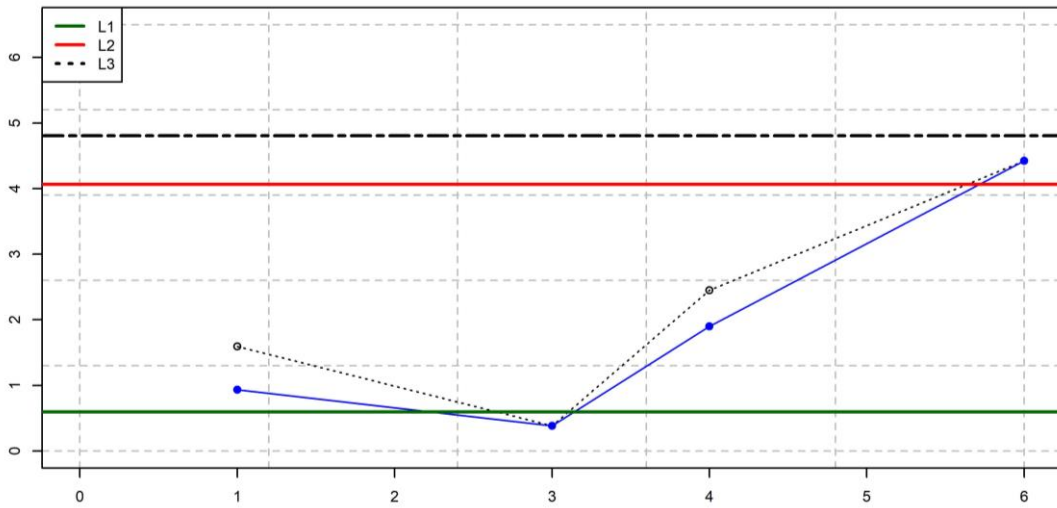

Figure 52 – DS S² chart (Setting 4: δ = 1.5, σ_m = 0.7)
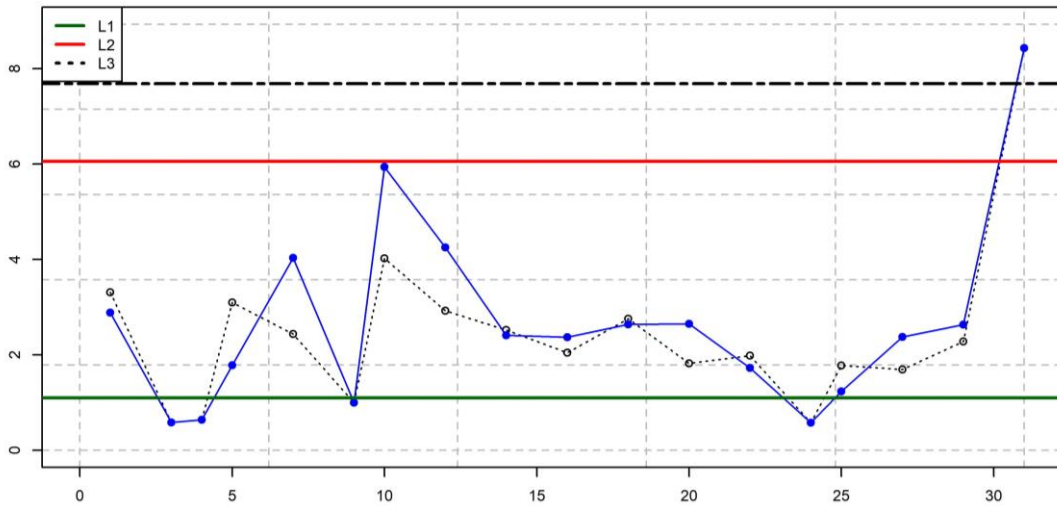
Figure 53 – S² chart (δ = 1.5, σ_m = 0.7)
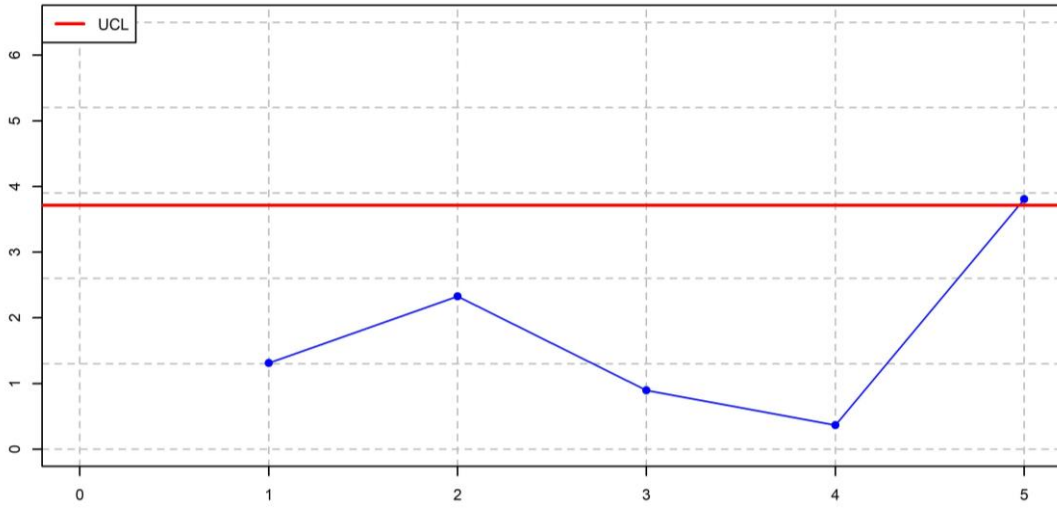
Figure 54 – DS S² chart (Setting 0: δ = 2.0, σ_m = 0.7)
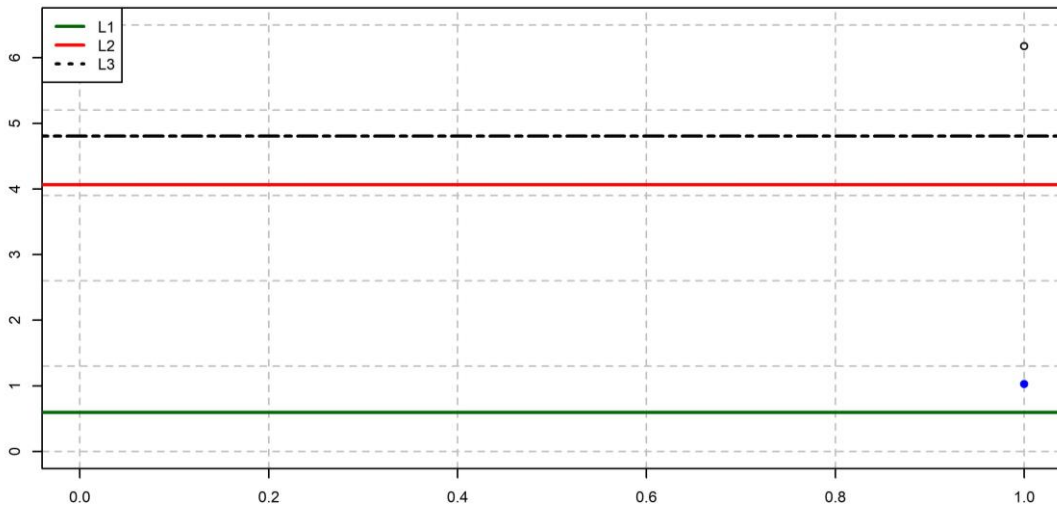
Figure 55 – DS S² chart (Setting 4: δ = 2.0, σ_m = 0.7)
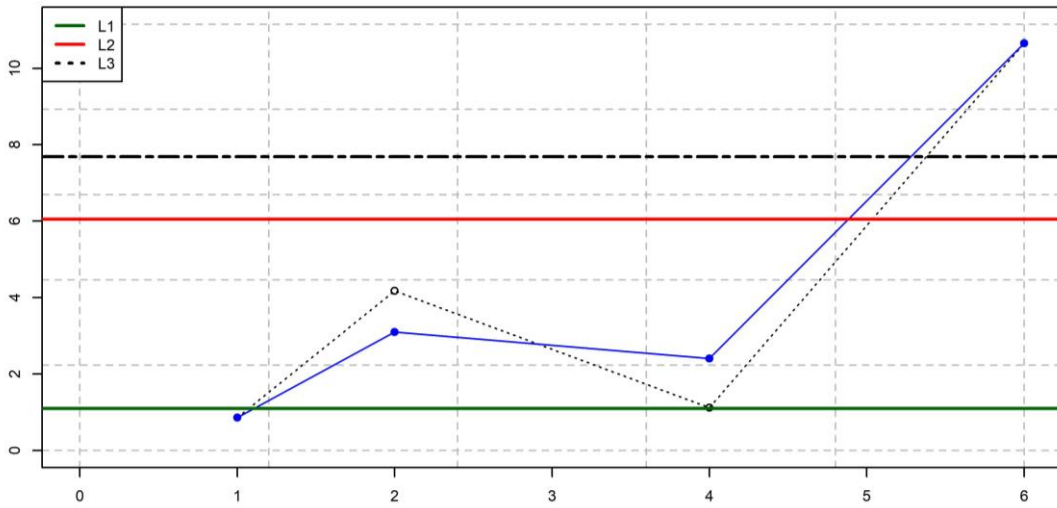
Figure 56 – S² chart ($\delta = 2.0$, $\sigma_m = 0.7$)
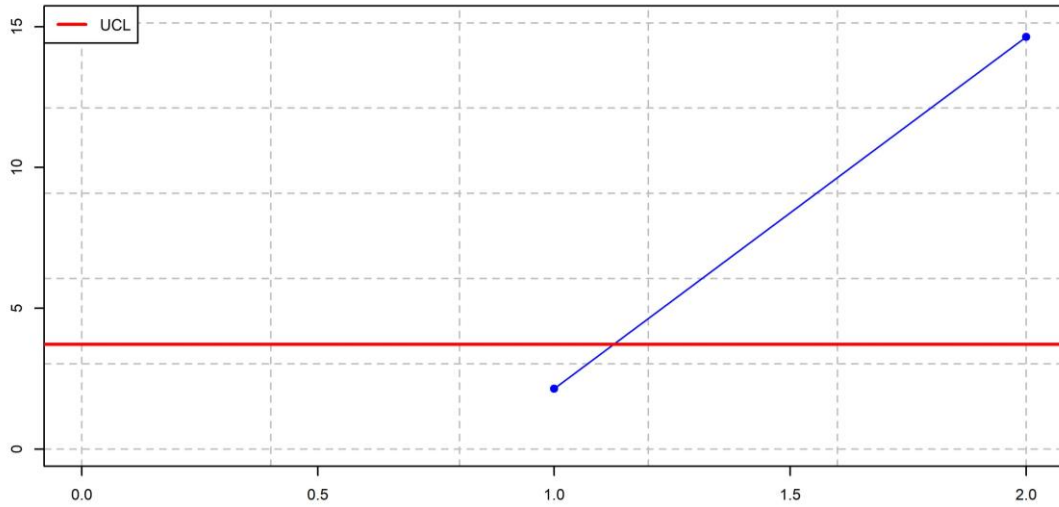
5.2. FINAL REMARKS

Based on the results presented in chapters 4 and 5, it is observed that the presence of measurement errors degrades the performance of the Double Sampling S^2 control chart in terms of ARL. For cases where the process operates under statistical control, the presence of measurement error tends to reduce the ARL value, with a greater impact as the error value increases. For cases where the process shift, the ARL result may be masked by the presence of measurement error, indicating a higher number of false alarms as the measurement error increases. Furthermore, when measurement errors are present, the DS S^2 control chart tends to consult Stage 2 more frequently, increasing the expected value of n as the measurement error increases.

It is observed that even small modifications to the control chart parameters significantly alter the obtained performance results. Considering the sample size reduction as an optimization problem and solving it using the genetic algorithm technique, a parameter table is obtained through the proposed optimization that allows using the Double Sampling S^2 control chart for different measurement error values. The utilization of the parameter table is useful for practical applications, particularly for larger measurement error values.

6. CONCLUSIONS

As a result of technological advancements, a greater quantity and variety of sensors and measuring systems are now being employed in production processes. Therefore, discussing the quality of these processes without bringing up their measurement error is becoming increasingly impractical.

One of the ways to quantify the quality of production processes is by controlling their variability. In this sense, control charts are an easy-to-use statistical tool that allows monitoring of different types of processes. Double Sampling charts have been studied recently as an alternative to improve monitoring performance. According to the systematic literature review findings, studies are still required to determine how measurement errors affect different Double Sampling control charts.

In this work, we propose to study the impact of measurement errors on the Double Sampling S^2 control chart. The present study initially investigated the effects of measurement errors for Double Sampling S^2 control charts with fixed limits. The average run length (ARL) value is used as the performance measure. It can be seen that the measurement error affects the ARL value both while the process is under control and when it shifts. Additionally, it has been noted that the measurement effect differs depending on the Double Sampling S^2 chart construction parameters.

Considering such changes in the performance of the DS S^2 control chart caused by modifying its parameters, a study of parameter optimization using a genetic algorithm is proposed. Through the optimization study, the DS S^2 control chart optimal parameters were obtained for different scenarios with and without the presence of measurement errors.

Through simulation, an illustrative example was proposed to show the use of optimized parameters. The simulation example results show that using optimized parameters for the measurement error case is beneficial compared to the no measurement error optimization. This result is even more expressive when the control chart is used in processes with measurement errors of greater magnitude.

It is worth noting that although results have been presented for the traditional S^2 chart, the objective of this work is not to make a comparative study of the performance of Double Sampling with the S^2 chart but rather to show the impacts of different measurement error values on the performance of the DS S^2 chart and to show the advantage of parameter optimization when it is not possible to change the measurement system used.

6.1. LIMITATIONS AND SUGGESTIONS FOR FUTURE WORK

Many of the studies that use genetic algorithm optimization in the literature use paid software, as the present study worked only with R programming language and with the researcher's private computer, the simulation time and computer's capacity for simulations were a limitation of the study.

This study was limited to observing the performance of the DS S^2 control chart using data simulation. A study that explores the practical application of optimization for a real case with known measurement error is suggested.

As shown in the systematic literature review, the effects of measurement errors and the optimization of Double Sampling control charts for the presence of measurement error still require further investigation. Expanding the study to other types of Double Sampling control charts is suggested, such as the effect of measurement error on the double sampling range control chart.

For this study, a process with known parameters was considered. However, true process parameters are rarely known and are usually estimated using retrospective in-control data. In practice, the estimates used to set the Phase II control chart limits are calculated based on the Phase I data obtained by measurements. Since no measurement is accurate, and the measuring system used in Phase I and Phase II are not always the same, the need for further investigation of the effects of measurement errors on both Phase I and Phase II measurements is evident. It is then suggested that this study be extended to the case in which the parameters are unknown.

Also, it would be interesting to investigate a wider range of sample size variations, such as considering a sample of size $n_1 = 1$ in the first stage and a larger sample in the second stage. Additionally, it would be worthwhile to evaluate the chart's performance results when measuring each item more than once and assess the variation of measurements for the same piece.

REFERENCES

ADAMS, B. M. Control Charts, Selection of. **Encyclopedia of Statistics in Quality and Reliability**, 2008.

ALEVIZAKOS, V.; CHATTERJEE, K.; KOUKOUVINOS, C. The extended homogeneously weighted moving average control chart. **Quality and Reliability Engineering International**, v. 37, n. 5, p. 2134–2155, 2021.

ALI, S. et al. On Designing Mixed Nonparametric Control Chart for Monitoring the Manufacturing Processes. **Arabian Journal for Science and Engineering**, v. 46, n. 12, p. 12117–12136, 2021.

AMERICAN SOCIETY FOR QUALITY. **Walter A. Shewhart, Father of statistical quality control**. Disponível em: <https://asq.org/about-asq/honorary-members/shewhart>. Acesso em: 20 dez. 2022.

AMIRI, A.; MOSLEMI, A.; DOROUDYAN, M. H. Robust economic and economic-statistical design of EWMA control chart. **Springer**, v. 78, n. 1–4, p. 511–523, 2015.

ANIS, M. Z. Basic process capability indices: An expository review. **International Statistical Review**, 2008.

ASLAM, M. et al. A mixed control chart for monitoring failure times under accelerated hybrid censoring. **Journal of Applied Statistics**, 2020.

ASLAM, M. et al. A new CUSUM control chart under uncertainty with applications in petroleum and meteorology. **PLoS ONE**, v. 16, n. 2 February 2021, p. e0246185, 2021.

BAKIR, S. T. A Quality Control Chart for Work Performance Appraisal. **Quality Engineering**, v. 17, n. 3, p. 429–434, 1 jul. 2005.

BAR-LEV, S. K.; BOUKAL, B. On a ump and curtailed double sampling test for proportions. **Communications in Statistics - Theory and Methods**, v. 29, n. 12, p. 2791–2803, 1 jan. 2000.

BERTRAND, J. W. M.; FRANSOO, J. C. Operations management research methodologies using quantitative modeling. **International Journal of Operations and Production Management**, v. 22, n. 2, p. 241–264, fev. 2002.

BEST, M.; NEUHAUSER, D. Walter A Shewhart, 1924, and the Hawthorne factory. **Quality and Safety in Health Care**, v. 15, n. 2, p. 142–143, 1 abr. 2006.

BIPM. **JCGM 200:2012 International vocabulary of metrology – Basic and general concepts and associated terms (VIM)**. [s.l: s.n.].

BOONE, J. M.; CHAKRABORTI, S. Two simple Shewhart-type multivariate nonparametric control charts. **Applied Stochastic Models in Business and Industry**, v. 28, n. 2, p. 130–140, 2012.

BRADFORD, P. G.; MIRANTI, P. J. Information in an Industrial Culture: Walter A. Shewhart and the Evolution of the Control Chart, 1917–1954. **Information & Culture**, 2019.

CAMPUZANO, M. J.; CARRIÓN, A.; MOSQUERA, J. Characterisation and optimal design of a new double sampling c chart. **European Journal of Industrial Engineering**, v. 13, n. 6, p. 775–793, 2019.

CAROT, V.; JABALOYES, J. M.; CAROT, T. Combined double sampling and variable sampling interval X chart. **International Journal of Production Research**, v. 40, n. 9, p. 2175–2186, 2002.

CASTAGLIOLA, P.; OPRIME, P. C.; KHOO, M. B. C. The double sampling S2 chart with estimated process variance. **Communications in Statistics - Theory and Methods**, v. 46, n. 7, p. 3556–3573, 2017.

CHAKRABORTI, S.; GRAHAM, M. A. **Nonparametric Statistical Process Control**. [s.l.] John Wiley & Sons, 2018.

CHAKRABORTI, S.; GRAHAM, M. A. Nonparametric (distribution-free) control charts: An updated overview and some results. **Quality Engineering**, v. 31, n. 4, p. 523–544, 2 out. 2019.

CHAMP, C. W.; APARISI, F. Double sampling Hotelling's T2 charts. **Quality and Reliability Engineering International**, v. 24, n. 2, p. 153–166, 2008.

CHEN, G. The run length distributions of the R, s and s 2 control charts when σ is estimated . **Canadian Journal of Statistics**, v. 26, n. 2, p. 311–322, 1998.

CHENG, Y.; SUN, L.; GUO, B. Phase II synthetic exponential charts and effect of parameter estimation. **Quality Technology & Quantitative Management**, v. 15, n. 1, p. 125–142, 2018.

CHONG, Z. L. et al. Group runs double sampling np control chart for attributes. **Journal of Testing and Evaluation**, v. 45, n. 6, 2017.

CHONG, Z. L.; KHOO, M. B. C.; CASTAGLIOLA, P. Synthetic double sampling np control chart for attributes. **Computers and Industrial Engineering**, v. 75, n. 1, p. 157–169, 2014.

CLARO, F. A. E.; COSTA, A. F. B.; MACHADO, M. A. G. Double sampling $\bar{X}$ control chart for a first order autoregressive process. **Pesquisa Operacional**, v. 28, n. 3, p. 545–562, 2008.

COSTA, A. The double sampling range chart. **Quality and Reliability Engineering International**, v. 33, n. 8, p. 2739–2745, 2017.

COSTA, A. F. B.; CLARO, F. A. E. Double sampling $\bar{x}$ control chart for a first-order autoregressive moving average process model. **International Journal of Advanced Manufacturing Technology**, v. 39, n. 5–6, p. 521–542, 2008.

COSTA, A. F. B.; MACHADO, M. A. G. Bivariate control charts with double sampling. **Journal of Applied Statistics**, v. 35, n. 7, p. 809–822, 2008.

CROASDALE, R. Control charts for a double-sampling scheme based on average production run lengths. **International Journal of Production Research**, v. 12, n. 5, p. 585–592, 1974.

DAUDIN, J. J. Double Sampling $\bar{X}$ Charts. **Journal of Quality Technology**, v. 24, n. 2, p. 78–87, 1992.

DE ARAÚJO RODRIGUES, A. A.; EPPRECHT, E. K.; DE MAGALHÃES, M. S. Double-sampling control charts for attributes. **Journal of Applied Statistics**, v. 38, n. 1, p. 87–112, 2011.

DEMING, W. E. **Out of the Crisis**. [s.l.] MIT press, 1986.

DIKO, M. D. et al. Phase II control charts for monitoring dispersion when parameters are estimated. **Quality Engineering**, v. 29, n. 4, p. 605–622, 2017.

DODGE, H. F.; ROMIG, H. G. A method of sampling inspection. **The Bell System Technical Journal**, v. 8, n. 4, p. 613–631, 1929.

EIZI, A.; SADEGHPOUR GILDEH, B.; EHSAN MONABBATI, S. Comparison between two methods of the economic-statistical design of profile monitoring under the double sampling scheme. **Journal of Statistical Computation and Simulation**, v. 90, n. 18, p. 3400–3421, 2020.

EPPRECHT, E. K.; LOUREIRO, L. D.; CHAKRABORTI, S. Effect of the amount of phase I data on the phase II performance of S2 and S control charts. **Journal of Quality Technology**, v. 47, n. 2, p. 139–155, 2015.

FABBRI, S. et al. **Improvements in the StArt tool to better support the systematic review process**. ACM International Conference Proceeding Series. **Anais**...2016

FARAZ, A.; HEUCHENNE, C.; SANIGA, E. Optimal T2 control chart with a double sampling scheme–an alternative to the MEWMA chart. **Quality and Reliability Engineering International**, v. 28, n. 7, p. 751–760, 2012.

GANGULY, A. **Economic Design of Control Charts Using Metaheuristic Approaches**National Institute of Technology Rourkela, , 2016.

GANGULY, A.; PATEL, S. K. A teaching-learning based optimization approach for economic design of X-bar control chart. **Applied Soft Computing Journal**, v. 24, p. 643–653, 2014.

GERALD, C. F.; WHEATLEY, P. O. Applied numerical analysis. **Reading, MA: Addison-Wesley Publishing Co, 1989.**, 1989.

GHAFFAR, Y. A.; ALI, F. A. M.; AHMED, A. R. Review of Economic Statistical Design X-bar Chart with Six Sigma Idea. **International Journal of Scientific & Engineering Research**, v. 12, n. 4, p. 254–264, 2021.

GHASEMI ESHKAFTAKI, Z.; ZEINAL HAMADANI, A.; AHMADI YAZDI, A. Evaluating Parameter Estimation Effect on the Polynomial Profile Monitoring Methods' Phase II Performance. **Advances in Industrial Engineering**, v. 55, n. 2, p. 133–150, 2021.

GODINA, R. et al. Improvement of the statistical process control certainty in an automotive manufacturing unit. **Procedia Manufacturing**, v. 17, p. 729–736, 2018.

GRIGORYAN, A.; HE, D. Multivariate double sampling |S| charts for controlling process variability. **International Journal of Production Research**, v. 43, n. 4, p. 715–730, 2005.

HACK, P. S.; TEN CATEN, C. S. **Effect of Measurement Uncertainty in Control Charts**.

XVIII International Conference on Industrial Engineering and Operations Management. **Anais**...Guimarães, Portugal: 2012

HAQ, A.; KHOO, M. B. C. A new double sampling control chart for monitoring process mean using auxiliary information. **Journal of Statistical Computation and Simulation**, v. 88, n. 5, p. 869–899, 2018.

HAQ, A.; KHOO, M. B. C. A synthetic double sampling control chart for process mean using auxiliary information. **Quality and Reliability Engineering International**, v. 35, n. 6, p. 1803–1825, 2019.

HE, D.; GRIGORYAN, A. Construction of double sampling s-control charts for agile manufacturing. **Quality and reliability engineering international**, v. 18, n. 4, p. 343–355, 2002.

HE, D.; GRIGORYAN, A. An improved double sampling s chart. **International Journal of Production Research**, v. 41, n. 12, p. 2663–2679, 2003.

HE, D.; GRIGORYAN, A. Multivariate multiple sampling charts. **IIE Transactions (Institute of Industrial Engineers)**, v. 37, n. 6, p. 509–521, 2005.

HE, D.; GRIGORYAN, A. Joint statistical design of double sampling $\bar{X}$ and s charts. **European Journal of Operational Research**, v. 168, n. 1, p. 122–142, 2006.

HE, D.; GRIGORYAN, A.; SIGH, M. Design of double-and triple-sampling X-bar control charts using genetic algorithms. **International Journal of Production Research**, v. 40, n. 6, p. 1387–1404, 2002.

HINDERKS, A. et al. **An SLR-Tool: Search Process in Practice : To conduct and manage Systematic Literature Review (SLR)**. Proceedings - 2020 ACM/IEEE 42nd International Conference on Software Engineering: Companion, ICSE-Companion 2020. **Anais**...2020

HRYNIEWICZ, O.; KACZMAREK-MAJER, K. Monitoring of non-stationary health-recovery processes with control charts. **Int. J. Adv. Life Sci**, 2018.

HSU, L. Note on 'Construction of Double Sampling s-Control Charts for Agile Manufacturing'. **Quality and Reliability Engineering International**, v. 23, n. 2, p. 269–272, 2007.

HSU, L. F. Note on "design of double- and triple-sampling X-bar control charts using genetic algorithms". **International Journal of Production Research**, v. 42, n. 5, p. 1043–1047, 2004.

HUANG, S.; YANG, J.; XIE, M. A double-sampling SPM scheme for simultaneously monitoring of location and scale shifts and its joint design with maintenance strategies. **Journal of Manufacturing Systems**, v. 54, p. 94–102, 2020.

INGHILLERI, R.; LUPO, T.; PASSANNANTI, G. An effective double sampling scheme for the c control chart. **Quality and Reliability Engineering International**, v. 31, n. 2, p. 205–216, 2015.

IRIANTO, D.; JULIANI, A. A two control limits double sampling control chart by optimizing producer and customer risks. **ITB Journal of Engineering Science**, v. 42 B, n. 2,

p. 165–178, 2010.

IRIANTO, D.; SHINOZAKI, N. An optimal double sampling $\bar{X}$ control chart. **International Journal of Industrial Engineering : Theory Applications and Practice**, v. 5, n. 3, p. 226–234, 1998.

IZIY, A.; GILDEH, B. S.; MONABBATI, E. Comparison between the economic-statistical design of double and triple sampling X control charts. **Stochastics and Quality Control**, v. 32, n. 1, p. 49–61, 2017.

JAFARIAN-NAMIN, S. et al. Robust Economic-statistical design of acceptance control chart. **Journal of Quality Engineering and Production Optimization**, v. 4, n. 1, p. 55–72, 2019.

JARDIM, F. S.; CHAKRABORTI, S.; EPPRECHT, E. K. X^- Chart with Estimated Parameters: The Conditional ARL Distribution and New Insights. **Production and Operations Management**, 2019.

JAVAID, A.; NOOR-UL-AMIN, M.; HANIF, M. Performance of Max-EWMA control chart for joint monitoring of mean and variance with measurement error. **Communications in Statistics: Simulation and Computation**, p. 1–26, 2020.

JENSEN, W. A. et al. Effects of parameter estimation on control chart properties: A literature review. **Journal of Quality Technology**, v. 38, n. 4, p. 349–364, 2006.

JOEKES, S.; SMREKAR, M.; BARBOSA, E. P. Extending a double sampling control chart for non-conforming proportion in high quality processes to the case of small samples. **Statistical Methodology**, v. 23, p. 35–49, 2015.

KANAZUKA, T. The Effect of Measurement Error on the Power of $\bar{X}$-R Charts. **Journal of Quality Technology**, v. 18, n. 2, p. 91–95, abr. 1986.

KATEBI, M.; KHOO, M. B. C. Optimal economic statistical design of combined double sampling and variable sampling interval multivariate T 2 control charts. **Journal of Statistical Computation and Simulation**, v. 91, n. 10, p. 2094–2115, 2021.

KATEBI, M.; MOGHADAM, M. B. A double sampling multivariate T2 control chart with variable sample size and variable sampling interval. **Communications in Statistics: Simulation and Computation**, v. 51, n. 7, p. 3578–3595, 2022.

KATEBI, M. S. M.; RAHIM, A. A special double sampling three-level control chart. **Communications in Statistics: Simulation and Computation**, 2022.

KHEE YONG SI, K. S. et al. The economic design of the double sampling x chart with measurement errors. **International Journal of Difference Equations**, v. 15, n. 2, p. 259–274, 2021.

KHIRED, A. A.; ASLAM, M.; DOBBAH, S. A. Refined double sampling scheme with measures and application. **Stat**, v. 10, n. 1, 2021.

KHOO, M. B. C. S2 control chart based on double sampling. **International Journal of Pure and Applied Mathematics**, v. 13, n. 2, p. 249–258, 2004.

KHOO, M. B. C. et al. A synthetic double sampling control chart for the process mean. **IIE**

Transactions (Institute of Industrial Engineers), v. 43, n. 1, p. 23–38, 2011.

KHOO, M. B. C. **Power functions of the Shewhart control chart**. Journal of Physics: Conference Series. **Anais**...IOP Publishing, 2013

KHOO, M. B. C. et al. A multivariate synthetic double sampling T2 control chart. **Computers and Industrial Engineering**, v. 64, n. 1, p. 179–189, 2013.

KNOBLOCH, K.; YOON, U.; VOGT, P. M. Preferred reporting items for systematic reviews and meta-analyses (PRISMA) statement and publication bias. **Journal of Cranio-Maxillofacial Surgery**, v. 39, n. 2, p. 91–92, mar. 2011.

LEE, M. H. et al. The effect of measurement errors on the double sampling X chart. **Compusoft**, v. 8, n. 9, p. 3395–3401, 2019.

LEE, M. H.; KHOO, M. B. C. Combined double sampling and variable sampling interval np chart. **Communications in Statistics - Theory and Methods**, v. 46, n. 23, p. 11892–11917, 2017a.

LEE, M. H.; KHOO, M. B. C. Synthetic double sampling s chart. **Communications in Statistics - Theory and Methods**, v. 46, n. 12, p. 5914–5931, 2017b.

LEE, M. H.; KHOO, M. B. C. Economic-statistical design of double sampling S control chart. **International Journal for Quality Research**, v. 12, n. 2, p. 337–362, 2018a.

LEE, M. H.; KHOO, M. B. C. Double sampling| S| control chart with variable sample size and variable sampling interval. **Communications in Statistics-Simulation and Computation**, v. 47, n. 2, p. 615–628, 2018b.

LEE, P.-H. et al. Monitoring the coefficient of variation using a double-sampling control chart. **Communications in Statistics-Simulation and Computation**, p. 1–15, 2021.

LEE, P.-H.; CHANG, Y.-C.; TORNG, C.-C. A design of s control charts with a combined double sampling and variable sampling interval scheme. **Communications in Statistics - Theory and Methods**, v. 41, n. 1, p. 153–165, 2012.

LEE, P.-H.; TORNG, C.-C.; LIAO, L.-F. An economic design of combined double sampling and variable sampling interval X control chart. **International Journal of Production Economics**, v. 138, n. 1, p. 102–106, 2012.

LEWICKI, P.; HILL, T. **Statistics : Methods and Applications - A comprehensive reference for science, industry and data mining**. [s.l.] StatSoft, Inc., 2006. v. 1

LI, J.; HUANG, S. Regression-based process monitoring with consideration of measurement errors. **IIE Transactions**, v. 42, n. 2, p. 146–160, 2009.

LIBERATI, A. et al. The PRISMA statement for reporting systematic reviews and meta-analyses of studies that evaluate health care interventions: explanation and elaboration. **Journal of clinical epidemiology**, v. 62, n. 10, p. e1–e34, 2009.

LINNA, K. W.; WOODALL, W. H. Effect of Measurement Error on Shewhart Control Charts. **Journal of Quality Technology**, v. 33, n. 2, p. 213–222, 2001.

MABUDE, K.; MALELA-MAJIKA, J. C.; SHONGWE, S. C. A new distribution-free generally weighted moving average monitoring scheme for detecting unknown shifts in the process location. **International Journal of Industrial Engineering Computations**, v. 11, n. 2, p. 235–254, 2020.

MACHADO, M. A. G.; COSTA, A. F. B. The double sampling and the EWMA charts based on the sample variances. **International Journal of Production Economics**, v. 114, n. 1, p. 134–148, 2008.

MACII, D.; CARBONE, P.; PETRI, D. Management of measurement uncertainty for effective statistical process control. **IEEE Transactions on Instrumentation and Measurement**, v. 52, n. 5, p. 1611–1617, 2003.

MALEKI, M. R. et al. The effect of gauge measurement errors on double sampling control chart. **Communications in Statistics - Theory and Methods**, v. 52, n. 8, p. 2702–2717, 2023.

MALEKI, M. R.; AMIRI, A.; CASTAGLIOLA, P. Measurement errors in statistical process monitoring: A literature review. **Computers and Industrial Engineering**, v. 103, p. 316–329, 2017.

MALEKI, M. R.; AMIRI, A.; CASTAGLIOLA, P. An overview on recent profile monitoring papers (2008–2018) based on conceptual classification scheme. **Computers and Industrial Engineering**, v. 126, p. 705–728, 2018.

MALEKI, M. R.; MALEKI, F.; DIZABADI, A. K. Decreasing the effect of measurement errors on detecting and diagnosing performance of MAX-EWMAMS control chart in Phase II. **International Journal of Quality Engineering and Technology**, v. 6, n. 1–2, p. 54–66, 2016.

MALEKI, M. R.; SALMASNIA, A.; YARMOHAMMADI SABER, S. The Performance of Triple Sampling X Control Chart with Measurement Errors. **Quality Technology and Quantitative Management**, v. 19, n. 5, p. 587–604, 2022.

MALELA-MAJIKA, J.-C. et al. Distribution-free double-sampling precedence monitoring scheme to detect unknown shifts in the location parameter. **Quality and Reliability Engineering International**, v. 37, n. 8, p. 3580–3599, 2021.

MALELA-MAJIKA, J.-C.; RAPOO, E. M. Side-sensitive synthetic double sampling $\bar{X}$ control charts. **European Journal of Industrial Engineering**, v. 13, n. 1, p. 117–148, 2019.

MALELA-MAJIKA, J. C.; MOTSEPA, C. M.; GRAHAM, M. A. A new double sampling control chart for monitoring an abrupt change in the process location. **Communications in Statistics: Simulation and Computation**, v. 50, n. 3, p. 917–935, 2021.

MARAVELAKIS, P. E. **An investigation of some characteristics of univariate and multivariate control charts**. [s.l: s.n.].

MCCRACKEN, A. K.; CHAKRABORTI, S. Control charts for joint monitoring of mean and variance: An overview. **Quality Technology and Quantitative Management**, 2013.

MEIRA, M. R. M. DE; OPRIME, P. C.; MERGULHÃO, R. C. Analysis of deviation from

nominal control chart performance on short production runs. **Production**, v. 32, 2022.

MEREDITH, J. R. et al. Alternative research paradigms in operations. **Journal of Operations Management**, v. 8, n. 4, p. 297–326, 1989.

MIGUEL, P. A. C. et al. Metodologia de pesquisa em engenharia de produção e gestão de operações. 2010.

MIRABI, M.; FATEMI GHOMI, M. T.; JOLAI, F. Hybrid genetic algorithm for the economic-statistical design of variable sample size and sampling interval x-bar control chart. **Journal of Industrial Engineering and Management Studies**, v. 8, n. 2, p. 160–174, 2022.

MITTAG, H. J.; STEMANN, D. Gauge imprecision effect on the performance of the $\bar{X}$-S control chart. **Journal of Applied Statistics**, 1998.

MONTGOMERY, D. . . **Introduction to Statistical Quality Control**. [s.l.] Arizona State University, John Wiley & Sons, 2013.

MOSQUERA, J.; APARISI, F. Optimal double sampling control chart based on gauges. **Quality Engineering**, v. 32, n. 4, p. 693–704, 2020.

MOTSEPA, C. M. et al. Double sampling monitoring schemes: a literature review and some future research ideas. **Communications in Statistics: Simulation and Computation**, p. 1–29, 2021.

MOYA-FERNÁNDEZ, P. J.; ÁLVAREZ, E.; SKALSKÁ, H. The performance of control charts in the presence of assignable causes. **International Journal of Recent Technology and Engineering**, v. 7, n. 6, p. 458–463, 2019.

MUÑOZ, J. J.; CAMPUZANO, M. J.; MOSQUERA, J. Optimized np Attribute Control Chart Using Triple Sampling. **Mathematics**, v. 10, n. 20, 2022.

NELSON, L. S. Notes on the Shewhart Control Chart. **Journal of Quality Technology**, v. 31, n. 1, p. 124–126, 1999.

NOOROSSANA, R.; SHEKARY A, M.; DEHESHVAR, A. Combined variable sample size, sampling interval, and double sampling (CVSSIDS) adaptive control charts. **Communications in Statistics-Theory and Methods**, v. 44, n. 6, p. 1255–1269, 2015.

PAGE, E. S. Continuous Inspection Schemes. **Biometrika**, v. 41, n. 1/2, p. 100, 1954.

PATINO-RODRIGUEZ, C.; PÉREZ, D. M.; MANCO, O. U. Simulation approach for assessing the performance of the γEWMA control chart. **International Journal of Quality and Reliability Management**, 2021.

PEKIN ALAKOC, N.; APAYDIN, A. A Fuzzy Control Chart Approach for Attributes and Variables. **Engineering, Technology & Applied Science Research**, v. 8, n. 5, p. 3360–3365, 2018.

PERDIKIS, T. et al. An EWMA signed ranks control chart with reliable run length performances. **Quality and Reliability Engineering International**, v. 37, n. 3, p. 1266–1284, 2021.

QUINTERO-ARTEAGA, C. et al. Statistical design of an adaptive synthetic $\bar{X}$–X control chart for autocorrelated processes. **Quality and Reliability Engineering International**, 2022.

RAMLIE, F. et al. Classification performance of thresholding methods in the Mahalanobis–Taguchi system. **Applied Sciences**, v. 11, n. 9, p. 3906, 2021.

RAZALI, H. et al. Application of Fuzzy Control Charts: A Review of Its Analysis and Findings. **Lecture Notes in Mechanical Engineering**, p. 483–490, 2020.

RIAZ, M. Monitoring of process parameters under measurement errors. **Journal of Testing and Evaluation**, v. 42, n. 4, p. 980–988, 2014.

RIAZ, M. A sensitive non-parametric EWMA control chart. **Journal of the Chinese Institute of Engineers**, v. 38, n. 2, p. 208–219, 17 fev. 2015.

ROBERTS, S. W. Control Chart Tests Based on Geometric Moving Averages. **Technometrics**, v. 1, n. 3, p. 239–250, 1959.

ROZI, F. et al. Optimal Design of a Revised Double Sampling $\bar{X}$ Chart Based on Median Run Length. **Journal of Hunan University Natural Sciences**, v. 48, n. 7, 2021.

SABAHNO, H.; CASTAGLIOLA, P.; AMIRI, A. A variable parameters multivariate control chart for simultaneous monitoring of the process mean and variability with measurement errors. **Quality and Reliability Engineering International**, 2020.

SAEMIAN, M.; MALEKI, M. R.; SALMASNIA, A. Performance of Max-HEWMAMS control chart for simultaneous monitoring of process mean and variability in the presence of measurement errors. **International Journal of Applied Decision Sciences**, v. 16, n. 2, p. 165–188, 2023.

SAGHIR, A. et al. A EWMA control chart based on an auxiliary variable and repetitive sampling for monitoring process location. **Communications in Statistics: Simulation and Computation**, v. 48, n. 7, p. 2034–2045, 2019.

SAHA, S. et al. A side-sensitive modified group runs double sampling (SSMGRDS) control chart for detecting mean shifts. **Communications in Statistics: Simulation and Computation**, v. 47, n. 5, p. 1353–1369, 2018.

SALMASNIA, A.; MALEKI, M. R.; MIRZAEI, M. Double Sampling Adaptive Thresholding LASSO Variability Chart for Phase II Monitoring of High-Dimensional Data Streams. **Journal of Industrial Integration and Management**, 2023.

SATO, S. **Growing Importance of Fundamental Understanding of the Source of Process Variations**. 2006 14th IEEE International Conference on Advanced Thermal Processing of Semiconductors. **Anais**...2006

SCRUCCA, L. GA: A package for genetic algorithms in R. **Journal of Statistical Software**, v. 53, n. 4, p. 1–37, 2013.

ŞENTÜRK, S.; ANTUCHEVICIENE, J. Interval Type-2 Fuzzy c-Control Charts: An Application in a Food Company. **Informatica (Netherlands)**, v. 28, n. 2, p. 269–283, 2017.

SHEWHART, W. A. The Application of Statistics as an Aid in Maintaining Quality of a Manufactured Product. **Journal of the American Statistical Association**, v. 20, n. 152, p. 546–548, 1925.

SHEWHART, W. A. Economic Quality Control of Manufactured Product. **Bell System Technical Journal**, v. 9, n. 2, p. 364–389, 1930.

SHORE, H. Determining measurement error requirements to satisfy statistical process control performance requirements. **IIE Transactions (Institute of Industrial Engineers)**, v. 36, n. 9, p. 881–890, set. 2004.

SMITH, G. T. **Machine tool metrology: An industrial handbook**. [s.l.] Springer, 2016.

STATSOFT, I. Electronic statistics textbook. **Tulsa, OK: StatSoft**, 2011.

STOUMBOS, Z. G. et al. The state of statistical process control as we proceed into the 21st century. In: **Statistics in the 21st Century**. [s.l: s.n.].

TANG, A. et al. A new nonparametric adaptive EWMA control chart with exact run length properties. **Computers and Industrial Engineering**, v. 130, p. 404–419, 2019.

TEOH, W. L. et al. Optimal design of the double sampling X chart with estimated parameters based on median run length. **Computers & Industrial Engineering**, v. 67, p. 104–115, 2014.

TEOH, W. L. et al. A median run length-based double-sampling $\bar{X}$ chart with estimated parameters for minimizing the average sample size. **International Journal of Advanced Manufacturing Technology**, v. 80, n. 1–4, p. 411–426, 2015.

TEOH, W. L. et al. Exact run length distribution of the double sampling X chart with estimated process parameters. **South African Journal of Industrial Engineering**, v. 27, n. 1, p. 20–31, 2016.

THANWANE, M. et al. The effect of measurement errors on the performance of the homogenously weighted moving average X monitoring scheme. **Transactions of the Institute of Measurement and Control**, v. 43, n. 3, p. 728–745, 2021a.

THANWANE, M. et al. The use of fast initial response features on the homogeneously weighted moving average chart with estimated parameters under the effect of measurement errors. **Quality and Reliability Engineering International**, v. 37, n. 6, p. 2568–2586, 2021b.

TOMOHIRO, R.; ARIZONO, I.; TAKEMOTO, Y. Economic design of double sampling Cpm control chart for monitoring process capability. **International Journal of Production Economics**, v. 221, 2020.

TORNG, C.-C. et al. An economic design of double sampling over(X, -) charts for correlated data using genetic algorithms. **Expert Systems with Applications**, v. 36, n. 10, p. 12621–12626, 2009.

TORNG, C.-C.; CHUNG, S.-P.; CHEN, Y.-C. An economic-statistical design of the joint and S control charts with double sampling and variable sampling intervals. **Journal of Industrial and Production Engineering**, v. 31, n. 7, p. 452–457, 2014.

TORNG, C.-C.; LEE, P.-H. The performance of double sampling $\bar{X}$ control charts under non

normality. **Communications in Statistics: Simulation and Computation**, v. 38, n. 3, p. 541–557, 2009a.

TORNG, C.-C.; LEE, P.-H. **A modified statistical design model of double sampling $\overline{X}$ control chart**. Proceedings of the International MultiConference of Engineers and Computer Scientists. **Anais**...Citeseer, 2009b

TORNG, C.-C.; TSENG, C.-C.; LEE, P.-H. Non-normality and combined double sampling and variable sampling interval control charts. **Journal of Applied Statistics**, v. 37, n. 6, p. 955–967, 2010.

TUH, M. H. et al. Optimal statistical design of the double sampling np chart based on expected median run length. **Frontiers in Applied Mathematics and Statistics**, v. 8, 2022.

TUH, M. H. et al. Evaluating the Performance of Synthetic Double Sampling np Chart Based on Expected Median Run Length. **Mathematics**, v. 11, n. 3, 2023.

UMAR, A. A. et al. A combined variable sampling interval and double sampling control chart with auxiliary information for the process mean. **Transactions of the Institute of Measurement and Control**, v. 42, n. 6, p. 1151–1165, 2020.

VACHÁLEK, J. et al. Intelligent dynamic identification technique of industrial products in a robotic workplace. **Sensors**, v. 21, n. 5, p. 1–20, 2021.

VAN DINTER, R.; TEKINERDOGAN, B.; CATAL, C. Automation of systematic literature reviews: A systematic literature review. **Information and Software Technology**, v. 136, p. 106589, 2021.

WETHERILL, G. B.; ROWLANDS, R. J. **Reducing variation in the process industries**. International Conference on Control 1991. Control '91. **Anais**...1991

WILEY. Giants of quality - Walter Shewhart. **Quality and Reliability Engineering International**, v. 27, n. 8, p. 979, dez. 2011.

WOODALL, W. H.; MONTGOMERY, D. C. Research issues and ideas in statistical process control. **Journal of Quality Technology**, v. 31, n. 4, p. 376–386, 1999.

WOON, Y. H. Run length distribution of synthetic double sampling chart. **International Journal of Applied Engineering Research**, v. 12, n. 24, p. 14268–14272, 2017.

WU, Z. et al. An np control chart for monitoring the mean of a variable based on an attribute inspection. **International Journal of Production Economics**, v. 121, n. 1, p. 141–147, 2009.

XIE, M.; MUKHERJEE, A. "Advances in the theory and application of Statistical Process Control" – Celebrate the Quasquicentennial (125th) Birth Anniversary of the Father of Statistical Quality Control – Dr. Walter Andrew Shewhart. **Quality Technology & Quantitative Management**, v. 14, n. 4, p. 341–342, 2 out. 2017.

YANG, S.-F.; CHEN, L.-P.; LIN, C.-K. **Adjustment of Measurement Error Effects on Dispersion Control Chart with Distribution-Free Quality VariableSustainability**, 2023.

YANG, S.-F.; WU, S.-H. A double sampling scheme for process variability monitoring. **Quality and Reliability Engineering International**, v. 33, n. 8, p. 2193–2204, 2017a.

YANG, S.-F.; WU, S.-H. A double sampling scheme for process mean monitoring. **IEEE Access**, v. 5, p. 6668–6677, 2017b.

YANG, S. F. et al. A new phase II EWMA dispersion control chart. **Quality and Reliability Engineering International**, 2021.

YEONG, W. C. et al. Optimal designs of the side sensitive synthetic chart for the coefficient of variation based on the median run length and expected median run length. **Plos one**, v. 16, n. 7, p. e0255366, 2021.

YOU, H. W. Performance of Synthetic Double Sampling Chart with Estimated Parameters Based on Expected Average Run Length. **Journal of Probability and Statistics**, v. 2018, 2018.

YU, Y.; ZHANG, M. Control chart recognition based on the parallel model of CNN and LSTM with GA optimization. **Expert Systems with Applications**, v. 185, p. 115689, 2021.

ZADEH, L. Optimality and non-scalar-valued performance criteria. **IEEE transactions on Automatic Control**, v. 8, n. 1, p. 59–60, 1963.

ZAIRI, M. The TQM legacy - Gurus' contributions and theoretical impact. **TQM Journal**, v. 25, n. 6, p. 659–676, 2013.

ZHOU, W. et al. A joint-adaptive np control chart with multiple dependent state sampling scheme. **Communications in Statistics - Theory and Methods**, v. 46, n. 14, p. 6967–6979, 2017.

ZIBETTI, A. **Probabilidade - Estatística: Material de apoio à engenharia**. Disponível em: <https://www.inf.ufsc.br/~andre.zibetti/>. Acesso em: 20 jan. 2022.

APPENDIX A - ANALYSIS OF THE DISTRIBUTION OF $S_Y{}^2$

Analyzing the distribution of the variable $S_Y{}^2$, we will make the following considerations:

1) $Y \sim N(A + B\mu, B^2\sigma_p{}^2 + \sigma_m{}^2)$

2) $Z = \dfrac{Y-(A+B\mu)}{\sqrt{B^2\sigma_p{}^2+\sigma_m{}^2}}$

3) $Z \sim N(0,1)$

4) $Z^2 = \left(\dfrac{Y-(A+B\mu)}{\sqrt{B^2\sigma_p{}^2+\sigma_m{}^2}}\right)^2$

5) $Z^2 = \dfrac{(Y-(A+B\mu))^2}{B^2\sigma_p{}^2+\sigma_m{}^2}$

6) $Z^2 \sim \chi^2_{(1)}$

So, let $W = \sum_{j=1}^{n} Z^2$, we have that

$$W = \sum_{j=1}^{n}\left[\frac{\left(Y_j-(A+B\mu)\right)^2}{B^2\sigma_p{}^2+\sigma_m{}^2}\right]$$

So, $W \sim \chi^2_{(n)}$, and:

$$W = \sum_{j=1}^{n}\left[\frac{\left(Y_j-(A+B\mu)-\bar{Y}+\bar{Y}\right)^2}{B^2\sigma_p{}^2+\sigma_m{}^2}\right]$$

$$= \sum_{j=1}^{n}\left[\frac{\left(\left(Y_j-\bar{Y}\right)+\left(\bar{Y}-(A+B\mu)\right)\right)^2}{B^2\sigma_p{}^2+\sigma_m{}^2}\right]$$

$$= \sum_{j=1}^{n}\left[\frac{\left(Y_j-\bar{Y}\right)^2}{B^2\sigma_p{}^2+\sigma_m{}^2}\right] + 2\left(\frac{\bar{Y}-(A+B\mu)}{B^2\sigma_p{}^2+\sigma_m{}^2}\right)\sum_{j=1}^{n}\left(Y_j-\bar{Y}\right) + \sum_{j=1}^{n}\left[\frac{\left(\bar{Y}-(A+B\mu)\right)^2}{B^2\sigma_p{}^2+\sigma_m{}^2}\right]$$

Since,

$$\sum_{j=1}^{n}(Y_j - \bar{Y}) = \sum_{j=1}^{n}(Y_j) - \sum_{j=1}^{n}(\bar{Y})$$

$$= \sum_{j=1}^{n}(Y_j) - n\bar{Y}$$

And, $\sum_{j=1}^{n} Y_j = n\bar{Y}$, we have that:

$$\sum_{j=1}^{n}(Y_j - \bar{Y}) = n\bar{Y} - n\bar{Y} = 0$$

Thus,

$$W = \sum_{j=1}^{n}\left[\frac{(Y_j - \bar{Y})^2}{B^2\sigma_p{}^2 + \sigma_m{}^2}\right] + \sum_{j=1}^{n}\left[\frac{(\bar{Y} - (A + B\mu))^2}{B^2\sigma_p{}^2 + \sigma_m{}^2}\right]$$

$$= \frac{\sum_{j=1}^{n}(Y_j - \bar{Y})^2}{B^2\sigma_p{}^2 + \sigma_m{}^2} + \frac{n(\bar{Y} - (A + B\mu))^2}{B^2\sigma_p{}^2 + \sigma_m{}^2}$$

Considering the Central Limit Theorem, the sample mean of a random variable is normally distributed. So,

$$\bar{Y} \sim N\left(A + B\mu, \left(B^2\sigma_p{}^2 + \sigma_m{}^2\right)/n\right)$$

$$Z = \left(\frac{\sqrt{n}(\bar{Y} - A + B\mu)}{\sqrt{B^2\sigma_p{}^2 + \sigma_m{}^2}}\right)$$

$$Z \sim N(0,1)$$

$$Z^2 = \left(\frac{\sqrt{n}(\bar{Y} - A + B\mu)}{\sqrt{B^2\sigma_p{}^2 + \sigma_m{}^2}}\right)^2$$

$$Z^2 = \frac{n(\bar{Y} - (A + B\mu))^2}{B^2\sigma_p{}^2 + \sigma_m{}^2}$$

$$Z^2 \sim \chi^2_{(1)}$$

As previously shown,

$$W = \frac{\sum_{j=1}^{n}(Y_j - \bar{Y})^2}{B^2\sigma_p{}^2 + \sigma_m{}^2} + \frac{n(\bar{Y} - (A + B\mu))^2}{B^2\sigma_p{}^2 + \sigma_m{}^2}$$

where

$W \sim \chi^2_{(n)}$, and:

$$\frac{n(\bar{Y} - (A + B\mu))^2}{B^2\sigma_p{}^2 + \sigma_m{}^2} \sim \chi^2_{(1)}$$

Therefore,

$$\frac{\sum_{j=1}^{n}(Y_j - \bar{Y})^2}{B^2\sigma_p{}^2 + \sigma_m{}^2} = \begin{cases} W \\ \sim \chi^2_{(n)} \end{cases} - \begin{cases} \dfrac{n(\bar{Y} - (A + B\mu))^2}{B^2\sigma_p{}^2 + \sigma_m{}^2} \\ \sim \chi^2_{(1)} \end{cases}$$

So,

$$\frac{\sum_{j=1}^{n}(Y_j - \bar{Y})^2}{B^2\sigma_p{}^2 + \sigma_m{}^2} \sim \chi^2_{(n-1)}$$

Since,

$$S_Y{}^2 = \frac{\sum_{j=1}^{n}(Y_j - \bar{Y})^2}{n - 1}$$

Thus,

$$\frac{\sum_{j=1}^{n}\left(Y_j - \bar{Y}\right)^2}{B^2\sigma_p{}^2 + \sigma_m{}^2} = \frac{(n-1)S_Y{}^2}{B^2\sigma_p{}^2 + \sigma_m{}^2} \sim \chi^2_{(n-1)}$$
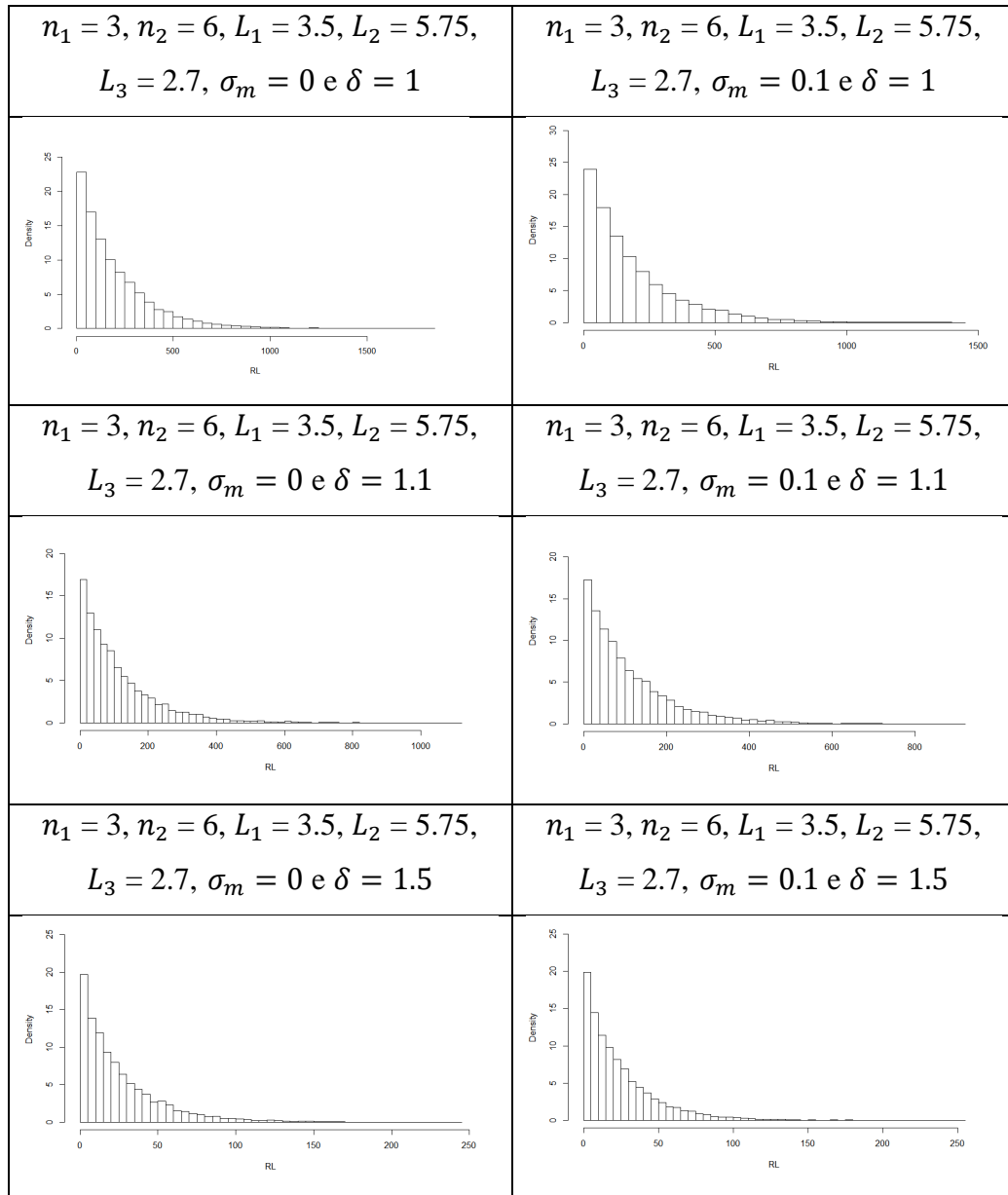
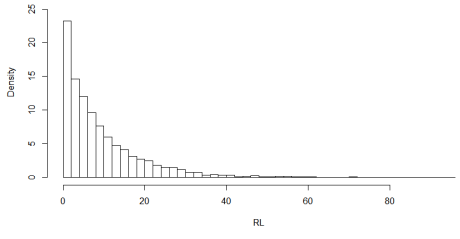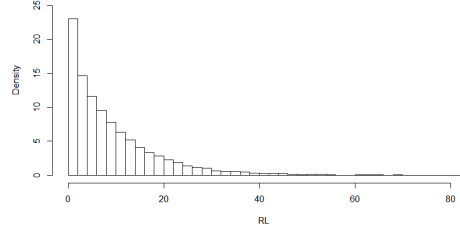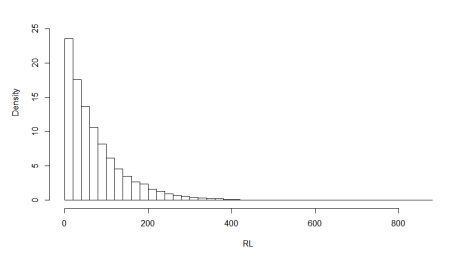**Reference:** ZIBETTI, André. Probabilidade - Estatística: Material de apoio à engenharia. Available on: https://www.inf.ufsc.br/~andre.zibetti/. Accessed on: 20/01/2022.
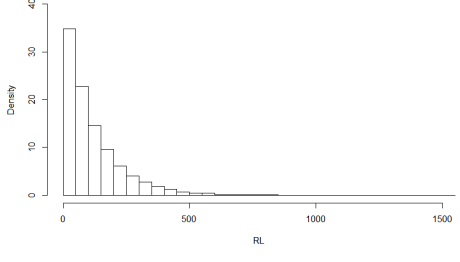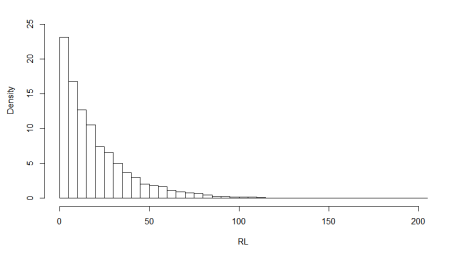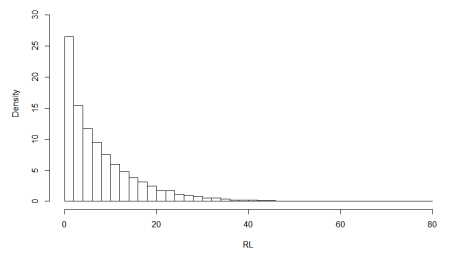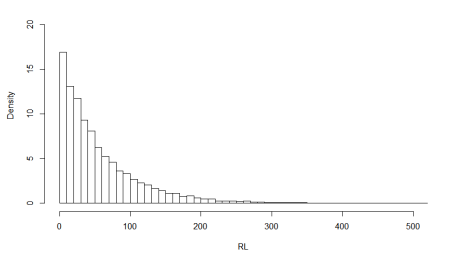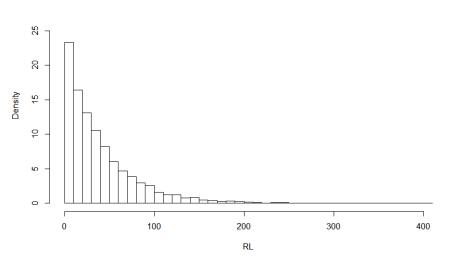
APPENDIX B – EXAMPLES OF THE SIMULATION GRAPHS

This appendix shows examples of the RL distribution results from the simulation described in Chapter 4.

- **RL distributions for simulated data**

$n_1 = 3, n_2 = 6, L_1 = 3.5, L_2 = 5.75,$ $L_3 = 2.7, \sigma_m = 0$ e $\delta = 1$	$n_1 = 3, n_2 = 6, L_1 = 3.5, L_2 = 5.75,$ $L_3 = 2.7, \sigma_m = 0.1$ e $\delta = 1$
$n_1 = 3, n_2 = 6, L_1 = 3.5, L_2 = 5.75,$ $L_3 = 2.7, \sigma_m = 0$ e $\delta = 1.1$	$n_1 = 3, n_2 = 6, L_1 = 3.5, L_2 = 5.75,$ $L_3 = 2.7, \sigma_m = 0.1$ e $\delta = 1.1$
$n_1 = 3, n_2 = 6, L_1 = 3.5, L_2 = 5.75,$ $L_3 = 2.7, \sigma_m = 0$ e $\delta = 1.5$	$n_1 = 3, n_2 = 6, L_1 = 3.5, L_2 = 5.75,$ $L_3 = 2.7, \sigma_m = 0.1$ e $\delta = 1.5$

$n_1 = 3, n_2 = 6, L_1 = 3.5, L_2 = 5.75,$ $L_3 = 2.7, \sigma_m = 0$ e $\delta = 2$	$n_1 = 3, n_2 = 6, L_1 = 3.5, L_2 = 5.75,$ $L_3 = 2.7, \sigma_m = 0.1$ e $\delta = 2$
$n_1 = 3, n_2 = 6, L_1 = 3.5, L_2 = 5.75,$ $L_3 = 2.7, \sigma_m = 0.3$ e $\delta = 1$	$n_1 = 3, n_2 = 6, L_1 = 3.5, L_2 = 5.75,$ $L_3 = 2.7, \sigma_m = 0.3$ e $\delta = 1.1$
$n_1 = 3, n_2 = 6, L_1 = 3.5, L_2 = 5.75,$ $L_3 = 2.7, \sigma_m = 0.3$ e $\delta = 1.5$	$n_1 = 3, n_2 = 6, L_1 = 3.5, L_2 = 5.75,$ $L_3 = 2.7, \sigma_m = 0.3$ e $\delta = 2$
$n_1 = 3, n_2 = 6, L_1 = 3.5, L_2 = 5.75,$ $L_3 = 2.7, \sigma_m = 0.5$ e $\delta = 1$	$n_1 = 3, n_2 = 6, L_1 = 3.5, L_2 = 5.75,$ $L_3 = 2.7, \sigma_m = 0.5$ e $\delta = 1.1$

$n_1 = 3, n_2 = 6, L_1 = 3.5, L_2 = 5.75,$ $L_3 = 2.7, \sigma_m = 0.5$ e $\delta = 1.5$	$n_1 = 3, n_2 = 6, L_1 = 3.5, L_2 = 5.75,$ $L_3 = 2.7, \sigma_m = 0.5$ e $\delta = 2$
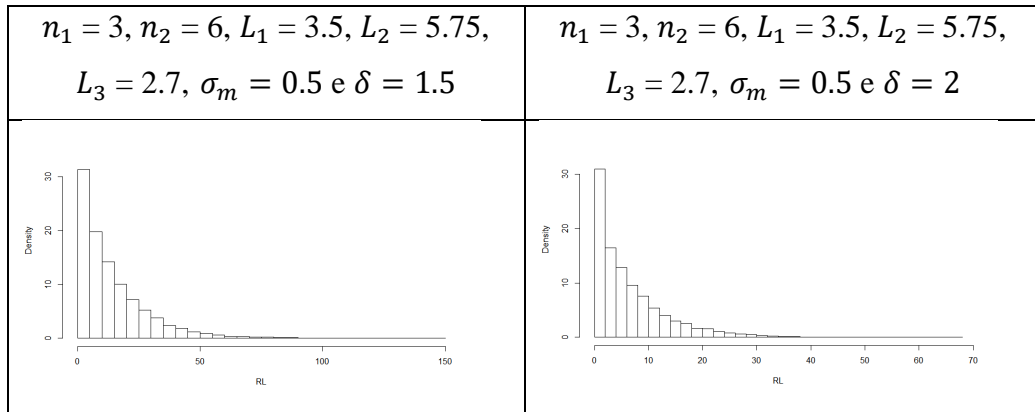
APPENDIX C - INTERVAL STUDIES

Let $z = \frac{(n_1-1)S_{Y1}^2}{B^2\sigma_p'^2+\sigma_m^2}$

Since S_{Y1}^2 is in interval $\Omega_2 = (L_1, L_2]$, then

$$L_1 \leq S_{Y1}^2 < L_2 = k_1(B^2\sigma_p^2 + \sigma_m^2) \leq S_{Y1}^2 < k_2(B^2\sigma_p^2 + \sigma_m^2)$$

For the case there is no shift in the process $(\sigma_p'^2 = \sigma_p^2)$, multiplying the both sides by $\frac{(n_1-1)}{B^2\sigma_p^2+\sigma_m^2}$, give us

$$(n_1 - 1)k_1 \leq z < (n_1 - 1)k_2$$

Then Ω_2^* can be written as

$$\Omega_2^* = ((n_1 - 1)k_1, (n_1 - 1)k_2]$$

Where there is a shift in the process standard deviation, then the interval Ω_2^{**} can be obtained consider

$$k_1(B^2\sigma_p^2 + \sigma_m^2) \leq S_{Y1}^2 < k_2(B^2\sigma_p^2 + \sigma_m^2)$$

Multiplying the both sides by $\frac{(n_1-1)}{B^2\sigma_p'^2+\sigma_m^2}$, give us

$$\frac{(n_1 - 1)k_1(B^2\sigma_p^2 + \sigma_m^2)}{B^2\sigma_p'^2 + \sigma_m^2} \leq z < \frac{(n_1 - 1)k_2(B^2\sigma_p^2 + \sigma_m^2)}{B^2\sigma_p'^2 + \sigma_m^2}$$

Then Ω_2^{**} can be written as

$$\Omega_2^{**} = (\frac{(n_1 - 1)k_1(B^2\sigma_p^2 + \sigma_m^2)}{B^2\sigma_p'^2 + \sigma_m^2}, \frac{(n_1 - 1)k_2(B^2\sigma_p^2 + \sigma_m^2)}{B^2\sigma_p'^2 + \sigma_m^2}]$$